CRYOGENICS

An International Journal of Low Temperature Engineering and Research

VOL. 2 NO. 2 DECEMBER 1961

Towards Superconductive Computers

J. M. Lock Royal Radar Establishment, Malvern

Received 24 March 1961

Digital computer circuitry

The possibility of making digital computers depends on the existence of non-linear devices capable in general of taking up two or more discrete states. Babbage's pioneer attempts to make calculating machines in the nineteenth century,[1] for example, and indeed the design of all our modern desk calculators, depend essentially on the use of the discrete positions of toothed wheels to represent the digits 0 to 9 of the decimal system. Although a few early electronic computers also used the decimal system, and incorporated devices or groups of devices with the necessary ten stable states, it soon became apparent that greater speed and economy of operation could be achieved using the binary code of numbers, so that only two stable states needed to be used. The logical operations entailed in computation can also be conveniently specified by means of a binary switching algebra, so that exactly the same code can be used for instructions and for the numbers to which these instructions relate.

All modern electronic digital computers, therefore, make use of binary physical devices. Their circuitry may be divided conveniently into two categories—a section which accomplishes the actual logical operations on numbers required by the calculation, and a section devoted to the storage of numbers and instructions at all the intermediate stages involved. Because the number of different operations is comparatively small, whereas the possible quantity of numerical data is almost unlimited, it has turned out that a fast and flexible computer needs a far larger number of binary devices in its store than it does in its logical circuits. To give an idea of the order of magnitude involved, a large modern machine may store a million or more binary digits (bits) of information, while using only ten thousand or so binary elements in its logical circuitry. (Even this refers only to its rapid access store; additional slow magnetic tape stores may be used to accommodate a hundred million or more bits.) Because of this, computers have in the past used quite different devices for the store and for the logical circuitry, a major consideration in the former being that of cost. In particular, whereas valve or transistor 'flip-flops' are widely used as high speed switches with inherent power gain in the logical circuits, their expense prohibits their use for the storage of information. This is now usually accomplished by means of magnetic ferrite cores, which although they are much slower in switching from one state to another, and do not possess power gain, are nevertheless at least an order of magnitude cheaper per bit. The presence or absence of available power gain in a device is often indicated by describing it as 'active' or 'passive', respectively. Passive devices, such as the ferrite core, must be used in conjunction with separate amplifiers to boost up their output, whereas active binary devices are capable of switching one another independently. At the present time large ferrite core stores have been constructed, into and out of which information can be passed in roughly 1 microsecond, and it seems that this sort of speed is getting near the limit set by the physical properties of this device. Transistor flip-flop circuits for handling this information can be made which will switch at rather more than ten times this rate. Most computations, however, require a number of logical operations in between each reference to store, so that the relatively low speed of the latter is not such a handicap as might appear at first sight.

Considerable efforts are being made in a number of laboratories to develop devices which will overcome the limitations of the present generation of computers, and it is the purpose of this review article to describe one such field of development, namely the utilization of the non-linear properties of superconductors in computer circuits.

Superconductivity

Shortly after his successful liquefaction of helium at Leiden in 1908, Kamerlingh Onnes began a series of investigations[2] on the electrical resistance of metals in the new range of low temperatures which had thus been opened up. It was in the course of these experiments that in May, 1911 he first observed the abrupt drop in the resistivity of mercury at 4·15° K, and thus discovered the phenomenon of superconductivity. At the present day some twenty metallic elements and a large number of alloys are known to become superconductive, with transition temperatures (T_c) ranging from about 0·5° K (cadmium, ruthenium, titanium) up to about 18° K for a compound of tin and niobium (Nb_3Sn).

The question as to whether the resistance of a metal in the superconducting state is truly zero or merely exceedingly small cannot yet be said to be finally settled. From the experimental point of view no trace of resistance has ever been measured, but of course this *may* mean only that the sensitivity of the experiments is not sufficiently refined; the persistence of a current in the superconducting circuit known as the Crowe cell (see below) has proved that the maximum possible resistance is less than 4×10^{-14} of its normal value. The recent theories of superconductivity due to Bardeen, Cooper, and Schrieffer,[3] and Bogolyubov,[4] while remarkably successful in explaining many of the thermal and magnetic properties of superconductors, have so far failed to account satisfactorily for the disappearance of resistance (the phenomenon which gave superconductivity its name!), although they suggest the lines along which the search for the true explanation of this phenomenon should proceed. In the absence of such an explanation it is clearly impossible to say whether the theory of superconductivity will predict a genuinely zero resistance or not.

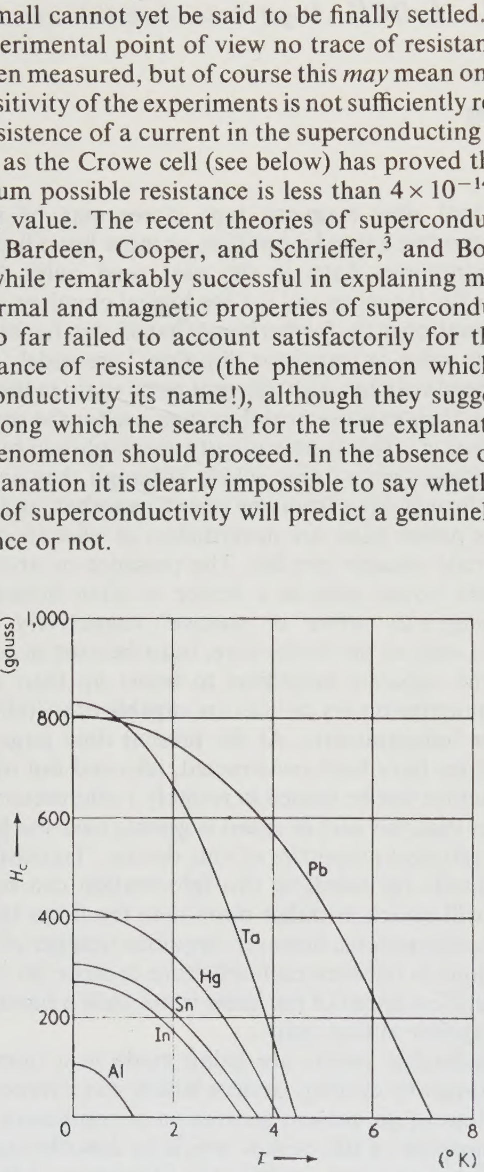

Figure 1. H_c–T curves of some superconductors

From the point of view of non-linear circuit elements the most important property of superconductors is the fact that their normal resistance can always be restored by the application of a large enough external magnetic field, which for a given pure superconductor is a well-defined function of temperature and is known as the critical field (H_c). The critical field curves of a number of typical superconductors are shown in Figure 1, and the restoration of resistance in a thin mercury film as the applied magnetic field is increased in Figure 2. It is seen that, just as in the case of the change of resistance with temperature, this transition is an abrupt one.

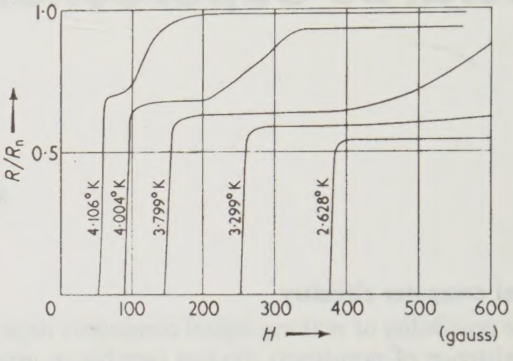

Figure 2. Transition curves of mercury film 2,410 Å thick

For about twenty years after the discovery of superconductivity it was assumed that the property of zero resistance, together with its restoration above the critical field, were sufficient to explain all the facts about superconductors. Below H_c any change in the applied field would induce currents in the surface of the metal just big enough to prevent any change of flux inside it, and because its resistivity was zero these currents would persist without any observable decay. The flux inside a superconductor would therefore remain constant at the value existing when the metal first went into the superconducting state. However, in 1933, Meissner and Ochsenfeld[5] showed conclusively that if a superconductor was cooled in a magnetic field from *above* its transition temperature (so that the initial value of the flux inside it was *not* zero), then the onset of superconductivity was accompanied by a sudden expulsion of flux from the interior of the specimen. This was shown by the ballistic galvanometer deflection observed as the specimen was cooled down, with a search coil surrounding it connected in series with the galvanometer. This classic experiment proved for the first time that it is not just the change in magnetic induction B which is zero in the interior of a superconductor, but the induction B itself. Instead of there being an infinite number of possible equilibrium magnetic states, only one, that with $B=0$, represents the true stable state of the material. A superconductor thus behaves like a perfectly diamagnetic material of susceptibility $\kappa = -1/(4\pi)$, (since $H+4\pi I = B = 0$). This discovery of the Meissner effect, as it is called, was of the greatest importance because it provided the justification for the application of the theory of reversible thermodynamics to superconductors in a magnetic field, and enabled the correlation between their magnetic properties, such as critical field, and thermal properties, such as specific heat, to be worked out.

An important corollary to the destruction of superconductivity by an external magnetic field is its destruction by a current flowing in the superconductor itself. This was actually discovered by Onnes[6] before the discovery of the magnetic field effect, but is closely connected with it, the critical current in a superconducting wire of macroscopic dimensions being simply that current which will produce the critical field at the surface of the wire. The suggestion that this was the true explanation of the effect was first made by Silsbee[7] and is known as the Silsbee hypothesis.

One final property of superconductors needs to be mentioned before we pass on to a discussion of actual switching devices. The change in magnetic induction from zero inside a superconductor to a finite value outside, when the specimen is in an applied field, is not discontinuous but takes place over a finite distance known as the penetration depth λ, typically $\sim 10^{-5}$ cm. In other words, the surface currents, which keep the induction zero inside the metal, flow in a skin of finite thickness, and this is the penetration depth layer. Penetration effects become of particular importance in specimens in the form of thin metallic films whose thickness is of the same order of magnitude as the penetration depth. Two important changes then take place, an increase in the critical field required to destroy superconductivity in the film, and a decrease in its critical current. These effects will be described in greater detail when we come to consider devices based on superconducting thin films.

Early superconducting switches

The idea of using the superconducting transition as a switching mechanism is not a new one, and superconducting switches have been used in laboratory apparatus for more than twenty years. One of the earliest of these was incorporated in the circuit of a superconducting galvanometer designed by Grayson Smith and his coworkers at Toronto in 1935.[8] This galvanometer consisted of a moving copper coil suspended in superconducting lead field coils, and was designed for the measurement of persistent currents induced in these field coils. The purpose of the superconducting switch was to introduce a small resistance in series with the field coils so that the persistent current dropped rapidly to zero, enabling the zero reading of the galvanometer to be obtained. The switch consisted simply of a short section of the superconducting circuit around which was wound a small copper coil, so that when a large enough current was passed through the latter the critical field of the superconductor was exceeded. A similar arrangement was used in conjunction with a much more sensitive superconducting galvanometer constructed by Pippard and Pullan,[9] except that their switch was an evaporated film of lead which could be heated above its transition temperature by means of a heating strip of german silver. In this way a resistance of about $5 \times 10^{-3}\,\Omega$ could be introduced into the circuit, effectively 'open circuiting' a very small shunt across the superconducting galvanometer itself, and thereby enabling its sensitivity to be varied at will (a second resistance of about $2 \times 10^{-5}\,\Omega$ was permanently in series with the galvanometer).

A further development of the superconducting switch was its use in superconducting 'chopper' amplifiers by Templeton[10] and de Vroomen and van Baarle.[11] In these instruments the switch is driven alternately normal and superconducting by an alternating magnetic field so that a d.c. current in a circuit of very low resistance in series with the switch is modulated by it, producing an a.c. component which can be transformed up and amplified in a conventional way. The frequencies used by these authors were not high, 800 c/s and 10 c/s, respectively, but even so a serious difficulty was caused by pick-up due to stray fields from the coil. In spite of this both these amplifiers were capable of detecting signals as low as a few times 10^{-11} V.

The first deliberate attempt to apply the switching capabilities of superconductors to the development of computer components was made by Buck in 1956,[12] who called the new device the 'cryotron'. Like the switch used by Grayson Smith it depends on the destruction of superconductivity by a magnetic field, and consists of a straight piece of superconducting wire, or 'gate', on which is wound a single layer coil through which a control current can be passed in order to drive the gate normal and thus restore its resistance. This control winding is itself made of a superconductor with a much higher transition temperature and critical field than the gate wire, so that even when it carries a current large enough to generate a field greater than the critical field of the gate it remains superconducting itself. Suitable materials used by Buck for his cryotrons were tantalum for the gate ($T_c = 4{\cdot}3°$ K) and niobium for the control winding ($T_c = 8°$ K); at the normal boiling point of liquid helium (4·215° K) the critical field of the gate was then about 40 oersteds.

An important feature of the cryotron is that, by a suitable choice of the dimensions of the gate and control circuits, it is easy to arrange for the critical current i_g of the gate wire to be larger than the current i_c in the control winding needed to restore the gate resistance, or 'critical control current'. Then if H_c is the critical field of the gate wire we have (by Silsbee's hypothesis)

$$H_c = 4i_g/d \qquad \ldots (1)$$

and

$$H_c = 4\pi n i_c \qquad \ldots (2)$$

where d is the diameter of the gate wire and n is the number of turns per unit length of control winding. Thus

$$i_g/i_c = \pi n d = K \qquad \ldots (3)$$

The number K may be called the 'current gain' of the cryotron. For the cryotron dimensions used by Buck (gate diameter 0·009 in., control winding 250 turns per inch of

0·003 in. insulated niobium wire), $K = 7$. In practice the observed value of current gain was usually somewhat smaller than that calculated, presumably due to small flaws in the tantalum gate wire. Provided that K is greater than unity it is possible to construct switching circuits with identical cryotrons (using superconducting interconnections) without any additional power amplification, in just the same way as is done with relays. The value of K also fixes the allowable tolerance on the cryotron parameters, for a circuit in which there is a statistical spread of these parameters will always work satisfactorily provided that the ratio of the highest to the lowest critical current is less than the smallest current gain. Since in the steady state the current in such a circuit will always flow along a completely superconducting path there is no power dissipation and heat is generated only during the actual switching process. The basic simplicity and universality of the cryotron for the purpose of switching circuitry are almost unique among digital devices, and it is therefore not surprising that they have, as we shall see, attracted so much attention in recent years.

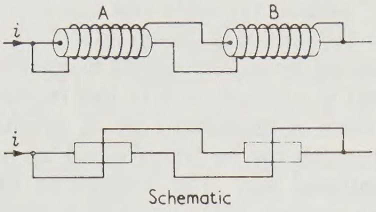

Figure 3. Cryotron flip-flop

The simplest example of a cryotron switching circuit is the bistable element or flip-flop, shown in Figure 3, consisting of two cryotrons A and B connected in parallel with the gate of one in series with the control circuit of the other. The current i supplied externally can flow either through gate A and control winding B, holding gate B resistive, or through gate B and control winding A, holding gate A resistive. It is, of course, necessary that $i_g > i > i_c$. Furthermore this circuit as it stands provides no means of controlling the current path: two further cryotrons C and D (Figure 4) are needed to act as 'write-in' triggers, and one more E as a 'read-out' circuit. The complete flip-flop therefore consists of five cryotrons.

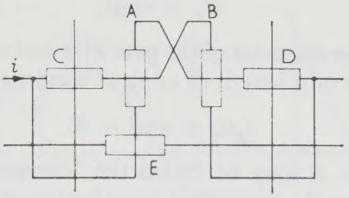

Figure 4. Complete flip-flop

The rate at which the current i can be switched from one path to the other depends on the self-inductance of the whole loop and on the normal gate resistance R associated with each cryotron. If most of the self-inductance is due to the control winding, as is usually the case, it turns out that the overall switching time is about $7L/R$, where L is the self-inductance of one control winding, and in the case of the cryotrons described above this time is of the order of 100 μsec. A further limitation to the speed of the device is set by the heat generated during switching while current is still flowing momentarily through a resistive arm of the flip-flop. Since the rate of heating is Ri^2 and since the time for which it continues is of the order of L/R the total heat generated is roughly Li^2. This heat warms up the gate wire, and it is found in practice that, because the maximum permissible temperature rise of the tantalum is less than 0·1° K, this effect limits the frequency at which the flip-flop may be switched to about 1,000 c/s.

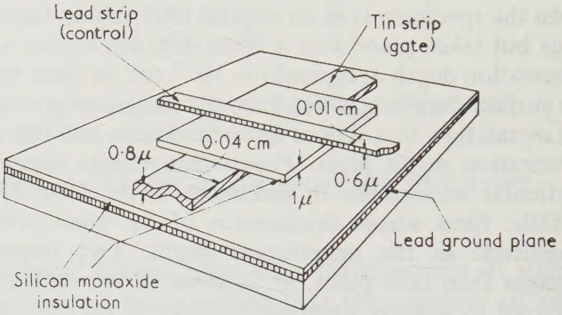

Figure 5. Strip cryotron

We see, therefore, that the Buck wire-wound cryotron is severely limited in its speed of operation, mainly by its comparatively large self-inductance. The efforts made in the last few years to overcome this limitation, and the extent to which they have been successful will be described below.

Fast superconductive devices

A simple modification of the basic design of the cryotron in order to reduce its self-inductance, and at the same time to increase its normal resistance, immediately suggests itself. This is to make both gate and control circuits of thin evaporated superconducting films, instead of macroscopic wires, in the way shown schematically in Figure 5. In this construction a current through the lead control strip gives rise to a magnetic field between it and the ground plane, so that the narrow region of the tin gate lying immediately beneath the control strip can thereby be driven normal. The geometrical design of this device has given rise to the name 'planar cryotron' to distinguish it from Buck's original invention. It was first tested at the laboratories of I.B.M. in America, but has shown so many promising features that many other industrial laboratories in the

U.S.A. have started working vigorously on it, though it has so far been almost entirely neglected by industry in the U.K.

The chief problem encountered in fabricating the planar cryotron has proved to be that of achieving a useful current gain. The first tests were made on two crossed strips with no ground plane, and showed not only that the gate in this arrangement had a disappointingly low critical current but also, from the width of its transition as the control current was raised, that the magnetic field due to the latter was too spread out. The presence of the ground plane not only concentrates this field (and incidentally thereby considerably reduces the self-inductance of the circuit), but probably also makes the current distribution in the gate much more uniform across its width, thereby raising its critical current. If the widths of the gate and control strips are w_g and w_c, respectively, then the fields beneath them produced by unit current are $4\pi/w_g$ and $4\pi/w_c$ and, assuming again that Silsbee's hypothesis holds in this case, the current gain K of the cryotron should be w_g/w_c, or width ratio W. In practice it is found extremely difficult even using a ground plane to achieve this ideal current gain, so it is useful to introduce a cryotron efficiency e defined by $e = K/W$.

The I.B.M. workers have so far been the most successful in attaining values of e close to unity, and have traced one particular cause of trouble which is of some interest. The gate strip is usually made by evaporating tin (or indium) on to the substrate (after the ground plane and silicon monoxide insulation), through a suitable mask, and in doing so the edges of the strip always show a 'penumbral' region in which the thickness of the strip gradually falls off to zero. Now, as was mentioned above, such a region of very thin film has a critical field greater than the bulk metal, so that it will remain superconducting, and thus short out the central region of film, after the latter has been driven normal by the control current. The presence of the penumbra thus increases the effective critical control current and thereby decreases the current gain, and it appears that its removal, either by physically scoring through it or by other means such as depositing on a pre-heated substrate (which has the effect of causing the penumbra to disintegrate into isolated 'islands' of film), can increase the current gain by a factor of 2 or 3.

The increased critical field of a very thin film is, as we have seen, due to the penetration of the magnetic field into the surface layer of the superconductor, and it sets a lower limit to the useful thickness of the gate in the planar cryotron. If current gain were the only important factor there would be no point in making the films as thin as possible, but considerations of switching speed show that this is not so. Once again it is L/R which is the important factor. If the main contribution to self-inductance in a cryotron circuit is that of the control strip, then if the insulation thickness is d cm and the gate thickness and resistivity are t cm and ρ Ωcm, respectively, we have

$$L = 4\pi \times 10^{-9}\, dw_g/w_c \text{ H} \qquad \ldots(4)$$

and

$$R = \rho w_c/tw_g\ \Omega \qquad \ldots(5)$$

so that

$$L/R = 4\pi \times 10^{-9}\, dtW^2/\rho \text{ sec}$$
$$= 4\pi \times 10^{-9}\, dtK^2/\rho e^2 \text{ sec} \qquad \ldots(6)$$

For a given current gain L/R has a minimum value for some thickness t usually somewhat greater than the penetration depth of the superconductor, owing to the rapid decrease in e as t is reduced. The theory of the destruction of superconductivity in thin films both by external fields and by currents is not yet sufficiently well understood to say whether the best observed values of e are 'ideal' or still limited by imperfections in the film. However, for gate thicknesses of about 8,000 Å, efficiencies of over 0·9 have been reported by Rosenberger,[13] so that no order of magnitude improvement can be expected. The value of L/R predicted by equation (6) is then about 2×10^{-8} sec for $K = 4$, $\rho = 10^{-7}$ Ωcm, $d = 1$ micron, and agrees quite well with the observed switching time ($7L/R$) of an actual flip-flop.

Further improvements in the speed of the planar cryotron may be expected from developments in two directions. First one may expect a significant improvement in the figures quoted above for the factors in equation (6)—the use of alloys may enable ρ to be increased, the insulation thickness may be further reduced, and it may prove possible to decrease t without a corresponding deterioration of e. Better control of evaporating conditions will probably result in cryotrons of greater reproducibility, thus enabling a smaller current gain to be used. Conventional improvements of this kind will probably result in a reduction of L/R by a further factor of 5 to 10. In the second place a recent development in the geometrical design of the planar cryotron at I.B.M. may lead to even higher speeds. This is the use of what I.B.M. call the 'in-line' cryotron, in which the control and gate strips, instead of crossing one another at right angles, are actually parallel, so that the entire length of gate lying below the control strip is driven normal, instead of just a narrow section. At first sight this geometry would seem inapplicable, since the current gain must inevitably be less than unity. However, by the use of a further biasing control strip placed above the ordinary control, advantage can be taken of the fact that with parallel gate and control their magnetic fields can be either parallel (currents flowing in the same direction) or anti-parallel (currents opposed). A steady biasing field can thus be made to increase the control field but decrease the self-field due to the gate, and a current gain greater than unity can thus be achieved. The in-line cryotron has a normal gate resistance very much larger than the conventional design, and it is hoped ultimately that it can actually be matched approximately to the characteristic impedance of the circuitry linking the cryotrons together. This circuitry consists of evaporated superconducting lead strips just like the control strips of the cryotrons themselves, and forms, with the ground plane, a set of strip transmission lines of roughly 1 Ω characteristic impedance. At present it requires an in-line cryotron gate about 4 cm long to match this resistance, but this length can probably be considerably reduced. If such matching can be achieved the speed of switching of cryotron circuits will be increased to such an extent that it becomes limited mainly by the propagation time along the circuit at the velocity of electromagnetic waves in the dielectric insulation.

The planar cryotron is not the only fast superconductive computer device to appear in the last few years. It was mentioned earlier that one of the limitations of present computers is the comparatively slow rate of access to the store set by the switching speed of the ferrite core. In the quest for higher speed, therefore, considerable attention has been devoted to the development of faster passive devices suitable for information storage. One such device which shows promise makes use of the possibility of setting up persistent currents in a superconducting circuit, the direction of these currents representing the two states required to store information. It was invented by Crowe[14] at I.B.M. and has now been studied in some detail both in the U.S.A. and also in the U.K. at R.R.E. and at S.E.R.L.

The Crowe cell consists of a thin film of tin or lead of the shape shown in Figure 6(a) on a glass or mica substrate. The two states of the device are represented by currents flowing in the directions shown in Figure 6(b) and 6(c), and are set up by current pulses of opposite polarity and appropriate amplitude in the drive wire, which is closely linked inductively with the superconducting circuit. Changes of state are detected by means of the pick-up wire beneath the 'crossbar'. Because the superconducting circuit acts as a perfect screen for flux through the two D-shaped holes, a signal is only obtained when the crossbar is driven normal, and it can be shown that this occurs only when the drive current pulse is of opposite polarity to the previous one. Thus the 'information' which is stored in the cell can always be read out destructively, in the same way as with a ferrite core, by 'interrogating' it with a current pulse of the appropriate polarity to drive it into the '0' state. A previously stored '1' will then give an output signal, but a previously stored '0' none.

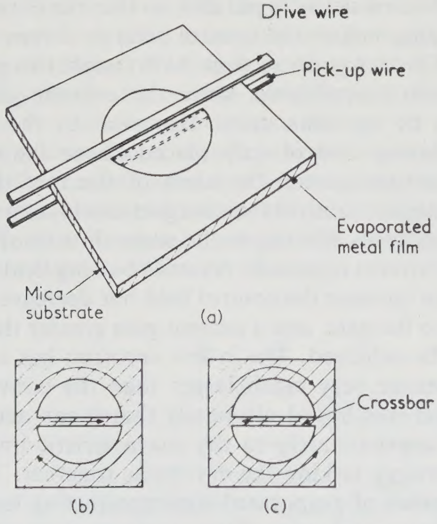

Figure 6. Diagram of Crowe cell: (a) General view; (b) '0' state; (c) '1' state

The Crowe cell depends on the destruction of superconductivity in the crossbar when the induced current in it exceeds the critical value. It differs in this respect from the cryotron whose operation depends upon the external application of the critical magnetic field of the gate. For this reason there is no inherent disadvantage in using much thinner films for the Crowe cell, and the switching speed can be thereby increased. As usual, this depends mainly on the L/R time constant of the circuit when the normal resistance of the crossbar is restored; and the self-inductance is in fact appreciably larger than in the planar cryotron, about 10^{-9} H. However, the crossbar resistance can be quite large, a few tenths of an ohm, so that the switching speed of the Crowe cell is high. The best figure reported so far[15] is about 3×10^{-9} sec, or some 100 times faster than the highest speed attainable with the ferrite core. With this high speed, with its fairly small drive current (~ 100 mA), and with the possibility of evaporating it in large arrays at low cost, the Crowe cell offers attractive possibilities for a large rapid access computer store. Whether these can be fulfilled or not depends largely on the question of reproducibility, for the tolerance allowable on the critical current of the crossbar is much smaller than is the case for the gate of the planar cryotron.

Cryotron circuitry

Those who have worked on the planar cryotron are so confident of its ultimate success that a considerable amount of work has been devoted to the design of cryotron computer circuits, well before the cryotrons themselves have become available in appropriate numbers. It is important to stress here that the ultimate goal in this field is the construction of a computer whose circuits, apart from the input and output, are built exclusively with cryotrons; no other type of circuit element is either needed or desired.

It has been pointed out by Haynes[16] that the cryotron has the unique property among digital computer devices of providing a means of storing information without power dissipation, and at the same time of yielding a d.c. indication of its state. This can be achieved, as we shall see, by using the cryotron in a persistent current loop, as in the Crowe cell, but at the same time causing the persistent current to act as the control for a second cryotron. All other types of fast storage device belong to one of two categories: either they give a d.c. indication of their state, but require power dissipation to maintain that state (for example the transistor flip-flop), or they require no continuous power dissipation but yield no d.c. indication of their state (for example, the ferrite core).

A single cryotron performs exactly the same logical function in a circuit as a simple relay with a normally closed contact. Thus, when no current flows in the control strip, then current may flow in the gate and vice versa.

Just as in the case of relays, any logical function whatever may be built up by a suitable combination of cryotrons. This similarity between cryotrons and relays enables computer circuitry to be designed on an asynchronous principle, or in other words without the need for a synchronizing clock pulse generator. One can set up a network of cryotron gates by means of the control currents appropriate to any chosen input function, and then apply a probing current to the entire network of cryotrons. This probing current will distribute itself through the network as rapidly as possible in a pattern of paths which is switched successively from one arrangement to another until it attains the stable state yielding the corresponding output function.

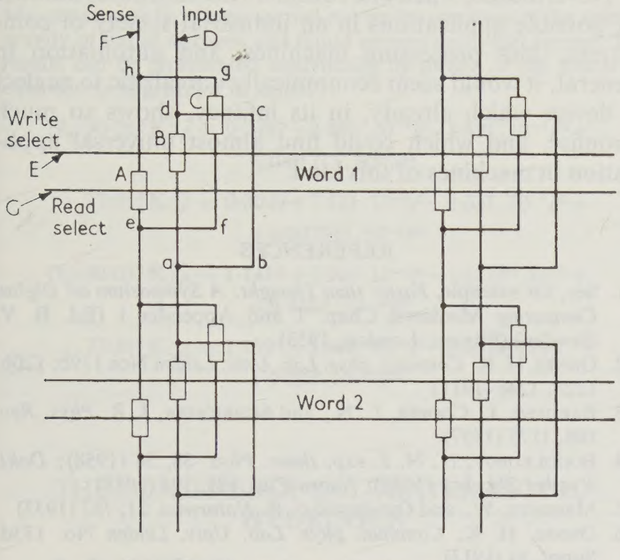

Figure 7. Cryotron persistent current store

It is clearly of primary importance to devise a cryotron circuit suitable for a large random access store, provided with a convenient method of address selection. A solution to this problem has been given by Haynes[16] by means of the circuit of Figure 7 which requires three cryotrons per bit of storage, and uses the presence or absence of a persistent current in the loop abcd to represent a '1' or a '0', respectively. Figure 7 shows a portion containing 4 bits, of a two-dimensional store arranged in rows of *words* so that a given *column* contains bits of the same degree of significance in all words. Two-dimensional selection for writing and completely separate non-destructive reading is provided by 'input' and 'write select', 'sense' and 'read select' lines, respectively.

To store a '1' in the loop abcd, current is passed through the appropriate digit input line D and the write select line E for word 1 is pulsed. This drives the gate of cryotron B resistive so that the input current must switch to the shunting loop abcd, of appreciably higher self-inductance than the direct path ad. Flux is now linked with the loop abcd, and on removing the currents from E and then D a persistent current will remain in the loop, large enough to control the gate of cryotron C. To store a '0' or to switch a '1' to a '0' the write select line is pulsed with no current flowing in the input line.

Similarly, to read the contents of loop abcd current is applied to the digit sense line F while the read select line G is pulsed. The latter drives the gate of cryotron A resistive, and, if the loop abcd contains no persistent current so that gate C is superconducting, the sense current is switched to the shunting loop hgfe but continues to flow in line F. If, however, a '1' is stored in loop abcd, gates A and C are both resistive and the current in F is switched to some other superconducting path in parallel with F (not shown in Figure 7), thereby controlling a digit register cryotron which will then sense the presence of the stored '1'. The separation of the read and write selection circuits in this way enables simultaneous reading of one word and writing of another to be performed if necessary. The same basic storage unit, in conjunction with slightly more complicated access circuits, makes it possible to perform more sophisticated logical operations such as transfer of data from one word or register to another, right shifting in storage, or interchange of data between two registers.

As a final example of cryotron circuitry we give the binary full adder for a single bit.[16] This circuit requires fourteen cryotrons, and is shown in Figure 8. A full adder has three inputs, namely the carry from the previous stage and the two digits to be added, and two outputs, the sum and the carry to the next stage. These are indicated in Figure 8 by the letters C_0, A, B (the inputs), S_1, and C_1 (the outputs), respectively. A bar over the letter indicates a '0' and its absence a '1'. The first stage of the operation

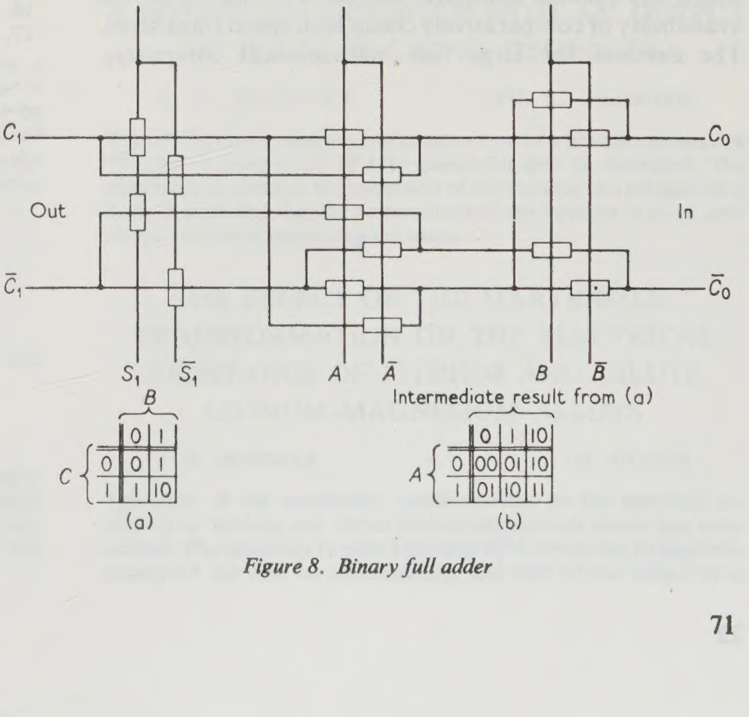

Figure 8. Binary full adder

involves acting on the input carry by the B input and must produce the intermediate sum shown in Figure 8(a) which has the three possible values, 0, 1, and 10. Thus the two lines corresponding to $C_0 . \bar{B}$ and $\bar{C}_0 . B$ (remembering that the presence of control current in a cryotron denies current to its gate line) are recombined, giving three intermediate result lines. These must now split into six so that either A or $\bar{A}$ can operate to produce the required full sum shown in Figure 8(b), in which the first digit is the C_1 carry and the second the S_1 sum. Again recombination takes place to give the four possible results 00, 01, 10, and 11 on four lines which generate the sum output via the gates in lines S_1 and $\bar{S}_1$ and themselves recombine into the two carry lines C_1 and $\bar{C}_1$.

The future of cryotrons

Of all the factors which determine the success or failure of a new invention such as the cryotron the most important is probably also the most difficult to assess—namely the economic factor. As regards its technical capabilities the planar cryotron seems to be ideally suited for future mathematical computers; it combines simplicity, versatility, compactness, high speed, negligible power dissipation, and, above all, ease for translating the logical requirements of the computer designer into an actual circuit, since it is a digital device *par excellence*, needing no other ancillary circuit elements in combination with it. The need for a liquid helium refrigerator in a cryotron computer should be no barrier, since modern cryogenic techniques have shown that such machines can be made reliable over running periods of over 1,000 hr.[17] If it were economically feasible to spend as much money on the development of the cryotron as has been spent on, say, the transistor it might lead the field in computer design. But, of course, the economics of the transistor depend, not on computers, but on its tremendous market in commercial radio and television, among other things, and it is this which has enabled computer designers to cash in on the availability of comparatively cheap high speed transistors. The demand for large fast mathematical computers, particularly in the U.K., is a very restricted one, and unfortunately some of the chief customers, the universities, are not able to buy as many as they would like because of lack of funds. The electronics industry is, in fact, loth to sink capital on a completely new project such as the cryotron, restricted entirely to the computer field.

Nevertheless, when one considers the enormous number of possible applications in an industrial society of computers, data processing machines, and automation in general, it would seem economically unrealistic to neglect a device which already, in its infancy, shows so much promise, and which could find almost universal application in machines of this kind.

REFERENCES

1. See, for example, *Faster than Thought: A Symposium on Digital Computing Machines*, Chap. 1 and Appendix 1 (Ed. B. V. Bowden) (Pitman, London, 1953)
2. Onnes, H. K. *Commun. phys. Lab. Univ. Leiden* Nos 119b, 120b, 122b, 124c (1911)
3. Bardeen, J., Cooper, L. N., and Schrieffer, J. R. *Phys. Rev.* **108,** 1175 (1957)
4. Bogolyubov, N. N. *J. exp. theor. Phys.* **34,** 58 (1958); *Dokl. Vysshei Shkoly* **1** (1958); *Nuovo Cim.* **VII,** 794 (1958)
5. Meissner, W., and Ochsenfeld, R. *Naturwiss.* **21,** 787 (1933)
6. Onnes, H. K. *Commun. phys. Lab. Univ. Leiden* No. 133d, Suppl. 34 (1913)
7. Silsbee, F. B. *J. Wash. Acad. Sci.* **6,** 597 (1916)
8. Grayson Smith, H., and Tarr, F. G. A. *Trans. roy. Soc. Can.* **29,** 23 (1935); Grayson Smith, H., Mann, K. C., and Wilhelm, J. O. *Trans. roy. Soc. Can.* **30,** 13 (1936)
9. Pippard, A. B., and Pullan, G. T. *Proc. Camb. phil. Soc.* **48,** 188 (1952)
10. Templeton, I. M. *J. sci. Instrum.* **32,** 314 (1955)
11. de Vroomen, A. R., and van Baarle, C. *Physica* **23,** 785 (1957)
12. Buck, D. A. *Proc. Inst. Radio Engrs, N.Y.* **44,** 482 (1956)
13. Rosenberger, G. B. *Solid State Electron.* **1,** 388 (1960)
14. Crowe, J. W. *I.B.M. J. Res. Develop.* **1,** 295 (1957)
15. Rhoderick, E. H., and Broom, R. F. Unpublished work at the Services Electronics Research Laboratory
16. Haynes, M. K. *Solid State Electron.* **1,** 399 (1960)
17. McMahon, H. O., and Gifford, W. E. *Solid State Electron.* **1,** 273 (1960); also private communication

Abstracts

THE VARIATION OF THE DENSITY OF LIQUID NITROGEN AND LIQUID OXYGEN AS A FUNCTION OF PRESSURE

A. VAN ITTERBEEK　　O. VERBEKE

MEASUREMENTS have been carried out on the variation of the specific gravity of liquid nitrogen and liquid oxygen up to 850 kg/cm². The results can be represented analytically by means of the following equation (ρ in g/cm³, P in kg/cm²):

$$N_2: 90{\cdot}26^\circ K; \rho = 0{\cdot}7497 + 3{\cdot}493 . 10^{-4}P - 3{\cdot}431 . 10^{-7}P^2 + \\ + 0{\cdot}01713 . 10^{-8}P^3$$

$$77{\cdot}31^\circ K; \rho = 0{\cdot}8079 + 2{\cdot}521 . 10^{-4}P - 2{\cdot}031 . 10^{-7}P^2 + \\ + 0{\cdot}007995 . 10^{-8}P^3$$

$$O_2: 90{\cdot}07^\circ K; \rho = 1{\cdot}1419 + 1{\cdot}969 . 10^{-4}P - 1{\cdot}233P^2 . 10^{-7} + \\ + 0{\cdot}4682 . 10^{-10}P^3$$

$$77{\cdot}35^\circ K; \rho = 1{\cdot}1997 + 1{\cdot}608 . 10^{-4}P - 0{\cdot}8078P^2 . 10^{-7} + \\ + 0{\cdot}298 . 10^{-10}P^3$$

THE DENSITIES OF SATURATED LIQUID HYDROGEN

R. D. GOODWIN　　D. E. DILLER
H. M. RODER　　L. A. WEBER

DENSITIES of *para*-hydrogen from 17° to 32° K are obtained by extrapolating newly determined compressed liquid isotherms to corresponding vapour pressures. Results are combined with earlier data for the range 14° to 20° K and compared with normal hydrogen by means of density–temperature relationships.

SMALL SCALE HYDROGEN LIQUEFACTION

B. YATES　　F. E. HOARE

A DESCRIPTION is given of the procedure adopted in designing a hydrogen liquefier to produce a required output. The procedure is applied to a case where 5 l. of liquid hydrogen were required to be produced without the use of a compressor. Constructional details of the purification and liquefaction systems of an accessible and easily constructed machine are included, together with performance figures.

TOLERANCES ASSOCIATED WITH THE OPERATION OF THE CROWE STORAGE CELL IN THE COINCIDENT CURRENT MODE

R. V. PEACOCK

THE coincident current mode of operation of the Crowe storage cell is considered. The relationship between the tolerances on the device parameters and the drive currents is calculated as a function of the shape of the adiabatic curve of resistance against current of the crossbar.

A METHOD FOR MEASURING THE HEAT CAPACITY OF CONDENSED GASES ABOVE THEIR BOILING POINT

A. V. VORONEL　　P. G. STRELKOV

A METHOD has been developed for measuring the heat capacity with stirring at pressures up to several tens of atmospheres. The heat capacity of the calorimeter, which is approximately 105 cm³ in volume and can stand 70 atm, amounted to 13–20 per cent of the measured quantity. The magnetic stirrer working at low temperature and high pressure, does not introduce any noticeable heating and reduces the time for achieving equilibrium by 1·5 to 2 times. Trial measurements were made of the heat capacity of nitrogen in the critical region.

THE MEASUREMENT OF THERMAL EXPANSION OF METALS AT LOW TEMPERATURES

K. ANDRES

AN apparatus for measuring thermal expansion at low temperatures is described. By means of an optical technique, it is possible to detect length changes of 1 Å (10^{-8}cm) in a specimen 7 cm long. Results are given for the lattice and electronic contributions to thermal expansion in the metals Al, Pb, Ta, Nb, Mg, and W.

CARBON RESISTANCE THERMOMETERS FOR LOW TEMPERATURES

N. N. MIKHAILOV　　A. YA. KAGANOVSKII

THE technique of preparation from petroleum pitch and the properties of carbon thermometers, for measuring low temperatures with high sensitivity and satisfactory reproducibility are described. The form of the temperature dependence of the resistance of these thermometers is determined by the firing temperature.

A HYDROGEN LIQUEFIER WITH AN OUTPUT OF 50 l./hr OF LIQUID HYDROGEN

A. G. ZEL'DOVICH　　YU. K. PILIPENKO

THE principal of operation and construction of a liquefier producing 50 l./hr of normal, or 30 l./hr *para*-hydrogen is described. The possibility is noted of the operation of the liquefier in a refrigerating cycle. A table showing the performance of the liquefier is given, and also the results of measuring the losses.

THE EFFECT OF THE MARTENSITIC TRANSFORMATION ON THE ELECTRICAL RESISTANCE OF LITHIUM AND DILUTE LITHIUM–MAGNESIUM ALLOYS

J. S. DUGDALE　　D. GUGAN

THE effect of the martensitic transformation on the electrical resistivity of lithium and dilute lithium–magnesium alloys has been studied. The resistivity of pure lithium at 80° K decreases by approximately 0·5 per cent on transforming, and that of the alloys by a

great deal more. By means of experiments using thermal cycling and mechanical deformation we find that the intrinsic residual resistivities of the h.c.p. and f.c.c. phases of lithium and the magnesium–lithium alloys are, respectively, about 10 and 15 per cent greater than that of the b.c.c. phase. The experiments show that there are large departures from Matthiesen's rule in all three phases of the alloys and in at least the b.c.c. phase of quite pure lithium. These departures account for the much larger changes in resistance that are observed when the alloys transform than are observed when lithium transforms.

A LIQUID HELIUM LEVEL INDICATOR

A. E. ROVINSKII

THE idea of using the phenomenon of the transition of pure tantalum into the superconducting state at 4·3°K for measuring the level of liquid helium was proposed by Feldmeier, and first applied by Rasor in an apparatus for continuous measurement of the quantity of liquid in a closed vessel. In a liquid level indicator with a feeler in the form of a probe it is desirable to reduce the dimensions and mass of the immersed tantalum element, so that it is advantageous to change the electrical circuit of the instrument somewhat in order to maintain a sufficiently high sensitivity.

Résumés

LA VARIATION DE LA DENSITE DE L'AZOTE ET DE L'OXYGENE LIQUIDE EN FONCTION DE LA PRESSION

A. VAN ITTERBEEK　　O. VERBEKE

ON a fait des mesures de variation de masse spécifique d'azote liquide et d'oxygène liquide jusqu'à 850 kg/cm². Les résultats peuvent être représentés à l'aide des équations suivantes (ρ en g/cm³, P en kg/cm²):

$$\begin{aligned}
N_2\text{: } 90{\cdot}26^\circ\text{K}; \rho &= 0{\cdot}7497+3{\cdot}493\,.\,10^{-4}P-3{\cdot}431\,.\,10^{-7}P^2+\\
&\quad +0{\cdot}01713\,.\,10^{-8}P^3\\
77{\cdot}31^\circ\text{K}; \rho &= 0{\cdot}8079+2{\cdot}521\,.\,10^{-4}P-2{\cdot}031\,.\,10^{-7}P^2+\\
&\quad +0{\cdot}007995\,.\,10^{-8}P^3\\
O_2\text{: } 90{\cdot}07^\circ\text{K}; \rho &= 1{\cdot}1419+1{\cdot}969\,.\,10^{-4}P-1{\cdot}233\,P^2\,.\,10^{-7}+\\
&\quad +0{\cdot}4682\,.\,10^{-10}P^3\\
77{\cdot}35^\circ\text{K}; \rho &= 1{\cdot}1997+1{\cdot}608\,.\,10^{-4}P-0{\cdot}8078\,P^2\,.\,10^{-7}+\\
&\quad +0{\cdot}298\,.\,10^{-10}P^3
\end{aligned}$$

LA DENSITE DE L'HYDROGENE LIQUIDE SOUS SA PRESSION DE VAPEUR SATURANTE

R. D. GOODWIN　　D. E. DILLER
H. M. RODER　　L. A. WEBER

LES densités d'hydrogène para entre 17° et 32°K ont été obtenues en extrapolant aux pressions de vapeur correspondantes les isothermes du liquide comprimé nouvellement déterminées. Les résultats sont combinés avec des valeurs antérieures dans l'intervalle de 14 à 20°K et comparés avec l'hydrogène normal à l'aide des relations densité–température.

LIQUEFACTION DE L'HYDROGENE A PETITE ECHELLE

B. YATES　　F. E. HOARE

DESCRIPTION du procédé adopté pour réaliser un liquéfacteur de débit donné. La méthode est appliquée ici, pour obtenir 5 litres d'hydrogène liquide sans l'aide de compresseur. On trouvera dans ce texte, les détails de construction des systèmes de purification et de liquéfaction d'un appareil accessible et facile à construire, ainsi que ses performances.

TOLERANCES ASSOCIES AVEC L'OPERATION DE L'ELEMENT D'EMMAGASINAGE CROWE DANS LE MODE PAR COURANT COINCIDENT

R. V. PEACOCK

LE mode d'opération par courant coincident de l'élément d'emmagasinage Crowe est considéré. Le rapport entre les tolérances sur les paramètres de l'appareil et les courants de transmission est calculé comme fonction de la forme de la courbe de résistance adiabatique contre le courant de la traverse.

UNE METHODE DE MESURE DE LA CAPACITE THERMIQUE DE GAZ CONDENSES AU DESSUS DE LEUR POINT D'EBULLITION

A. V. VORONEL　　P. G. STRELKOV

ON a mis au point une méthode de mesure de la capacité thermique, avec agitation, à des pressions allant jusqu'à plusieurs dizaines d'atmosphères. La capacité thermique du calorimètre, d'un volume d'environ 105 cm³ et pouvant résister à 70 atmosphères, était de 13–20 pour cent de la quantité mesurée. L'agitateur magnétique, fonctionnant à basse température et haute pression, n'a pas créé de chaleur appréciable et a réduit le temps nécessaire pour obtenir l'équilibre de 1,5 à 2 fois. Des mesures expérimentales de la capacité thermique de l'azote dans la région critique ont été réalisées.

MESURE DE LA DILATATION THERMIQUE DES METAUX A BASSE TEMPERATURE

K. ANDRES

DESCRIPTION d'un appareil permettant de mesurer les dilatations thermiques à basse température. Une technique optique permet de détecter des variations de longueur de 1 Å (10^{-8} cm) sur un échantillon de 7 cm de long. Les contributions à la dilatation thermique des électrons et du réseau sont données pour les métaux Al, Pb, Ta, Nb, Mg, et W.

THERMOMETRE A RESISTANCE DE CARBONE POUR BASSES TEMPERATURES

N. N. MIKHAILOV　　A. YA. KAGANOVSKII

DESCRIPTION d'une technique de préparation à partir des goudrons de pétrole et propriétés des thermomètres à carbone pour la mesure avec grande sensibilité et reproductibilité satisfaisante des basses températures. La variation de la résistance de ces thermomètres en fonction de la température dépend de la température de combustion.

LIQUEFACTEUR D'HYDROGENE DE DEBIT 50 l./hr EN HYDROGENE LIQUIDE

A. G. ZEL'DOVICH　　YU. K. PILIPENKO

LES auteurs décrivent l'essentiel de l'utilisation et de la construction d'un liquéfacteur produisant 50 l./hr d'hydrogène normal et 30 l./hr de parahydrogène. Le liquèfacteur peut également travailler en cycle réfrigérant. Un tableau montre les possibilités de ce liquéfacteur et le résultat de la mesure des pertes.

RÉSUMÉS

EFFET DE LA TRANSFORMATION MARTENSITIQUE SUR LA RESISTANCE ELECTRIQUE DU LITHIUM ET DES ALLIAGES DILUES LITHIUM–MAGNESIUM

J. S. DUGDALE D. GUGAN

Nous avons étudié l'effet de la transformation martensitique sur la résistivité électrique du lithium et des alliages dilués lithium–magnésium. La résistivité du lithium pur, à 80° K, décroit d'environ 0,5% lors de la transformation, celle des alliages dilués diminue encore bien plus. Des expériences de cyclage thermique et de déformation mécanique nous ont permis de trouver que les résistivités intrinsèques résiduelles des phases hexagonale compacte et cubique faces centrées du lithium et des alliages lithium–magnésium sont, respectivement, 10 et 15% plus élevées que celle de la phase cubique centrée. Les expériences montrent, pour les trois phases des alliages et au moins pour la phase cubique centrée du lithium très pur, de larges écarts à la règle de Matthiesen. Ces écarts expliquent que les variations observées de la résistance sont beaucoup plus importantes lors de la transformation des alliages que lors de la transformation du lithium pur.

UN INDICATEUR A NIVEAU D'HELIUM LIQUIDE

A. E. ROVINSKII

L'idée d'utiliser la transition du tantale pur état normal—état supraconducteur, à 4,3° K, pour mesurer le niveau de l'hélium liquide fut proposée par Feldmeier et mis en application pour la première fois par Rasor, dans un appareil pour la mesure continue de la quantité de liquide contenue dans un vase clos. Pour les indicateurs de niveau liquide à *élément sensible* en forme de sonde il est souhaitable de réduire les dimensions et la masse du tantale immergé, il est par suite, recommandé de changer le circuit électrique de l'instrument, de façon à conserver une sensibilité suffisante.

Auszüge

SCHWANKUNGEN DER DICHTE VON FLÜSSIGEM STICKSTOFF UND SAUERSTOFF ALS FUNKTION DES DRUCKS

A. VAN ITTERBEEK O. VERBEKE

Der Artikel bespricht Messungen der Dichte von flüssigem Stickstoff und Sauerstoff bei Drücken bis zu 850 kg/cm². Die Resultate können analytisch durch die folgenden Gleichungen wiedergegeben werden (ρ in g/cm³, P in kg/cm²):

$$\begin{aligned}
N_2\text{: } 90{\cdot}26^\circ\text{K; } \rho &= 0{\cdot}7497+3{\cdot}493\,.\,10^{-4}P-3{\cdot}431\,.\,10^{-7}P^2+ \\
&\quad +0{\cdot}01713\,.\,10^{-8}P^3 \\
77{\cdot}31^\circ\text{K; } \rho &= 0{\cdot}8079+2{\cdot}521\,.\,10^{-4}P-2{\cdot}031\,.\,10^{-7}P^2+ \\
&\quad +0{\cdot}007995\,.\,10^{-8}P^3 \\
O_2\text{: } 90{\cdot}07^\circ\text{K: } \rho &= 1{\cdot}1419+1{\cdot}969\,.\,10^{-4}P-1{\cdot}233\,P^2\,.\,10^{-7}+ \\
&\quad +0{\cdot}4682\,.\,10^{-10}P^3 \\
77{\cdot}35^\circ\text{K: } \rho &= 1{\cdot}1997+1{\cdot}608\,.\,10^{-4}P-0{\cdot}8078\,P^2\,.\,10^{-7}+ \\
&\quad +0{\cdot}298\,.\,10^{-10}P^3
\end{aligned}$$

DIE DICHTEN VON GESÄTTIGTEM, FLÜSSIGEM WASSERSTOFF

R. D. GOODWIN D. E. DILLER
H. M. RODER L. A. WEBER

Die Dichte von Parawasserstoff von 17 bis 32°K wird durch Extrapolation der neu bestimmten Isothermen der komprimierten Flüssigkeit auf die entsprechenden Dampfdrücke erhalten. Die Ergebnisse werden mit früheren Werten für den Bereich von 14 bis 20°K kombiniert und mit normalem Wasserstoff mittels der Dichte–Temperatur–Beziehungen verglichen.

DIE VERFLÜSSIGUNG KLEINER WASSERSTOFFMENGEN

B. YATES F. E. HOARE

Es wird ein Verfahren beschrieben, das beim Entwurf eines Wasserstoffverflüssigers für eine festgelegte Verflüssigungsmenge Anwendung fand. Es wird bei einem Bedarfsfall eingesetzt, bei dem 5 l. flüssigen Wasserstoffs ohne Verwendung eines Verdichters zu erzeugen waren. Konstruktive Einzelheiten des Reinigungs- und des Verflüssigungssystems einer zugänglich und einfach gebauten Maschine sowie Leistungsziffern werden angegeben.

TOLERANZEN BEIM BETRIEB DES CROWE–SPEICHERELEMENTES NACH DEM KOINZIDENZSTROMVERFAHREN

R. V. PEACOCK

Die Arbeitsweise eines Crowe-Speicherelementes in Koinzidenzstromschaltung wird beschrieben. Der Zusammenhang zwischen den Toleranzen in den Anordnungsgrößen und dem Betriebsstrom wird berechnet in Abhängigkeit vom Verlauf der adiabaten Widerstandskurve über dem Strom in der Querschiene (cross-bar).

EIN VERFAHREN ZUR MESSUNG DER WÄRMEKAPAZITÄT VON KONDENSIERTEN GASEN ÜBER DEREN SIEDEPUNKT

A. V. VORONEL P. G. STRELKOV

Ein Verfahren zur Messung der Wärmekapazität unter Wirbelung bei Drücken bis zu einigen Zehnereinheiten von Atmosphären wurde entwickelt. Die Wärmekapazität des Kalorimeters mit einem Inhalt von ca 105 cm³ und einer Belastbarkeit bis zu 70 at lag zwischen 13–20% der gemessenen Menge. Der bei niedrigen Temperaturen und hohem Druck arbeitende Magnetwirbler führt zu keiner bemerkenswerten Erwärmung und setzt die Zeit bis zur Herstellung des Gleichgewichts um das 1,5 bis 2-fache herab. Versuchsmessungen der Wärmekapazität von Stickstoff im kritischen Gebiet wurden durchgeführt.

DIE MESSUNG DER WÄRMEDEHNUNG VON METALLEN BEI TIEFEN TEMPERATUREN

K. ANDRES

Ein Apparat zur Messung der Wärmedehnung bei tiefen Temperaturen wird beschrieben. Mit Hilfe eines optischen Verfahrens ist es

möglich, Längenänderungen in der Größe von 1 Å (10^{-8} cm) bei Proben von 7 cm Länge zu bestimmen. Es werden Ergebnisse angegeben für den Gitteranteil und den elektronischen Anteil an der Wärmedehnung von Al, Pb, Ta, Nb, Mg, und W.

KOHLEWIDERSTANDSTHERMOMETER FÜR TIEFE TEMPERATUREN

N. N. MIKHAILOV A. YA. KAGANOVSKII

DIE Technik der Herstellung von Kohlethermometern aus Oelpech zur Messung tiefer Temperaturen mit hoher Empfindlichkeit und befriedigender Reproduzierbarkeit wird beschrieben. Der Temperaturverlauf des Widerstandes dieser Thermometer wird durch die Brenntemperatur bestimmt.

EIN WASSERSTOFFVERFLÜSSIGER MIT EINEM AUSSTOSS VON 50 l./h

A. G. ZEL'DOVICH YU. K. PILIPENKO

ARBEITSWEISE und Aufbau eines Verflüssigers für 50 l./h Normal oder 30 l./h Para-Wasserstoff werden beschrieben. Es wird auf die Möglichkeit hingewiesen, die Anlage in einem Kältekreislauf zu verwenden. In einer Tabelle wird die Verflüssigungsleistung angegeben, desgleichen die gemessenen Verluste.

STANDANZEIGER FÜR FLÜSSIGES HELIUM

A. E. ROVINSKII

DIE Idee, die Sprungtemperatur von reinem Tantal bei 4,3°K zur Bestimmung des Flüssigkeitsspiegels von Helium zu verwenden, stammt von Feldmaier und wurde erstmalig von Rasor in einem Apparat angewendet, mit dem die Heliumfüllung in einem geschlossenen Behälter fortlaufend gemessen wurde. Bei einem Standanzeiger in Form einer Sonde ist es wünschenswert, Abmessung und Masse des eingetauchten Tantalfühlers zu verringern, weshalb man zweckmäßigerweise einige Änderungen an der elektrischen Schaltung des Instrumentes vornimmt, um eine ausreichend hohe Empfindlichkeit zu gewährleisten.

DER EINFLUSS DER MARTENSITUMWANDLUNG AUF DEN ELEKTRISCHEN WIDERSTAND VON LITHIUM UND NIEDERPROZENTIGEN LITHIUM-MAGNESIUM-LEGIERUNGEN

J. S. DUGDALE D. GUGAN

DER Einfluß der Martensitumwandlung auf den elektrischen Widerstand von Lithium und niederprozentigem Lithium-Magnesium-Legierungen wurde untersucht. Der Widerstand von reinem Lithium bei 80°K fällt bei der Umwandlung um etwa 0,5%, der von Legierungen beträchtlich stärker. Versuche unter Anwendung von Wärmebehandlungen und mechanischen Deformationen ergaben, daß der eigentliche Restwiderstand bei dichtester hexagonaler Packung und bei kubisch flächenzentriertem Gitter jeweils etwa 10 bis 15% höher ist als der bei kubisch raumzentriertem Gitter. Die Versuche ergaben große Abweichungen von der Mathiesen'schen Regel in allen drei Gefügearten bei den Legierungen und zumindest in der kubisch raumzentrierten Anordnung von ziemlich reinem Lithium. Diese Abweichungen erklären die wesentlich größeren Widerstandsänderungen bei der Gefügeumwandlung in Legierungen verglichen mit den bei reinem Lithium beobachteten.

Sommari

LA VARIAZIONE DELLA DENSITA' DELL'AZOTO E DELL'OSSIGENO LIQUIDI IN FUNZIONE DELLA PRESSIONE

A. VAN ITTERBEEK O. VERBEKE

SONO state eseguite misure sulla variazione del peso specifico dell'azoto e dell'ossigeno liquidi fino a 850 Kg/cm². I risultati possono essere rappresentati analiticamente dalle seguenti equazioni (ρ in g/cm³, P in Kg/cm²):

$$N_2: 90{,}26^\circ K;\ \rho = 0{,}7497 + 3{,}493 \,.\, 10^{-4} \,.\, P - 3{,}431 \,.\, 10^{-7} \,.\, P^2 + \\ + 0{,}01713 \,.\, 10^{-8} \,.\, P^3$$

$$77{,}31^\circ K;\ \rho = 0{,}8079 + 2{,}521 \,.\, 10^{-4} \,.\, P - 2{,}031 \,.\, 10^{-7} \,.\, P^2 + \\ + 0{,}007995 \,.\, 10^{-8} \,.\, P^3$$

$$O_2: 90{,}07^\circ K;\ \rho = 1{,}1419 + 1{,}969 \,.\, 10^{-4} \,.\, P - 1{,}233 \,.\, P^2 \,.\, 10^{-7} + \\ + 0{,}4682 \,.\, 10^{-10} \,.\, P^3$$

$$77{,}35^\circ K;\ \rho = 1{,}1997 + 1{,}608 \,.\, 10^{-4} \,.\, P - 0{,}8078 \,.\, 10^{-7} \,.\, P^2 + \\ + 0{,}298 \,.\, 10^{-10} \,.\, P^3$$

LA DENSITA' DELL'IDROGENO LIQUIDO SATURO

R. D. GOODWIN D. E. DILLER
H. M. RODER L. A. WEBER

SONO state ottenute le densità del para-idrogeno tra 17° e 32°K estrapolando le isoterme, determinate nuovamente, del liquido compresso alle corrispondenti pressioni di vapore. I risultati soon stati combinati con dati precedenti per l'intervallo da 14° a 20° Ke confrontati con lo idrogeno normale per mezzo delle relazioni tra densità e temperatura.

UN LIQUEFATTORE DI IDROGENO DI PICCOLE DIMENSIONI

B. YATES F. E. HOARE

SI da una descrizione del procedimento adottato nel progettare un liquefattore di idrogeno per produrre una quantità di liquido desiderata. La procedura è applicata al caso ove siano richiesti 5 lt di

idrogeno liquido senza l'uso di un compressore. Sono inclusi i dettagli costruttivi dei sistemi di purificazione e liquefazione di una macchina accessibile nonchè facilmente costruibile, insieme alle curve di prestazione.

LE TOLLERANZE ASSOCIATE AL FUNZIONAMENTO DELLA PILA DI CROWE NEL MODO CORRENTE COINCIDENTE

R. V. PEACOCK

Si descrive il modo corrente coincidente di funzionamento nella pila di Crowe. E' calcolata la relazione tra le tolleranze sui parametri del dispositivo e le correnti in funzione della forma della curva adiabatica della resistenza funzione della corrente della barra di collegamento.

LA MISURA DELLA ESPANSIVITA' TERMICA DEI METALLI ALLE BASSE TEMPERATURE

K. ANDRES

E' descritta un apparecchiatura per la misura della espansività termica a basse temperature. Usando di una tecnica ottica, è possibile di rivelare variazioni di lunghezza di 1 Å (10^{-8} cm) in un campione lungo 7 cm. I risultati sono dati in vista dei contributi reticolare ed elettronico alla espansività termica nei metalli Al, Pb, Ta, Mg, e W.

UN TERMOMETRO A RESISTENZA DI CARBONE PER BASSE TEMPERATURE

N. N. MIKHAILOV A. YA. KAGANOVSKII

Sono descritte la tecnica di preparazione dal bitume di petrolio e le proprietà di termometri a carbone, per misure di basse temperature, con alta sensibilità e soddisfacente riproducibilità. L'andamento della dipendenza della temperatura dalla resistenza di questi termometri è determinata dalla temperatura di cottura.

UN LIQUEFATTORE DI IDROGENO CON UNA PRODUZIONE DI 50 lt/ora DI IDROGENO LIQUIDO

A. G. ZEL'DOVICH YU. K. PILIPENKO

Si descrivono le fondamentali caratteristiche di funzionamento e costruzione di un liquefattore che produce 50 lt/ora di liquido normale, ovvero 30 lt/ora di *para*-idrogeno. E' illustrata la possibilità di funzionamento del liquefattore in ciclo di refrigerazione. E' data una tabella di prestazione del liquefattore e inoltre i risultati sulle misure di perdita.

L'EFFETTO DELLA TRASFORMAZIONE MARTENSITICA SULLA RESISTENZA ELETTRICA DEL LITIO E DELLE LEGHE DILUITE LITIO–MANGANESE

J. S. DUGDALE D. GUGAN

E' stato studiato l'effetto della trasformazione martensitica sulla resistività elettrica del litio e delle leghe diluite litio–manganese. La resistività del litio puro a 80° K decresce approssimativamente del 0,5% durante la trasformazione e quella della lega decresce notevolmente di più. Eseguendo variazioni cicliche di temperatura e deformazioni meccaniche si trova che le resistività residue intrinseche delle fasi h.c.p. e f.c.c. del litio e delle leghe magnesio–litio sono circa il 10 e 15% rispettivamente, maggiori della fase b.c.c. Gli esperimenti mostrano che ci sono grandi discordanze dalla regola di Matthiesens in tutte e tre le fasi delle leghe ed in almeno nella fase b.c.c. del litio abbastanza puro. Queste discordanze spiegano come mai le variazioni della resistenza, osservate quando le leghe si trasformano, sono molto più grandi di quelle osservate quando si trasforma il litio.

UN INDICATORE DI LIVELLO PER ELIO LIQUIDO

A. E. ROVINSKII

L'idea di usare il fenomeno di transizione nello stato superconduttore a 4,3° K del tantalio puro per misurare il livello dell'elio liquido fu proposto da Feldmeier, e per la prima volta applicato da Rasor in un apparecchio per la misura continua della quantità di liquido in un recipiente chiuso. In un indicatore di livello del liquido, con l'elemento sensibile in forma di sonda, è desiderabile di ridurre le dimensioni e la massa dell'elemento di tantalio immerso, cosicchè è vantaggioso variare un poco il circuito elettrico dello strumento al fine di mantenere una sensibilità sufficientemente alta.

Резюме

ИЗМЕНЕНИЕ ПЛОТНОСТИ ЖИДКОГО АЗОТА И КИСЛОРОДА КАК ФУНКЦИЯ ДАВЛЕНИЯ

A. VAN ITTERBEEK O. VERBEKE

Измерилось изменение удельного веса жидкого азота и жидкого кислорода до 850 кг/см². Результаты можно представлять аналитически путем следующего уравнения (ρ в г/см³, P в кг/см²):

$$N_2:\ 90{\cdot}26^\circ\mathrm{K};\ \rho = 0{\cdot}7497 + 3{\cdot}493\,.\,10^{-4}\,P - 3{\cdot}431\,.\,10^{-7}\,P^2 + 0{\cdot}01713\,.\,10^{-8}\,P^3$$

$$77{\cdot}31^\circ\mathrm{K};\ \rho = 0{\cdot}8079 + 2{\cdot}521\,.\,10^{-4}\,P - 2{\cdot}031\,.\,10^{-7}\,P^2 + 0{\cdot}007995\,.\,10^{-8}\,P^3$$

$$O_2:\ 90{\cdot}07^\circ\mathrm{K};\ \rho = 1{\cdot}1419 + 1{\cdot}969\,.\,10^{-4}\,P - 1{\cdot}233\,.\,10^{-7}\,P^2 + 0{\cdot}4682\,.\,10^{-10}\,P^3$$

$$77{\cdot}35^\circ\mathrm{K};\ \rho = 1{\cdot}1997 + 1{\cdot}608\,.\,10^{-4}\,P - 0{\cdot}8078\,.\,10^{-7}\,P^2 + 0{\cdot}298\,.\,10^{-10}\,P^3$$

ПЛОТНОСТИ НАСЫЩЕННОГО ЖИДКОГО ВОДОРОДА

R. D. GOODWIN **D. E. DILLER**
H. M. RODER **L. A. WEBER**

Получаются плотности параводорода от 17° до 32° К путем экстраполяции ного-определенных изотерм сжатой жидкости до соответствующих давлений пара. Результаты соединяются с раньшими данными в пределах 14° до 20° К и сравниваются с нормальным водородом путем соотношений плотность — температура.

ОЖИЖАНИЕ ВОДОРОДА В МАЛОМ МАСШТАБЕ

B. YATES **F. E. HOARE**

Описание метода при конструкции ожижателя водорода, который производил бы требованную мощность. Метод используется для случая, когда требуется выход 5 л жидкого водорода без употребления компрессора. Присоединены конструктивные детали системы очистки и ожижания машины, которая была бы доступная и подходящая для конструкции, так же как и технические значения.

ДОПУСК ПРИ ЭКСПЛУАТАЦИИ АККУМУЛЯТОРНОГО ЭЛЕМЕНТА КРОВЕ В ВИДЕ С СОВПАДЕНИЕМ ТОКА

R. V. PEACOCK

Обсуждается вид эксплуатации с совпадением тока аккумуляторного элемента Крове. Вычислено отношение между допусками параметров установки и приводными токами в функции формы адиабатической кривой сопротивления в зависимости от тока ярма.

МЕТОДИКА ИЗМЕРЕНИЯ ТЕПЛОЕМКОСТИ КОНДЕНСИРОВАННЫХ ГАЗОВ ВЫШЕ ИХ ТОЧКИ КИПЕНИЯ

A. V. VORONEL **P. G. STRELKOV**

Разработана методика измерения теплоемкости с перемешиванием при давлениях до нескольких десятков *ат*. Теплоемкость калориметра, выдерживающего 70 *ат* в объеме ~ 105 *см*³, составляла от 13 до 20% измеряемой величины. Магнитная мешалка, работающая при низкой температуре и повышенном давлении, не создает заметного притока тепла и сокращает время установления равновесия в 1,5÷2 раза. Произведены пробные измерения теплоемкости азота в критической области.

ИЗМЕРЕНИЕ ТЕРМИЧЕСКОГО РАСЩИРЕНИЯ МЕТАЛЛОВ ПРИ НИЗКИХ ТЕМПЕРАТУРАХ

K. ANDRES

Описывается аппарат для измерения термического расщирения при низких температурах. С помощью оптических методов можно обнаружить в образцах длиной в 7 см. изменения длины 1Å (10^{-8} см). Показаны результаты для решетки и вклады электронов для термического расщирения в металлах Al, Pb, Ta, Nb, Mg и W.

УГОЛЬНЫЕ ТЕРМОМЕТРЫ СОПРОТИВЛЕНИЯ ДЛЯ НИЗКИХ ТЕМПЕРАТУР

N. N. MIKHAILOV **A. YA. KAGANOVSKII**

Описаны технология изготовления и свойства угольных термометров из нефтяного пека для измерения низких температур, обладающих высокой чувствительностью и удовлетворительной воспроизводимостью. Характер температурной зависимости сопротивления этих термометров определяется температурой обжига.

ВОДОРОДНЫЙ ОЖИЖИТЕЛЬ ПРОИЗВОДИТЕЛЬНОСТЬЮ 50 *л/ч* ЖИДКОГО ВОДОРОДА

A. G. ZEL'DOVICH **YU. K. PILIPENKO**

Описан принцип работы и конструкция ожижителя производительностью 50 *л/ч* нормального или 30 *л/ч* параводорода. Отмечается возможность работы ожижителя в цикле рефрижератора. Приведена таблица показателей работы ожижителя, а также результаты замера потерь.

ВЛИЯНИЕ МАРТЕНСИТНОГО ПЕРЕХОДА НА ЭЛЕКТРИЧЕСКОЕ СОПРОТИВЛЕНИЕ ЛИТИЯ И СПЛАВОВ МАГНИЯ С МАЛОЙ ПРИМЕСЬЮ ЛИТИЯ

J. S. DUGDALE **D. GUGAN**

Исследовалось влияние мартенситного перехода на электрическое сопротивление лития и сплавов магния с малой примесью лития. Сопротивление чистого лития при 80° К при переходе понижается приблизительно на 0,5%, в то время как сопротивление сплавов понижается более значительно. Посредством опытов по термической циклизации и механической деформации было найдено, что внутренние остаточные сопротивления кристаллических фаз лития и сплавов: гексагональной с плотной упаковкой и кубической гранецентрированной не превышают больше чем на 10 и 15% соответственно внутреннее остаточное сопротивление фазы с кубической объемноцентрированной решеткой. Эксперименты показали, что у всех трех фаз сплавов и у чистого лития по крайней мере в фазе с кубической объемноценрированной решеткой существуют большие отклонения от правила Матиесена. Этими отклонениями объясняется тот факт, что при переходе в сплавах наблюдаются гораздо большие изменения сопротивления, чем те, которые возникают при переходе в чистом литии.

ИНДИКАТОР УРОВНЯ ЖИДКОГО ГЕЛИЯ

A. E. ROVINSKII

Идея использования явления перехода чистого тантала в сверхпроводящее состояние при 4,3° *К* для измерения уровня жидкого гелия предложена Фельдмейером [1] и применена впервые Серином [2] в устройстве для непрерывного измерения количества жидкости в закрытом сосуде. В индикаторе уровня жидкости с датчиком в виде щупа желательно всемерно уменьшить размер и массу погружаемого танталового элемента, поэтому для сохранения достаточно высокой чувствительности целесообразно несколько изменить электрическую схему прибора.

The Variation of the Density of Liquid Nitrogen and Liquid Oxygen as a Function of Pressure

A. Van Itterbeek and O. Verbeke
Institut voor Lage Temperaturen en Technische Fysica, Louvain

Received 8 July 1961

COMPLETING our systematic investigation on the P, ρ, T relations of liquefied gases[1–3] some measurements have been carried out up to 850 kg/cm^2 on liquid nitrogen and liquid oxygen.

Only the variation of $(\partial\rho/\partial P)_T$ with pressure is measured, after integrating twice with respect to pressure and using as integrating constants values of the specific weights ρ and $(\partial\rho/\partial P)_T$ of earlier measurements at zero pressure, we obtained the density as a function of pressure.

Our apparatus is practically the same as that used for our earlier measurements; only an adaptation to the high pressure region is made.[1, 2]

The results for nitrogen are represented in Table 1 and graphically represented in Figure 1.

Table 1. Specific Gravity of Nitrogen as a Function of Pressure

T (°K)	P (kg/cm^2)	ρ (g/cm^3)
90·26	842·3	0·9030
	648·3	0·8782
	496·2	0·8599
	375·2	0·8423
	279·9	0·8232
	199·1	0·8073
	131·0	0·7901
	0	0·7497
77·31	574·2	0·9030
	431·0	0·8882
	319·2	0·8705
	227·1	0·8558
	150·3	0·8419
	82·0	0·8274
	0	0·8079

These two isotherms are evaluated as third degree curves with the aid of the least-squares method:

$$90{\cdot}26^\circ\,\mathrm{K};\ \rho = 0{\cdot}7497+3{\cdot}493.10^{-4}P-3{\cdot}431.10^{-7}P^2+ \\ +0{\cdot}01713.10^{-8}P^3$$

$$77{\cdot}31^\circ\,\mathrm{K};\ \rho = 0{\cdot}8079+2{\cdot}521.10^{-4}P-2{\cdot}031.10^{-7}P^2+ \\ +0{\cdot}007995.10^{-8}P^3$$

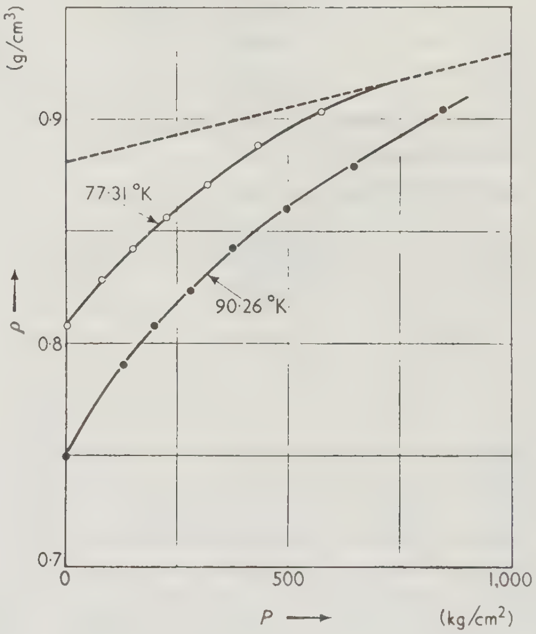

Figure 1. Specific weight of nitrogen as a function of pressure

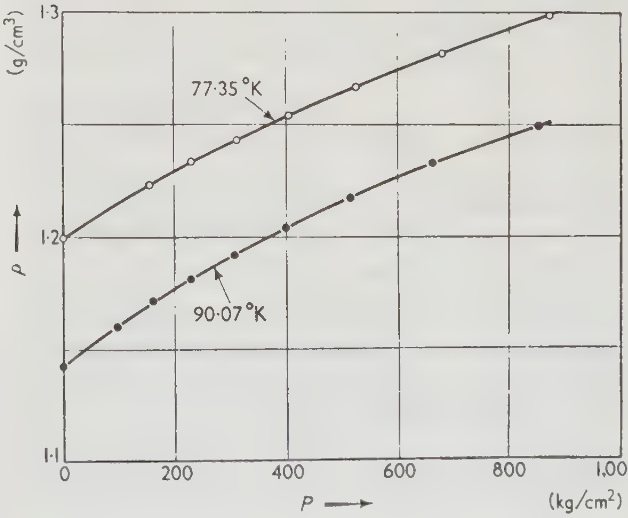

Figure 2. Specific weight of oxygen as a function of pressure

Table 2. Specific Weight of Oxygen as a Function of Pressure

T (°K)	P (kg/cm²)	ρ (g/cm³)
90·07	851·8	1·2490
	662·9	1·2322
	516·0	1·2170
	400·0	1·2039
	308·2	1·1918
	230·0	1·1808
	162·0	1·1712
	98·0	1·1597
77·35	874·5	1·2984
	680·0	1·2811
	527·0	1·2663
	406·0	1·2537
	312·8	1·2424
	232·0	1·2338
	158·2	1·2229

The calculated curves are:

$$90{\cdot}07^{\circ}\,\mathrm{K};\ \rho = 1{\cdot}1419+1{\cdot}969\,.\,10^{-4}P-1{\cdot}233P^{2}\,.\,10^{-7}+ +0{\cdot}4682\,.\,10^{-10}P^{3}$$

$$77{\cdot}35^{\circ}\,\mathrm{K};\ \rho = 1{\cdot}1997+1{\cdot}608\,.\,10^{-4}P-0{\cdot}8078P^{2}\,.\,10^{-7}+ +0{\cdot}298\,.\,10^{-10}P^{3}$$

The experimental results obtained for oxygen are represented in Table 2 and graphically represented in Figure 2.

Earlier measurements up to 150 kg/cm^2 suggested a linear dependence of specific weight with pressure. However, more accurate measurements showed a real dependence of $(\partial\rho/\partial P)_T$ with pressure.

Going up to the high pressure domain it appears very clearly a dependence of $(\partial\rho/\partial P)_T$ from pressure.

We express our thanks to Miss Deprit of the Centre for Electronic Calculations directed by Professor G. Lemaitre of the University of Louvain, who very kindly consented to calculate the analytic equation representing our measurements. We also express our sincere thanks to the Belgian Ministry of Education for the financial support of this research which was given to our laboratory as a division of the National Centre for Research at Low Temperatures.

REFERENCES

1. Van Itterbeek, A., and Verbeke, O. *Physica* **26**, 931 (1960)
2. Van Itterbeek, A., and Verbeke, O. *Cryogenics* **1**, 77 (1960)
3. Van Itterbeek, A., and Verbeke, O. *Physica*. To be published

The Densities of Saturated Liquid Hydrogen

R. D. Goodwin, D. E. Diller, H. M. Roder, and L. A. Weber

National Bureau of Standards, Boulder, Colorado

Received 12 July 1961

THIS laboratory is engaged in a programme for the determination of thermostatic, thermodynamic, and transport properties of *para*-hydrogen, emphasizing high densities. Reported here are new data for the density of saturated liquid *para*-hydrogen from boiling point to critical point. A review of hydrogen properties[1] includes densities of normal hydrogen from triple to critical points and of *para*-hydrogen up to the boiling point.[2] More recent determinations of vapour pressures and critical constants have been made for both hydrogen modifications.[3–5] Values of constants used in our computations are given in Table 1. To avoid confusion with amagat density, ρ, the symbol σ is employed for density in gram-moles per cubic centimetre. In following sections two approximate methods for representing the data are mentioned briefly, while two more-accurate methods are given in greater detail.

Table 1. Constants Used for Computations

		para	normal
T_c	=	32·984$^{(4)}$	33·180$^{(1)}$
T_t	=	13·803$^{(1)}$	13·947$^{(1)}$
$\sigma_t \times 10^3$	=	38·2029$^{(1)}$	38·3024$^{(1)}$
$\sigma_c \times 10^3$	=	15·2672$^{(4)}$	14·9370$^{(1)}$

Experimental

The Reichsanstalt method of Holborn and colleagues,[6] exemplified by recent work at the Ohio State University,[7] was employed to obtain the *PVT* isotherms.[8]

Saturated liquid densities are obtained by extrapolating forthcoming isotherms for compressed liquid *para*-hydrogen to the corresponding vapour pressures.[9] The 20° K equilibrium hydrogen (0·21 per cent *ortho*-hydrogen), herein called simply *para*-hydrogen, was produced by flow over iron oxide catalyst while filling the densitometer, and was confirmed by vapour pressure measurements.[3] The isotherms are characterized by reproducibility and accuracy for pressure and for temperature of about 1 part in 10,000. Platinum resistance thermometry, through calibration by the NBS temperature physics section, rests upon the NBS low temperature scale of Hoge and Brickwedde[10] as revised in 1955 by subtracting 0·01° C from the former temperatures for fixed points and throughout the range. For density, precision and accuracy are 2 and 10 parts in 10,000 respectively, the latter figure arising from the several volumetric determinations. By accuracy is meant here the authors' estimate of the probable total cumulative effect of all the calibration, adjustment, and observational errors.

To achieve the extrapolations, compressed liquid pressures are represented by polynomials in the density along isotherms, employing least-squares methods with a high speed digital computer. The tedious smoothing contemplated for the temperature dependence of the coefficients of these polynomials has not been applied here as the effect would not be significant. By means of the computer, an iteration procedure is applied for extraction of the density corresponding to an assigned (vapour) pressure. Accuracy of the extrapolations is not simply established. On some isotherms, data points occur virtually at the coexistence boundary, while on others they may be removed within limits ranging from 7·5 per cent of the saturation density at 32° to 2·0 per cent of the saturation density at 17° K. An important criterion therefore is the self-consistency of the set of densities obtained.

Results for *para*-hydrogen from 17° to 32° are presented in the lower portion of column 3, Table 2. The upper portion contains previously determined low pressure densities, the smoothed results selected being within the original experimental deviations.[2] Normal hydrogen densities are given for comparison in column 2 of Table 3. The upper group is from reference 2, while the lower group is from reference 11 as adjusted in reference 1.

Representation of the Data

Four expressions for representing the data have been examined.

(1) An approximate relation for the density of saturated liquid *para*-hydrogen up to 31° K is

$$(\sigma - \sigma_c) = -0{\cdot}001810 + 0{\cdot}0092597(T_c - T)^{1/3} \quad \ldots (1)$$

The simplicity of this expression renders it useful for some applications. In the range 14° to 31° maximum deviation in σ is $-0{\cdot}15$ per cent at 22° K. The deviation at 32° is $-0{\cdot}51$ per cent. This equation clearly does not extend to the critical temperature.

(2) A well known relation is derived from the Verschaffelt equation and law of the rectilinear diameter,[12]

$$2\sigma/\sigma_t = 1 - (1 - 2\sigma_c/\sigma_t)\,\theta + (1 - \theta)^n \quad \ldots (2)$$

where $$\theta \equiv (T-T_t)/(T_c-T_t)$$

Subscripts t and c refer to triple point and critical point, respectively, and $n = \frac{3}{10}$ or $n = \frac{1}{3}$. Equation (2) may be rearranged to the linear form

$$(\sigma-\sigma_c)/(T_c-T)^n = a+b(T_c-T)^{1-n} \qquad \dots (2a)$$

where a and b are constants.

The data plots of equation (2a) for *para*-hydrogen are markedly non-linear. Percentage deviations of σ calculated by equation (2) for $n = \frac{3}{10}$ are presented in Figure 1, relative to smoothed data from Table 2, column 4.

(3) A linear plot for experimental data is a valuable tool for its examination. There is a useful function for saturated liquid densities, valid nearly to the critical point,[13]

$$(T_c-T)^m/(\sigma-\sigma_c) = A+BT \qquad \dots (3)$$

where $m = \frac{4}{10}$. For *para*-hydrogen in the range 14° to 32° the function on the left-hand side of equation (3) varies only 7 per cent, while density varies 50 per cent of the mean value. E. H. Brown has shown at this laboratory that equation (3) is equivalent to

$$(1-\theta)^m/\Sigma = 1+\alpha\theta \qquad \dots (3a)$$

Table 2. Densities of Saturated Liquid *para*-Hydrogen

T (°K)	VP (atm)	σ (exper.)	σ (calc.)	$100\frac{\Delta\sigma}{\sigma}$
13·803		0·0382029	0·0381998	0·01
13·990		0·0381286	0·0381232	0·01
14·000	0·0778		0·0381191	
14·990		0·0377102	0·0377030	0·02
15·000	0·1327		0·0376987	
15·990		0·0372633	0·0372631	0·00
16·000	0·2130		0·0372586	
16·991		0·0367931	0·0368012	−0·02
17·992		0·0362989	0·0363159	−0·05
18·993		0·0357845	0·0358047	−0·06
19·995		0·0352509	0·0352642	−0·04
17·000	0·3250	0·0368288	0·0367970	0·09
18·000	0·4758	0·0362733	0·0363119	−0·11
19·000	0·6726	0·0357945	0·0358010	−0·02
20·000	0·9228	0·0352753	0·0352615	0·04
20·268	1·0000		0·0351115	
21·000	1·2341	0·0346992	0·0346898	0·03
22·000	1·6142	0·0341069	0·0340821	0·07
23·000	2·0714	0·0334638	0·0334330	0·09
24·000	2·6135	0·0327268	0·0327363	−0·03
25·000	3·2487	0·0319869	0·0319835	0·01
26·000	3·9854	0·0311607	0·0311635	−0·01
27·000	4·8315	0·0302443	0·0302610	−0·06
28·000	5·7950	0·0292449	0·0292534	−0·03
29·000	6·8890	0·0281325	0·0281060	0·09
30·000	8·1210	0·0267471	0·0267588	−0·04
31·000	9·5000	0·0250788	0·0250921	−0·05
32·000	11·0470	0·0227923	0·0227821	0·04
32·400			0·0214352	
32·700			0·0199780	
32·900			0·0182832	
32·984	12·7700	0·0152672		

where

$$\Sigma \equiv (\sigma-\sigma_c)/(\sigma_t-\sigma_c)$$

and α is a small arbitrary constant. For several cryogenic fluids the function on the left-hand side of equation (3a) varies linearly with T up to about $\theta = 0{\cdot}95$. It then must fall sharply to zero with eventual infinite slope at $\theta = 1$. Errors of several per cent in σ may be expected for $\theta > 0{\cdot}95$. Figure 2 presents data from Tables 2 and 3 plotted in the co-ordinates of equation (3). Filled circles represent new results of this report. Table 4 presents values for A and B of equation (3) determined by least squares, and the values for α of equation (3a) computed from the relation

$$\alpha = (T_c-T_t)/(A/B+T_t) \qquad \dots (3b)$$

(4) Data in the co-ordinates of equation (1) indicate a sigmoid plot, hence a polynomial in $(T_c-T)^{1/3}$. For trifluoromethane[14] and for nitrogen,[15] closely spaced data right up to the critical point have been represented accurately by

Table 3. Densities of Saturated Liquid Normal Hydrogen

T (°K)	σ (exper.)	σ (calc.)	$100\frac{\Delta\sigma}{\sigma}$
13·947	0·0383024	0·0383038	−0·00
13·990	0·0382860	0·0382861	−0·00
14·000		0·0382819	
14·990	0·0378680	0·0378653	0·01
15·000		0·0378609	
15·990	0·0374230	0·0374236	−0·00
16·000		0·0374190	
16·990	0·0369530	0·0369594	−0·02
17·000		0·0369546	
17·990	0·0364610	0·0364707	−0·03
18·000		0·0364656	
18·990	0·0359500	0·0359552	−0·01
19·000		0·0359498	
19·990	0·0354200	0·0354101	0·03
20·000		0·0354045	
20·380	0·0352100	0·0351889	0·06
21·000		0·0348263	
21·990	0·0342340	0·0342178	0·05
22·000		0·0342114	
23·000		0·0335549	
23·990	0·0328390	0·0328580	−0·06
24·000		0·0328506	
25·000		0·0320908	
25·990	0·0312540	0·0312737	−0·06
26·000		0·0312650	
27·000		0·0303590	
27·990	0·0293600	0·0293629	−0·01
28·000		0·0293522	
29·000		0·0282131	
29·990	0·0269260	0·0269034	0·08
30·000		0·0268889	
31·000		0·0252776	
31·990	0·0231420	0·0231499	−0·03
32·000		0·0231238	
33·000		0·0190252	
33·180	0·0149365		

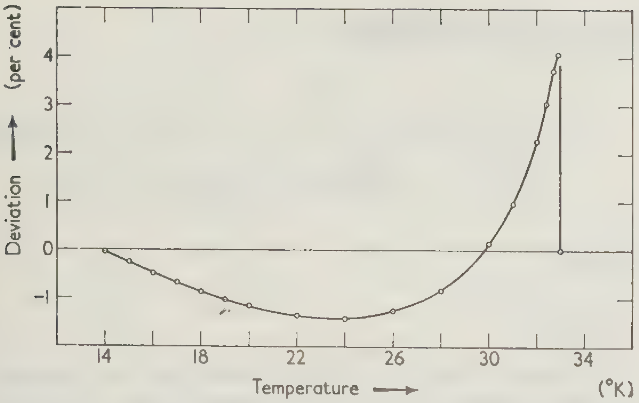

Figure 1. Relative deviations of equation (2). Results calculated by equation (2) minus smoothed data of Table 2, column 4, derived from equation (4)

$$(\sigma-\sigma_c) = \sum_{n=1}^{4} \alpha_n (T_c-T)^{n/3} \qquad \ldots (4)$$

Table 5 presents values for the constants of equation (4), determined by least squares. The calculated results from equation (4), with corresponding deviations in per cent of σ, are presented by Tables 2 and 3. The density of *para*-hydrogen is less than that of normal hydrogen at all temperatures. Figure 3 is an outline for the *para*-hydrogen results.

Table 4. Constants for Equations (3) and (3a)

		para	normal
A	=	+0·148 434	+0·145 985
B	=	−0·000 450 198	−0·000 447 314
α	=	−0·060 717	−0·061 563

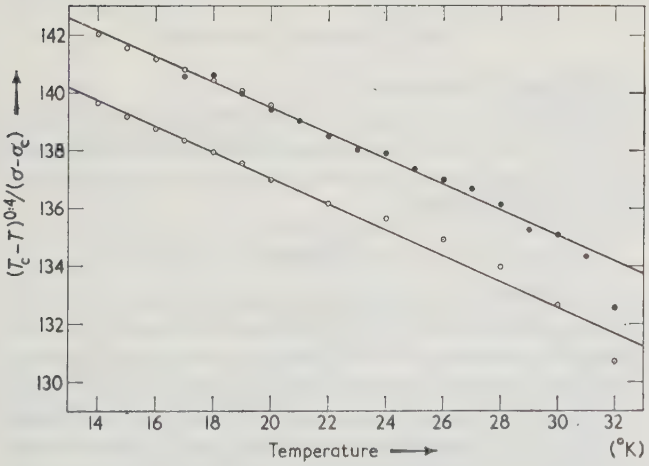

Figure 2. Density function. Open circles of the upper curve for para-*hydrogen are smoothed data from reference 2; filled circles are new data of this report. Data of the lower curve for normal hydrogen up to 20·390° K as smoothed from reference 2; above 21° K from reference 11 as adjusted in reference 1*

Table 5. Constants for Equation (4)

		para	normal
$a_1 \times 10^3$	=	+6·267 5345	+6·646 6259
$a_2 \times 10^3$	=	+1·497 3511	+1·026 5796
$a_3 \times 10^3$	=	−0·183 0690 3	+0·085 4904 60
$a_4 \times 10^3$	=	−0·020 6931 81	−0·067 0342 34

Mr. Thomas Strobridge contributed generously both advice and operable programmes for the digital computer. He brought to our attention reference 14. Continuing encouragement from R. J. Corruccini and R. B. Scott has made possible the programme on hydrogen properties.

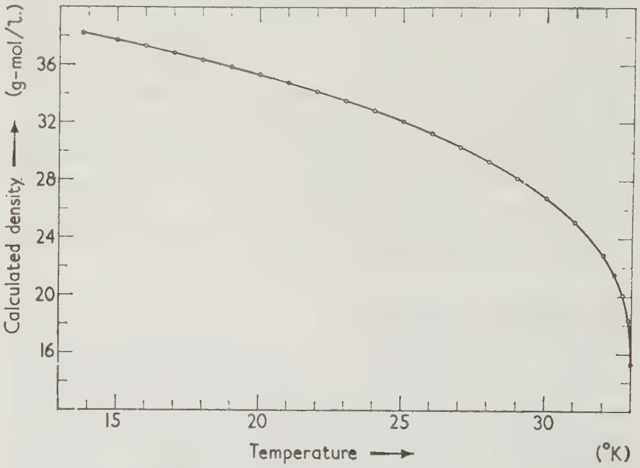

Figure 3. Outline of density–temperature relation for saturated liquid para-*hydrogen*

REFERENCES

1. Woolley, H. W., Scott, R. B., and Brickwedde, F. G. *J. Res. nat. Bur. Stand.* **41,** 379 (1948)
2. Scott, R. B., and Brickwedde, F. G. *J. chem. Phys.* **5,** 736 (1937)
3. Hoge, H. J., and Arnold, R. D. *J. Res. nat. Bur. Stand.* **47,** 63 (1951)
4. Hoge, H. J., and Lassiter, J. W. *J. Res. nat. Bur. Stand.* **47,** 75 (1951)
5. White, D., Friedman, A. S., and Johnston, H. L. *J. Amer. chem. Soc.* **72,** 3565, 3927 (1950)
6. Holborn, L., and Otto, J. *Z. Phys.* **38,** 359 (1926)
7. Johnston, H. L., Keller, W. E., and Friedman, A. S. *J. Amer. chem. Soc.* **76,** 1482 (1954)
8. Apparatus description and *PVT* data submitted to *J. Res. nat. Bur. Stand.* late in 1961
9. 'Tables of Thermal Properties of Gases.' *N.B.S. Circ.* 564, p. 287 (Ed. Hilsenrath, J., 1955)
10. Hoge, H. J., and Brickwedde, F. G. *J. Res. nat. Bur. Stand.* **22,** 351 (1939)
11. Mathias, E., Crommelin, C. A., and Kamerlingh Onnes, H. *Commun. phys. Lab. Univ. Leiden* 154b (1921)
12. Scott, A. F., and Dillon, R. *J. chem. Phys.* **17,** 1179 (1949)
13. Scott, R. B. Private communication (25 January 1961)
14. Hou, Y. C., and Martin, J. J. *Amer. Inst. chem. Engrs J.* **5** (1), 125 (1959)
15. Strobridge, T. Unpublished, this laboratory

Small Scale Hydrogen Liquefaction

B. Yates Bradford Institute of Technology
F. E. Hoare University of Leeds

Received 21 July 1961

THE refrigerants available in a number of laboratories which have entered the low temperature field in recent years are often limited to liquid helium and liquid nitrogen. A small supply of liquid hydrogen would provide a valuable extension of the facilities available in these laboratories, as well as providing a more economical alternative to liquid helium, to workers whose requirements do not call for temperatures below 10° K. For these reasons the design of a small and accessible hydrogen liquefier, of simple construction, is presented here in a form which will enable other workers to design liquefiers with outputs to meet their particular requirements.

The definitions of the symbols used in the equations are collected in the Appendix.

Basic initial considerations

From a knowledge of the variation of the enthalpy of hydrogen with temperature and pressure it is possible to calculate the rate of liquefaction at an expansion valve situated at the end of a countercurrent interchanger carrying gas under known conditions from the equation

$$H_i = H_o(1-E)+H_L E \qquad \ldots(1)$$

Using data from the work of Woolley, Scott, and Brickwedde,[1] and assuming a 100 per cent efficient interchanger, operating with a fore temperature of 70° K, calculation showed that an average of about 0·68 l. of liquid could be expected from a 165 ft^3 cylinder, the pressure of which fell from 120 to 30 atm during the liquefaction process. Allowing for the gas passed before the onset of liquefaction eight such cylinders are used in producing approximately 5 l. of liquid hydrogen.

The purification system

A schematic flow diagram of the liquefier is shown in Figure 1. The gas flows first through the dryer, which consists of a copper tube of 2½ in. o.d., 1 s.w.g. wall thickness, and length 18 in., containing silica gel. It then flows through the 'cleaner'. This consists of a similar, though shorter, tube. This contains packed nickel gauze and is immersed in liquid nitrogen, its purpose being to remove impurities with relatively high boiling points. From here the gas passes through two purifiers containing a total of about 300 g of granular activated charcoal. These take the form of helices, immersed in liquid nitrogen, each helix being made from a 9 ft length of ⅝ in. o.d. copper tubing of 13 s.w.g. wall thickness. Plugs of nickel gauze are included at the entries and exits of the dryer and purifiers, in order to prevent pieces of silica gel or charcoal from being dislodged, while a further nickel gauze filter is included at the position shown, as an additional precautionary measure. The silica gel and charcoal are both reactivated before a run by being pumped and baked.

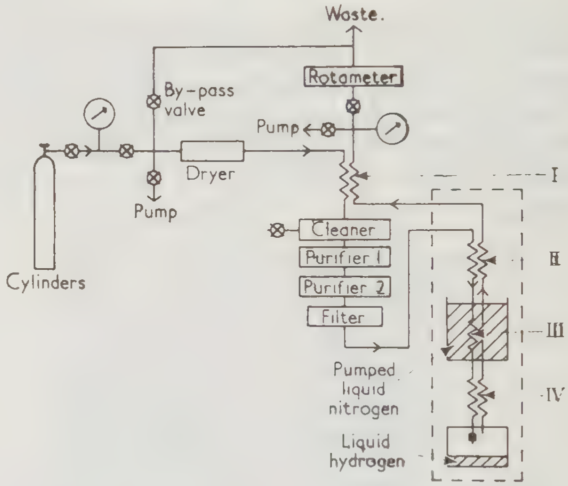

I. First interchanger
II. Second interchanger
III. Third interchanger
IV. Final interchanger

Figure 1. Schematic flow diagram

Interchanger dimensions

(1) *The final interchanger.* Assuming a rate of flow of 8·5 m^3/hr (i.e. 300 ft^3/hr), measured at room temperature before liquefaction commences, the corresponding mass rate of flow would be

$$0{\cdot}2076\ \text{g/sec} \qquad \ldots(2)$$

Assuming that the high pressure gas was cooled to 70° K before entering the final interchanger, for a 100 per cent efficient interchanger the mass of gas passing back through the low pressure side would increase from 0·1609 to 0·1900 g/sec as the high pressure fell from 120 to 30 atm.

Largely for simplicity of construction all interchangers have been constructed according to the tube-on-tube form, i.e. the high and low pressure tubes are soldered together along their lengths, and coiled into helices, as indicated in Figure 2. The relevant details of the interchangers are summarized in Table 1.

Table 1. Interchanger Dimensions

Interchanger	High pressure tubes		Low pressure tubes		Length (cm)	Material
	Outer diam. (in.)	Wall thickness (s.w.g.)	Outer diam. (in.)	Wall thickness (s.w.g.)		
1st	$\frac{1}{8}$	26	$\frac{1}{4}$	22	300	Copper
2nd	$\frac{3}{32}$	26	$\frac{5}{32}$	26	200	70% Copper–30% Nickel
3rd	$\frac{1}{8}$	26			100	Copper
Final	$\frac{3}{32}$	26	$\frac{5}{32}$	26	200	70% Copper–30% Nickel

The thermal exchange coefficients are calculated in the following manner.

(i) The convection coefficient per unit length, h_L. In accordance with the definition of this quantity,

$$h_L = 0{\cdot}10\bar{C}_p\bar{\eta}^{1/5}\left(\frac{1}{D}\cdot\frac{dm}{dt}\right)^{4/5} \qquad \ldots (3)$$

Substitution of the appropriate numerical data into this equation, corresponding to the situation where the high pressure tube is carrying gas at 120 atm pressure, gives

$$h_L = 6{\cdot}233\times10^{-2}\,\text{cal/deg. cm sec}$$

for the high pressure tube. The corresponding value for each of the low pressure tubes is

$$h'_L = 0{\cdot}984\times10^{-2}\,\text{cal/deg. cm sec}$$

(ii) The overall coefficient of heat transfer per unit length, $\bar{U}_L$.

Since there are two low pressure tubes in parallel, the appropriate form of the expression for $\bar{U}_L$ in the present case is

$$\frac{1}{\bar{U}_L} = \frac{1}{h_L}+\frac{1}{2h'_L}$$

neglecting the very small effect of the metal wall separating the gas streams. Therefore

$$\bar{U}_L = 1{\cdot}496\times10^{-2}\,\text{cal/deg. cm sec} \qquad \ldots (4)$$

The length of the interchanger is calculated in this manner. Defining the efficiency of the interchanger as

$$\epsilon = \frac{\theta'_H-\theta'_C}{\theta_H-\theta'_C} \qquad \ldots (5)$$

it may be shown that this is related to the overall coefficient of heat transfer per unit length by the equation

$$\bar{U}_L L = \frac{m_H m_L \bar{C}_H \bar{C}_L}{m_H \bar{C}_H - m_L \bar{C}_L}\ln\left(\frac{1-\epsilon . m_L \bar{C}_L/m_H \bar{C}_H}{1-\epsilon}\right) \qquad \ldots (6)$$

Assuming an efficiency of 95 per cent and substituting the value of m_L corresponding to a high pressure of 120 atm, 0·1609 g/sec together with results (2) and (4) in equation (6) gives $L = 123$ cm. Repeating this calculation using data corresponding to the situation where the high pressure is 30 atm yields an interchanger length of 144 cm, while a length of 245 cm would be required for an efficiency of 98 per cent. In practice a compromise length of 200 cm was used.

The pressure drops along the interchanger are calculated using the following method. The pressures dropped along the various tubes of the liquefier may be estimated from the equation

$$\frac{\Delta p}{\Delta L} = \frac{16R\bar{T}h_L}{10^6\pi^2\bar{C}_p D^4\bar{p}}\cdot\frac{dM}{dt}$$

Applying this equation to the most unfavourable case for the high pressure tube, when this is carrying gas at 30 atm pressure, shows that the pressure drop will be about 0·2 atm, while the corresponding pressure drop in the low pressure tubes will be about 0·03 atm. These are both acceptably low.

(2) *The second interchanger.* An attempt has been made to preserve the cooling obtained in passing through the purifiers by causing the high pressure tube to travel from the second purifier to the liquefier through an evacuated tube. The high pressure tube leaves this outer tube at K (Figure 2) and enters the second interchanger. A temperature of 150° K was assumed for the temperature of entry of the high pressure gas to the second interchanger, while the low pressure return gas was assumed to enter at 70° K and to leave at about 150° K. Substitution of the appropriate data into the equations given earlier yielded a value of 200 cm for the length of this interchanger, for an efficiency of 95 per cent. Subsequent observations of the low rate of boiling of the liquid nitrogen surrounding the second purifier have strongly suggested that the cooling derived in passing through the purifiers is greater than was assumed, indicating that a shorter second interchanger would suffice.

The highest temperature of emergence of the high pressure gas has been calculated as 103° K, and occurs when the high pressure is 120 atm.

(3) *The third interchanger.* Assuming this temperature of entry to the single-current interchanger, and aiming for a temperature of emergence of 70·1° K, the dimensions of a suitable interchanger may be calculated from the conventional equation

$$\theta_c-\theta_b = (\theta_h-\theta_b)\exp\left(\frac{-h_L L}{\bar{C}_p . dm/dt}\right) \qquad \ldots (7)$$

Assuming that $\frac{1}{8}$ in. o.d. tubing of 26 s.w.g. wall was to be used it was shown, with the aid of equations (3) and (7), that $L = 98$ cm.

(4) *The first interchanger.* In order to extract the cooling obtainable from the gas emerging from the second interchanger at a calculated temperature of 146° K, a further interchanger was included in the system before the cleaner. The returning low pressure tubes were arranged to share the vacuum jacketing tube with the ingoing high pressure tube, so as to preserve the cooling obtainable from the low

pressure stream before this entered the first interchanger. Application of the appropriate thermodynamic data indicated that this interchanger should have a length of about 300 cm for an efficiency of 95 per cent using the tubing listed in Table 1.

It may be added that the calculated values for Reynold's number were adequate for turbulent flow in every tube of every interchanger. The calculated overall pressure drops suffered during passage through the interchangers were approximately 1 atm in the high pressure line and 0·2 atm in the low pressure line.

The design

The design of the liquefier is reproduced, approximately to scale, in Figure 2. The vacuum jacketing tube, mentioned earlier, is soldered into a bush in the top plate A, and the vacuum jacket is continued a short distance into the liquefier in the form of a 1 in. o.d. 24 s.w.g. wall stainless steel tube, from which the gas tubes emerge at K. The purpose of the stainless steel termination is to prevent the O-ring seal of the plate A from becoming unduly cold. After passing through the second interchanger, D, the high pressure gas passes through the third interchanger, F, located at the bottom of the pumped nitrogen bath, E. This bath consists of a tube of stainless steel, 4 in. o.d., 16 s.w.g. wall, and 14 in. long. The level indicator consists of an aluminium wire supported by a float of foam polystyrene. This is covered by a glass tube and a seal is made by using a hat packing at J, where a protective slotted brass tube is also supported. The liquid nitrogen bath is pumped at C, and a vacuum gauge in the pumping line gives an indication of the temperature of the pumped liquid nitrogen. From this bath the high pressure gas flows through the final interchanger, H, and thence to the expansion valve within the liquid hydrogen receiver at L. The expansion valve control rod consists of a $\frac{1}{8}$ in. diameter stainless steel rod, sealed by metal bellows at the top, and controlled as shown. The helical spring B prevents the valve from closing during evacuation. With this design only low pressure gas enters the space between the control rod and its surrounding german silver tube, o.d. $\frac{3}{16}$ in. and 0·1 mm wall. The low pressure return gas follows the path shown.

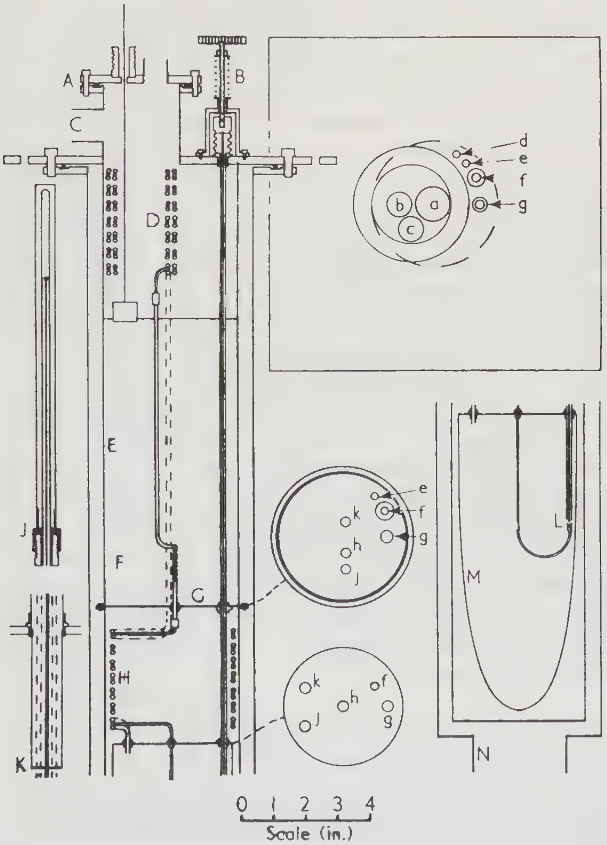

Positions of the bushes through which pass the following tubes:

a: Vacuum tube carrying high and low pressure tubes.
b: Float entry. c: Liquid nitrogen filling tube.
d: Vacuum/pressure gauge tube. e: Gas thermometer tube.
f: Siphon tube. g: Expansion valve control rod tube.
h: High pressure inlet tube. j, k: Low pressure return tubes.

Figure 2. Scale diagram of the liquefier

The liquid hydrogen receiver consists of a vessel of 22 s.w.g. spun copper, M, of capacity 1 litre. This is surrounded by a copper radiation shield attached to the base of the liquid nitrogen bath by screws. The liquid hydrogen is extracted via a $\frac{1}{8}$ in. o.d. german silver tube of wall thickness 0·1 mm, which extends from the bottom of the receiver to an extraction valve outside the liquefier. The tube is vacuum jacketed from its passage through the plate G to the tip of the extraction valve. Within the liquefier the vacuum jacket takes the form of a 1 cm o.d., 0·1 mm wall german silver tube, while this changes to standard $\frac{1}{2}$ in. bore copper tubing outside the liquefier. Mitred joints, similar to those described by Stout,[2] were used at the corners of the siphon tube and its vacuum jacket, asbestos spacers being used to prevent the inner and outer tubes from touching. The design of the extraction valve was based upon that of Fairbank.[3] A helium gas thermometer bulb is soldered to the top of the liquid hydrogen receiver and is connected to an external Bourdon gauge by 1 mm bore, 0·1 mm wall german silver tubing. This thermometer serves to indicate the time at which liquid hydrogen starts to collect in the receiver. The outer vacuum jacket is pumped via a 3 in. diameter tube N which feeds the throat of a diffusion pump. This high vacuum is shared with that surrounding the incoming and outgoing tubes, and with that surrounding the siphon tube. Detachable vacuum and water connections are used in the ancillary pipework, so that it is easily possible to lower the outer jacket and radiation shield for any servicing which may be found necessary in course of time. If, for any reason, access to the second or third interchangers should be required at any time these may be lifted out through the hole sealed by the plate A.

Performance

In cooling the cleaner, the purifiers, and the nitrogen bath within the liquefier, 20 l. of liquid nitrogen are used. During a run 25 l. are consumed. Recovery of the liquid nitrogen from the cleaner and purifiers at the end of a run indicates that, in all, approximately 35 l. are consumed. The time between the commencement of flow and the onset of liquefaction is 15 min. The intervals between the onset of liquefaction and the times of extraction of litres of liquid are approximately 17, 20, 23, 27, and 50 min.

If a compressor were to be used with the machine, to maintain the input pressure at 120 atm, and if the unliquefied return gas was to be recirculated the overall consumption of gaseous hydrogen would fall appreciably, whilst the output should rise to a constant value of just over 3 l./hr.

The total cost of constructional materials, gauges, and valves used in the liquefier and purification system was rather less than £200. The construction was undertaken by a technician without previous experience in this somewhat specialized field, assisted part of the time by one of the authors (B.Y.) and the total time taken, as nearly as can be assessed, was some three months.

The authors wish to thank two members of Bradford Institute of Technology: Dr. D. L. Smare for his support in obtaining the facilities which enabled the construction and installation to be undertaken, and Mr. D. Ives for his conscientious workmanship.

REFERENCES

1. Woolley, H. W., Scott, R. B., and Brickwedde, F. G. *J. Res. nat. Bur. Stand.* **41,** 379 (1948)
2. Stout, J. W. *Rev. sci. Instrum.* **25,** 929 (1954)
3. Fairbank, H. A. *Rev. sci. Instrum.* **17,** 473 (1946)

APPENDIX

Definitions of symbols, in order of their appearance in the text:

H_i = enthalpy per unit mass of inflowing gas (cal/g)
H_o = enthalpy per unit mass of outflowing gas (cal/g)
H_L = enthalpy per unit mass of liquid hydrogen (cal/g)
E = fraction of incoming gas which is liquefied
$\bar{C}_p$ = mean specific heat at constant pressure (cal/g. deg.)
$\bar{\eta}$ = mean viscosity (poise)
D = internal diameter of tube carrying gas (cm)
$\mathrm{d}m/\mathrm{d}t$ = mass rate of flow (g/sec)
θ_H = temperature at which high pressure gas enters interchanger (°K)
θ'_H = temperature at which low pressure gas leaves interchanger (°K)
θ'_C = temperature at which low pressure gas enters interchanger (°K)
L = length of interchanger (cm)
m_H = mass rate of flow of high pressure gas (g/sec)
m_L = mass rate of flow of low pressure gas (g/sec)
$\bar{C}_H$ = mean specific heat at constant pressure of high pressure gas (cal/g. deg.)
$\bar{C}_L$ = mean specific heat at constant pressure of low pressure gas (cal/g. deg.)
Δp = pressure (atm) dropped along a tube of length ΔL(cm)
R = gas constant (erg/mole. deg.)
$\bar{T}$ = mean absolute temperature (°K)
$\mathrm{d}M/\mathrm{d}t$ = rate of flow (mole/sec)
$\bar{p}$ = mean pressure in tube (dyn/cm^2)
θ_b = temperature of liquid nitrogen bath (°K)
θ_h = temperature of entry of gas to third interchanger (°K)
θ_c = emergent temperature of gas from third interchanger (°K)

Tolerances Associated with the Operation of the Crowe Storage Cell in the Coincident Current Mode

R. V. Peacock *Mullard Research Laboratories, Salfords*

Received 15 August 1961

THE Crowe cell and its mode of operation have been described by a number of authors.[1–6] This paper considers the tolerances on the device parameters and drive currents which are associated with the coincident current mode of operation.

Mode of operation

The two binary states of a Crowe cell are represented by the sense of the persistent supercurrents which may be made to flow round the D-shaped holes in the thin superconducting film (Figure 1(a) and (b)).

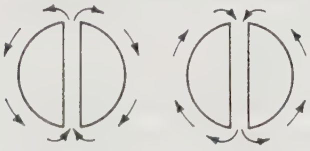
(a) (b)

Figure 1. (a) '1' stored; (b) '0' stored

Figure 2 illustrates a drive wire configuration for coincident current operation. Figure 3 shows graphically the relationship between the drive currents (solid lines) and the currents circulating in the film (dotted lines). Unity coupling is assumed between the drive wires and the crossbar of the 'D's, which may be shown theoretically to be a good approximation.

Let us assume that there is a circulating current I_1 flowing in the cell representing a '1' stored (Figure 3). Now it is necessary that the half read pulses shall have no destructive effect upon the stored information. Thus, if we apply a half read pulse $I_R/2$ along one of the drive wires of Figure 2, the sum of the current induced plus the circulating current must not be high enough for any appreciable resistance to be induced in the crossbar. Let the current at which the resistance becomes appreciable be $I_{C,1}$; then we may write the inequality

$$I_1 + I_R/2 < I_{C,1} \qquad \ldots(1)$$

It is necessary, however, that when a full read current pulse is applied to the cell the induced current plus the stored current should be sufficient to induce resistance in the crossbar which will dissipate energy and cause the circulating current to decay. The wattage dissipated in the now resistive bar by this current therefore decreases with time. The heat produced is dissipated away at a rate dependent upon the temperature of the bar. Thus, the crossbar will cool and become superconducting again after a certain time. If the current decays much more rapidly than the heat is conducted away, then the current falls very nearly to zero before the crossbar becomes superconducting, and therefore the current trapped in when the bar becomes superconducting, I_T, is almost zero. However, it may be shown that if the heat is conducted away quickly, then appreciable currents can be trapped in when the crossbar becomes superconducting.

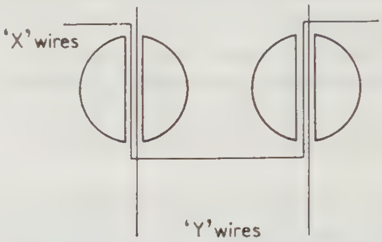

Figure 2

Now the resistance induced in the crossbar is a function of the drive current and, thus, the rate at which the circulating current decays is dependent upon the drive current. Thus, I_T, one of the parameters of the Crowe cell, is a function of the current being used to switch it; this

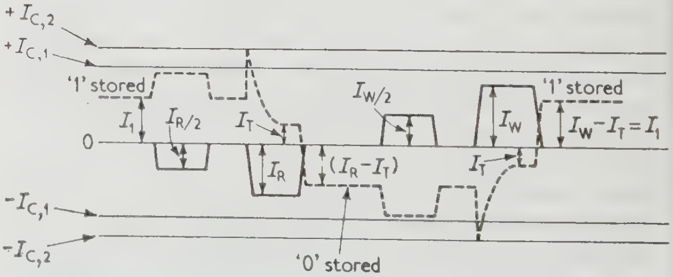

Figure 3. Coincident current mode of operation

clearly complicates the operation of the cell. However, in this analysis we shall make the simplifying assumption that if the sum of the induced current and the stored current exceeds a certain value $I_{C,2}$, and hence a sufficiently large resistance is induced in the crossbar, then the trapped current is fixed at a steady value I_T and that any lower value of this sum results in incomplete switching, and an unpredictable value of I_T.

This assumption is clearly an oversimplification and, in fact, the device is likely to have tighter tolerances in practice than the following analysis predicts.

Using the notation discussed above we may write the inequality which must be obeyed if a full read pulse I_R is to switch the cell

$$I_1 + I_R > I_{C,2} \qquad \ldots (2)$$

When this read-out pulse is removed, sometime after the crossbar has become superconducting again, only reversible changes take place, subject to certain limitations, to leave a circulating current of $I_R - I_T$, which represents a '0' stored.

As no information may be written in by a half write pulse we may write a third inequality

$$I_R - I_T + I_W/2 < I_{C,1} \qquad \ldots (3)$$

and we may express the necessary condition that writing takes place when I_W is applied by

$$I_R - I_T + I_W > I_{C,2} \qquad \ldots (4)$$

When this write pulse is removed we have a '1' stored again. Thus

$$I_W - I_T = I_1 \qquad \ldots (5)$$

Now if we write $I_{C,2}$ as $I_{C,1} + \Delta I_C$ and apply equation (5) to inequalities (1) to (3) we have

$$I_W + I_R/2 < I_{C,1} + I_T \qquad \ldots (6)$$

$$I_R + I_W > I_{C,1} + I_T + \Delta I_C \qquad \ldots (7)$$

$$I_R + I_W/2 < I_{C,1} + I_T \qquad \ldots (8)$$

Adding inequalities (6) and (8)

$$I_R + I_W < 4(I_{C,1} + I_T)/3 \qquad \ldots (9)$$

Thus we have a number of inequalities which have to be obeyed if the Crowe cell is to operate in a coincident current mode. We are therefore in a position to consider the tolerances on the drive currents, the device current parameters, and the relationship between them.

Tolerances

Let $\pm 100t$ per cent be the tolerance on the cell parameters, and $\pm 100q$ per cent be the drive current tolerances. Now if the device is to operate at all in the coincident current mode, the following inequalities modified from inequalities (7) and (9) must still be valid

$$(1-q)(I_R + I_W) > (1+t)(I_{C,1} + I_T + \Delta I_C) \qquad \ldots (10)$$

$$(1+q)(I_R + I_W) < 4(1-t)(I_{C,1} + I_T)/3 \qquad \ldots (11)$$

Thus, to find the limiting tolerances we must write these inequalities as equations, and dividing equation (10) by equation (11) we have

$$(1-q)/(1+q) = 3(1+t)(1+1/n)/4(1-t) \qquad \ldots (12)$$

where $n = (I_{C,1} + I_T)/\Delta I_C$

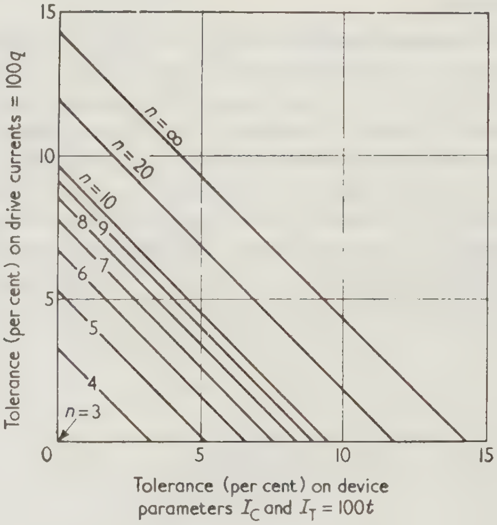

Figure 4

From equation (12) it is clear that if n equals 3 there is *no tolerance at all* on either $I_{C,1}$, I_W, I_R, or I_T, and if n is less than three the cell *cannot be used in a coincident current store.*

The relationship between the tolerances on the drive currents and the tolerances on the device parameters given by equation (12) is plotted in Figure 4.

Comments on the resistance against current transition

It is evident from Figure 4 that the value of n has a most marked effect upon the tolerance question. Let us therefore try to get some picture of the type of resistance against current transition which will be needed for the device to operate at all in the coincident current mode.

As the inductance of the cell for the original Crowe configuration is about 1 mμH, and in a working store a cell could conceivably spend as much as half of its time under the influence of half read pulses, then the resistance which is just tolerable for one hour of storage would be about $10^{-13}\ \Omega$. Thus, $I_{C,1}$ is the current at which R is approximately $10^{-13}\ \Omega$. As an order of magnitude $I_{C,2}$ may reasonably be assumed to be the current through the crossbar at which R is of the order of $0{\cdot}1\ \Omega$. Therefore ΔI_C is the current change required for the resistance to rise from about $10^{-13}\ \Omega$ by a factor of more than 10^{12}, on the graph of R against I taken with short pulses. (This adiabatic curve is considerably broader than the isothermal d.c. graph.[7])

The significance of this is made clearer when it is realized that there have been no adiabatic resistance against current characteristics published in the literature which have a transition width which would satisfy the inequality $(I_{C,1}+I_T)/\Delta I_C > 3$, which is necessary for coincident current operation, even making the most favourable assumption that $I_T = I_{C,1}$.

Conclusions

The tolerances which are to be expected in operating a coincident current matrix of Crowe cells are extremely tight, even when the most favourable assumptions that I_T can have a discrete value and that the coupling factor between the drive wire and the crossbar is the same for each cell in the matrix are made. In fact, unless the parameter '*n*' of the adiabatic *R* against *I* curve is greater than three the device cannot be used in a coincident current storage matrix.

The work reported in this paper was carried out in close collaboration with Mr. N. D. Richards, and the author would like to express his thanks to Mr. Richards for his help and for many useful discussions concerning this tolerance problem. He would also like to thank Dr. Parkinson and Dr. Lock, both of the Royal Radar Establishment, Malvern, for their help and interest.

REFERENCES

1. CROWE, J. M. *I.B.M. Journal* **1,** 295
2. RHODERICK, E. H. *Brit. J. appl. Phys.* **10,** 193 (1959)
3. GARWIN, R. L. *I.B.M. Journal* **1,** 304
4. KRAUS, C. J. *Digest of Technical Papers at 1959 I.R.E. Solid State Circuits Conference*, p. 20
5. LOCK, J. M. *Research, Lond.* **13,** 49 (1960)
6. LOCK, J. M. *Engineering, Lond.* **187,** 550
7. BREMER, J. W., and NEWHOUSE, V. L. *Phys. Rev.* **116,** 309 (1959)

A Method for Measuring the Heat Capacity of Condensed Gases above Their Boiling Point

A. V. Voronel and P. G. Strelkov

Scientific Research Institute for Physico-Technical and Radio-Technical Measurements, U.S.S.R.

Received 23 June 1961[†]

Kostryukov et al.[1] developed a method of measuring the heat capacity of condensed gases at pressures not more than 1–2 atm. The present work extends this range of attainable pressures to several tens of atmospheres. This improvement in the method makes it possible to measure the heat capacity of the liquid phase above the boiling point, and also of two-phase systems up to the critical point.

For elevated pressures it is very difficult to construct a calorimeter, which is light enough for its heat capacity, to be small compared with that of the specimen, while at the same time being sufficiently strong to stand the pressure without distortion. The construction shown in Figure 1 has turned out to be very successful. The calorimeter is made of two tubes (1) and (2), pressed out with the domes, of stainless steel with wall thickness 0·18 mm. One tube is fitted over the other to a depth of ~ 5 mm and soldered. At the join a wide (20 mm) ring (3) is put on, made of the same tubing, and also soldered. A thin walled steel tube (4), of diameter 5 mm, passes along the vertical axis of the calorimeter to take the platinum resistance thermometer (6) wound on the brass sleeves (5) at the ends of the calorimeter and soldered. With this construction the calorimeter, sealed with soft solder and of internal volume ~ 105 cm^3, stood up to above 70 atm without any noticeable deformation. The calorimeter weighed ~ 55 g and its own heat capacity was ~ 25 J/°C at room temperature. For the measurements of the heat capacity of nitrogen (see below) the heat capacity of the calorimeter amounted to 13–20 per cent of the total amount measured.

The calorimeter heater (7) was a 0·1 mm diameter constantan wire threaded through a copper capillary (external diameter 1 mm) formed into a spiral along the inner surface of the calorimeter. The capillary containing the heater was filled with BF4 paste which was then polymerized.

In many calorimetric experiments the fluid being investigated is stirred during the measurements. In particular, thermodynamic equilibrium of the system is very slowly established in measurements on the heat capacity of two-phase systems, and also near the critical temperature of liquids. Stirring considerably improves this and is even essential, in principle, for measurements in the critical region.[2]

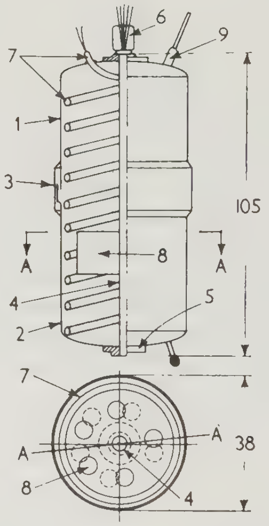

Figure 1

In the calorimeter described, stirring is achieved by the magnetic stirrer (8), consisting of two stainless steel disks fixed to the end of a hollow cylinder of permalloy strip. The stirrer is placed on the inner tube (4) as axis and is put into to-and-fro motion by switching a current through coils wound on the vacuum jacket at heights corresponding to the ends of the calorimeter. There are holes in the stirrer disks, which are displaced relative to one another, as shown in Figure 1, to improve the mixing. In order that the operating conditions of the calorimeter should not change under the action of the stirrer, the current in the coils is not switched off completely, but is only switched from one to the other. The method of thermal insulation and also the system for filling the calorimeter with gas were in principle the same as described previously.[1, 3] The development required only a high pressure valve.[4]

[†] Received by PTÉ Editor 28 October 1959: *Pribory i Tekhnika Éksperimenta* No. 6, p. 111 (1960).

The heat capacity of nitrogen in the critical region was measured in order to try out and study the method developed. The measurements were made on technical nitrogen, containing ~ 1·5 per cent oxygen. The heat capacity was measured at constant volume, close to the critical value, and at various temperatures up to the critical. The results are shown in Figure 2. It can be seen that the temperature dependence, on crossing the curve of coexistence of two phases, has a jump similar to that found for ethylene, oxygen, and carbon dioxide.[5–7] We were not concerned here with a special study of this discontinuity. The heat capacity obtained for the liquid phase is close to that given in the literature. The form of the discontinuity found on crossing the two phase curve does not contradict theoretical ideas.[8]

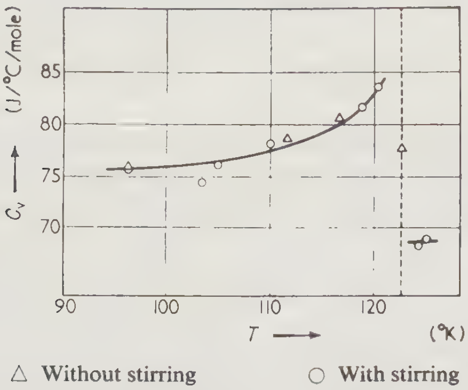

Figure 2. Temperature dependence of the heat capacity C_v for nitrogen (at a density $\rho = 0{\cdot}3$ g/cm^3)

Some heat capacity values were obtained without stirring in order to find how the stirrer worked. It can be seen from Figure 2 that these points show no systematic departure from the curve. Evidently the working of the stirrer produces no appreciable heat influx into the calorimeter during measurements. The time to reach equilibrium varied from 50 min far from the critical point to 1·5 hr in the critical region itself. On stirring this time decreases to 15–30 min depending on the vigour of stirring. This problem needs further study right in the critical region.

The error for a separate measurement of heat capacity does not exceed 1 per cent. The scatter of points on the curve, except for the point at 103·4° K is not outside this limit.

The authors thank V. N. Kostryukov for discussion and interest in the work.

REFERENCES

1. Kostryukov, V. N., Alikhanyants, R. A., Samoilov, B. N., and Strelkov, P. G. *J. phys. Chem., Moscou* **28,** 650 (1954)
2. 'Symposium on Critical Phenomena (Royal Society of Canada)'. *Chem. Rev.* **23,** 1 (1938)
3. Alikhanov, R. A. *Industr. Lab.* **22,** 1202 (1956)
4. Astrov, D. N., and Voronel, A. V. *Prib. i. Tekh. Eksper.* No. 3, 149 (1960)
5. Pall, D. B., Broughton, J. W., and Maass, O. *Canad. J. Res.* **B16,** 230 (1938)
6. Michels, A., and Strijland, J. *Physica* **18,** 613 (1952)
7. Hoge, H. *J. Res. nat. Bur. Stand.* **44,** 321 (1950)
8. Krichevskii, I. R., and Khazanova, N. E. *J. phys. Chem., Moscou* **29,** 1087 (1955)

This paper has been specially translated for CRYOGENICS and is included by permission of the Editors of *Pribory i Tekhnika Éksperimenta.* We are also indebted to the Instrument Society of America and the Plenum Press, who publish their own cover-to-cover translation of PTÉ by arrangement with the Russian publisher.

The Measurement of Thermal Expansion of Metals at Low Temperatures

K. Andres

Institut für kalorische Apparate und Kältetechnik der Eidgenössischen Technischen Hochschule, Zürich

Received 15 September 1961

It is well known that the thermal expansion coefficient β of solids tends to zero at low temperatures with the specific heat. This fact is expressed by the Grüneisen relation

$$\beta V/\kappa c = \gamma_G$$

where κ is the compressibility, c the specific heat per mole, V the molar volume, and γ_G the Grüneisen 'constant'. This is actually a mean value over the different $\gamma_{G(\omega)}$ corresponding to different vibration frequencies ω of the solid. γ_G may therefore exhibit changes with temperature which depend on the frequency spectrum and ultimately on the forces between the atoms or molecules of the solid.

At very low temperatures one may expect the Grüneisen constant of non-metals to become temperature independent, so that the thermal expansion coefficient β of a Debye solid should tend to zero as T^3. In metals, however, both the specific heat and the expansion cofficient should show an additional linear term due to the electrons (see below, under *Theoretical considerations*).

Whereas the order of magnitude of β at room temperature is about 10^{-5} per degree, it decreases to about 10^{-8} per degree in the region where the lattice and the electron contributions are comparable, that is, below 10° K. For this reason, only measurements above 10° K have been available so far (see, for instance, Nix and MacNair,[1] Bijl and Pullan,[2] Gibbons,[3] Swenson,[4] Fraser and Hollis Hallett[5]). Very recently, White[6,7] has described an apparatus which is capable of detecting relative length changes of about 10^{-9} by a condenser method; he has also given first results on the thermal expansion of copper, iron, beryllium, aluminium, palladium, and chromium at the temperature of liquid helium. The present author has developed an apparatus using an optical technique and having about the same sensitivity. Preliminary results on aluminium and lead have already been presented.[8,9] In this paper a description of the method is given, including some further results obtained with it.

Experimental method

(1) *Principle of measurement of length changes.* The working principle of the apparatus is the transformation of length changes into changes of light intensity. The light is passed through two closely spaced grids, one of which is held fixed, and the other of which is attached to the free end of the specimen whose expansion is to be measured. One grid is regular while the other has an irregularity in the middle as shown in Figure 1. Such a grid system has been described by Jones.[10,11] In position (a) no light can pass the lower half of the grids, in position (b), where the second grid is displaced with respect to the first by one line width, the situation is reversed. In position (c) the two halves are equally transparent. Thus the output of two differentially connected photocells placed behind the two halves of the grids is zero. When one grid is fixed and the other one attached to the specimen, changes in length of the latter will result in changes of the output of the photocells. This is a linear function of the grid displacement for not too large an intensity of illumination.

(2) *Cryostat construction.* For the sake of stability, the grids and the specimen have to be close together and it becomes necessary to place the grids within the helium bath. The problem of leading the light down into the cryostat has been solved by the use of Perspex light pipes as shown in Figure 2. The light, coming from a Philips high intensity lamp (type 13113 C/04 for 8 mm movie

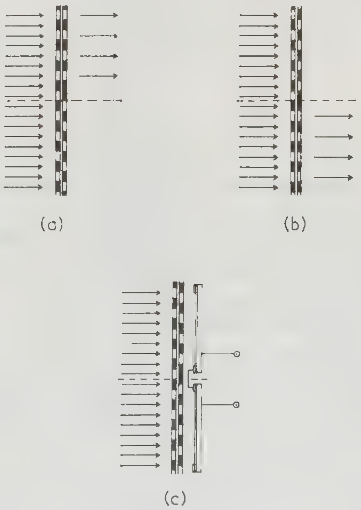
(a) (b)

(c)

Figure 1. Working principle of the grids

projectors), is focused into a light pipe after passing a cold light mirror and an interference filter (in order to remove the red and infra-red components). In the light pipe itself, it is totally reflected a few times on the polished surfaces until it falls on to the 45 degree surface at the bottom, where it is totally reflected towards the grids. Behind the grids, the light from each half is collected separately and led to the cryostat head again by two other light pipes at the end of which the photocells are mounted. The grids and the specimen are located in a brass framework which itself is firmly attached to the lower part of the three light pipes. The whole system is surrounded by a vacuum. The german silver tubes going to the top of the cryostat are connected to the light pipes at their lower ends. In this way, the apparatus is quite insensitive to shock. If the lower part of the cryostat moves with respect to the top (for instance, due to the boiling of liquid helium), then the grids and the light pipes move together so that in first order the illumination of the photocells is not changed.

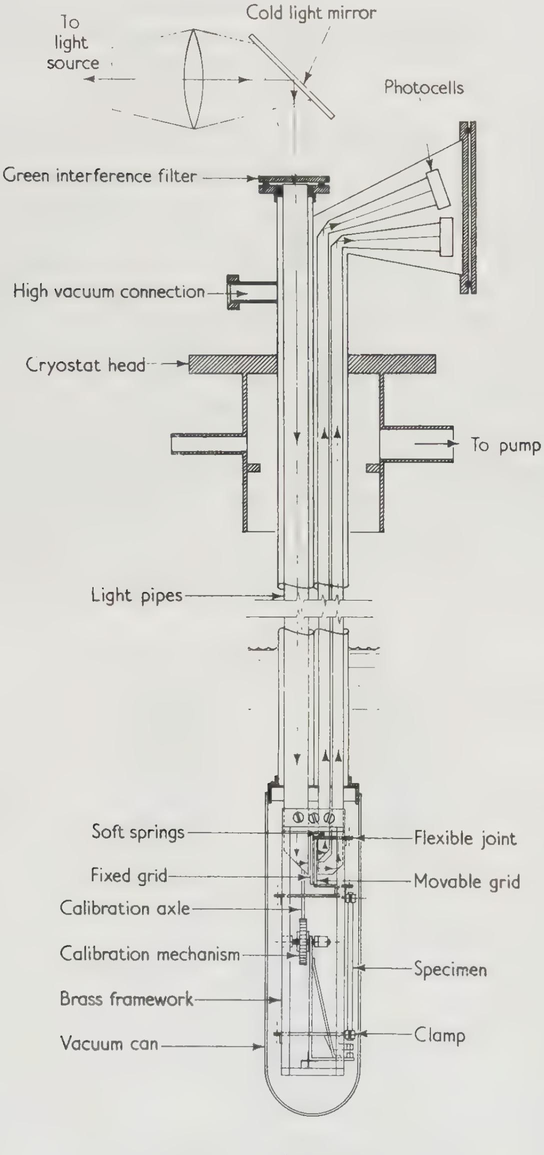

Figure 2. The cryostat

The grid connected to the specimen is suspended with flexible joints in the housing so that it can move up and down with its plane parallel to the other grid. This latter can be fixed by three adjusting screws so that the spacing between the two grids is about 0·05 mm. In a first execution, the grids were drawn on tracing paper and photographically reduced to the actual size of 10 × 11 mm with a line width of 0·15 mm. More recently a second pair of grids was kindly made for us by the firm Dr. E. Rüst AG, Präzisionsteilungen, Stäfa, Switzerland. These are made of optically flat pieces of glass (25 × 25 × 2 mm), one side of which is coated with a layer of chromium. On this side, the grid is scratched with a precision scaling machine. This pair of grids, which has a line width of 0·1 mm, has two advantages over the previous ones. Firstly, due to the greater precision, the optical efficiency is increased and, secondly, the light is reflected rather than absorbed by the lines so that less heat has to be carried away from the grids at low temperatures. This is important because the grids are in thermal contact with the housing and the absorbed heat has to be carried away by thermal conduction via the housing and a copper link to the helium bath, thus restricting the lowest temperature that can be obtained in the housing. If, for instance, the helium bath is at a temperature of 1·5° K, the temperature of the housing and the grids rises to about 2·5° K when the light is switched on.

The lower end of the specimen is attached via a calibration mechanism (see below) to the housing. Between the upper end of the specimen and the grid there is a system of lever arms with flexible joints as shown in Figure 2. This amplifies the length changes of the specimen by a factor of three. The specimen has a length of 7·5 cm and can be of a thickness between one and about three millimetres; it is held by two clamps. Between specimen and clamps some paper or hard rubber is inserted to isolate the specimen thermally from the housing. This insulation makes it possible to increase the temperature of the specimen above that of the housing. Heating the specimen from 1·6 to 10° K raises the temperature of the housing from 2·5 to 2·6° K, which does not affect the precision of the measurement.

(3) *Calibration.* The calibration is done by observing the voltage produced in the differential photocells when the lower end of the specimen is moved by a known amount. Figure 3 shows the working principle of the calibration mechanism. When the axle A leading from the top of the cryostat down to the housing H is turned one turn, the toothed wheel W turns by one tooth. The axle of the wheel W consists of a left thread on one side and a right thread on the other, so that if the wheel W turns, the nut N moves. The movement of the nut N is transferred to the lower end of the specimen S by means of the lever triangle T which itself can turn around the fixed point F.

The soft springs shown in Figure 2 tend to pull the specimen upwards and to push the nut N towards the wheel W thus minimizing the clearance between nut and thread.

One turn of the axle A corresponds to a displacement of the specimen of $3{\cdot}5 \times 10^{-4}$ cm with an error of about 3 per cent due to uncertainties in geometrical dimensions. Usually, a few calibration turns are made in the same direction. The corresponding output changes are traced by a pen recorder; they equal each other within about 3 per cent, so that the total uncertainty of the calibration is not greater than 6 per cent.

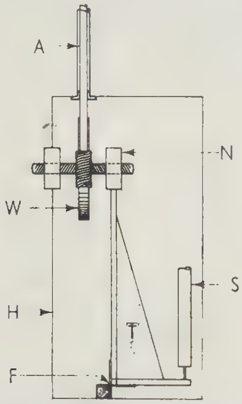

Figure 3. Calibration mechanism

(4) *Temperature measurement.* Since it was intended to detect electronic contributions to thermal expansion in metals, that is to measure the expansion coefficient below 10° K, carbon thermometers have been chosen for the temperature measurement. Two 100 Ω Allan Bradley resistors are soldered to the specimen either at the two ends or in the middle and at one end. Temperatures are calculated from the formula

$$T = \frac{\log R}{(A + B \log R)^2}$$

due to Clement and Quinell.[12] This should be valid in the temperature range from 1·5 to 20° K to within 0·02°. The constants A and B are determined in each experiment by calibration in the liquid helium range. It is believed that with the present procedure the accuracy of the temperature measurements around 10° K is about 0·1°. In the samples of aluminium, lead, magnesium, and tungsten of thickness 3 mm, the largest temperature differences between the two ends are observed at 10° K and amount to 0·1° K (the heater is attached at one end). In the thin sample of tantalum of thickness 0·5 mm, this temperature difference amounted to as much as 0·3° at 10° K due to its bad thermal conductivity and to insufficient thermal insulation from the clamps.

In all experiments the helium bath is kept at a temperature of 1·5° K. The sample, thermally isolated from the housing, is connected by a thermal link to the helium bath. It can be heated electrically while the temperature of the housing remains practically constant. With the light switched on, the sample has a temperature of about 1·6° K. Often, a constant drift is observed on the recorder corresponding to about 10 Å/min (1 Å = 10^{-8} cm), but this does not affect the accuracy of measurement, since the thermal relaxation time is about 2 sec. The heater is switched on during 20 sec and then switched off again. Figure 4 shows a typical recorder trace.

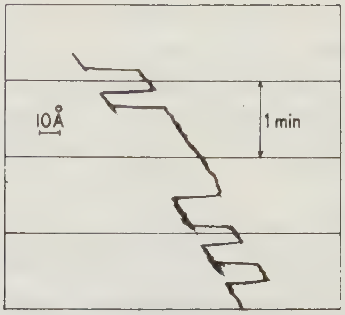

Figure 4. Typical recorder trace

The linear expansion coefficient is determined by graphical differentiation of the observed thermal expansion curve. In all samples measured so far the volume expansion is simply three times the linear expansion since they all had cubic structures except magnesium which was polycrystalline.

Results

The results in so far are of a preliminary nature as all measurements have been made on one sample of each element only. The reproducibility of the results from different samples of the same element has not yet been investigated, so that we know nothing of the dependence on purity.

In Figures 5 and 6 the volume expansion coefficient β of the elements investigated, divided by the temperature, is plotted against T^2. It is seen that β can be fairly well represented by the formula

$$\beta = aT + bT^3$$

This is indeed the temperature dependence one would expect from the theoretical considerations discussed below. The observed constants a and b are given in Table 1. The errors quoted are those estimated from each experiment and do not, as mentioned above, include the possible scatter between different samples. The rapid drop of β in the normal state of niobium below 4° K may be due to the presence of spurious superconducting inclusions at the ends of the sample. The magnet coil around the sample (made of superconducting niobium wire) produced only 3,100 oersteds, so that at the end the field was perhaps not high enough to destroy superconductivity. While heating from 1·6 to 4° K, these inclusions are 'pushed out', giving a negative contribution to the expansion because the volume of niobium in the superconducting state is greater than in the normal state.

Table 1. Thermal Expansion Data of Some Metals

Element	$a \times 10^{10} (deg^{-2})$	$b \times 10^{11} (deg^{-4})$
Al	33 ± 3	$6{\cdot}6 \pm 0{\cdot}6$
Mg	18 ± 10	30 ± 6
Ta (normal)	33 ± 2	27 ± 3
W	0 ± 2	$3 \pm 0{\cdot}6$
Pb (normal)	30 ± 60	420 ± 60
Pb (superconducting)	0 ± 30	360 ± 60
Nb (normal)	75 ± 30	45 ± 10

For lead and niobium the thermal expansion both in the normal and superconducting states have been measured. In superconducting lead, β seems to follow a T^3 law at the lowest temperatures, which would be in agreement with the theoretical expectation on the basis of the two fluid model for superconductivity (see end of next section). In superconducting niobium, β does not quite follow this law and we do not yet have an explanation for its behaviour.

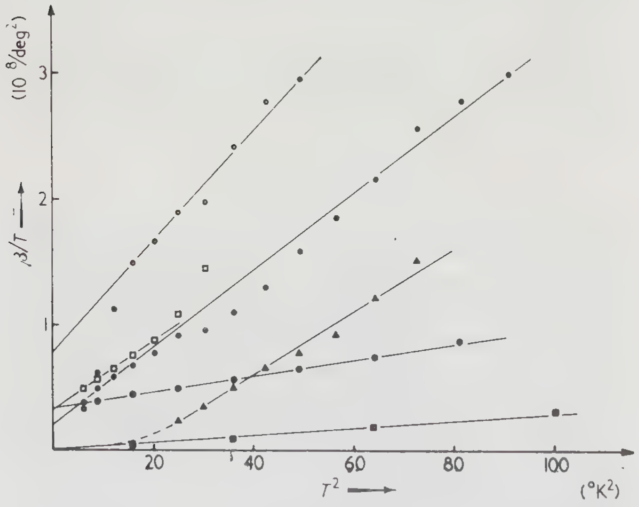

◐ Al ● Mg ☐ Ta (normal) ◧ W ○ Nb (normal)
△ Nb (superconducting)

Figure 5. The thermal expansion coefficient β, divided by T, for some metals plotted against T^2

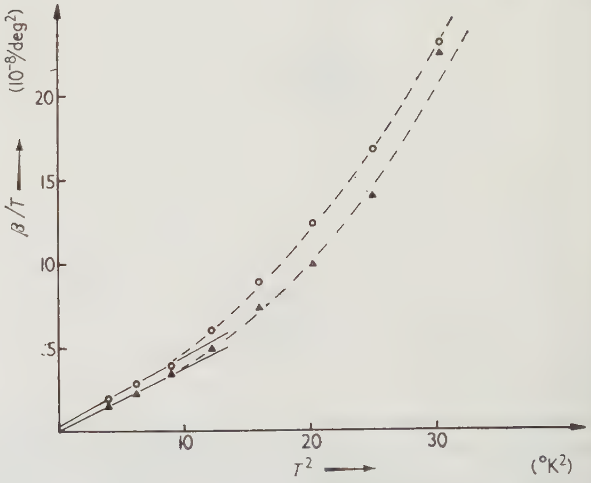

○ Normal △ Superconducting

Figure 6. The thermal expansion coefficient β, divided by T, for lead plotted against T^2

Theoretical considerations

Using one of the Maxwell relations

$$(\partial V/\partial T)_p = (\partial S/\partial p)_T$$

one can calculate the thermal expansion coefficient from the pressure dependence of the entropy at constant temperature. The entropy of a metal is the sum of a lattice and an electronic contribution:

$$S = S_L + S_e$$

and the temperature dependence of the expansion coefficient must also consist of two contributions due to the lattice and the electrons. At very low temperatures c_L, the lattice specific heat, varies as T^3 and in this region S_L also varies as T^3. This means that at very low temperatures the lattice contribution to thermal expansion β_L varies as T^3. At the higher temperatures S_L is usually a more complicated function of temperature. There, the Grüneisen parameter γ_G usually changes and various calculations exist to predict its temperature dependence (see, for instance, Barron,[13] Blackman,[14] Bijl and Pullan[2]). Calculations of the electron contribution have been given by Visvanathan[15] and Varley.[16] The entropy of the electrons equals γT, the electronic specific heat per mole. Therefore β_e, the electron contribution to the thermal expansion, also varies as T. In terms of γT, we calculate

$$\beta_e = \kappa(\gamma/V) g T$$

where g stands for $\partial \log \gamma / \partial \log V$ and $(\gamma/V)T$ is the electronic specific heat per unit volume. Since γ is proportional to $n(\xi)$, the electron density of states at the Fermi surface (see, for instance, Mott and Jones[17]), g is also equal to $\partial \log n(\xi)/\partial \log V$. The linear term in the thermal expansion coefficient of metals is thus a measure of the relative change of the density of electron states at the Fermi surface with volume. In Table 2, the observed g values of the measured metals are tabulated and compared with White's[7] results. It should be noted that the room temperature compressibilities have been used for the computation of our values of g.

Table 2. The Quantity $g = \partial \log n(\xi)/\partial \log V$ for Some Metals

Element	g *(this work)*	$\kappa \times 10^{12}$ *(cm²/dyn)*	g *(from White)*
Al	$1{\cdot}7 \pm 0{\cdot}2$	1·4	$1{\cdot}8 \pm 0{\cdot}2$
Mg	$0{\cdot}6 \pm 0{\cdot}3$	3·0	
Ta	$1{\cdot}3 \pm 0{\cdot}2$	0·5	1·4*
W	$0 \pm 0{\cdot}2$	0·3	
Pb	$0{\cdot}7 \pm 1{\cdot}5$	2·3	1·7*
Nb	$2{\cdot}1 \pm 1$	0·5	

* Private communication.

One can think of another more direct way of calculating the electron contribution to thermal expansion. The free electrons in a metal form a gas of particles which exerts a pressure on the metal walls. This internal pressure P can be calculated in a way similar to that in the kinetic theory of gases, if it is supposed that the Fermi surface is known. Its slight temperature dependence causes the electronic contribution to thermal expansion. For the special case of a Fermi surface with cubic symmetry, one can write

$$\beta_e = \kappa(\partial P/\partial T)_V$$

where κ is again the compressibility of the metal. A calculation of $(\partial P/\partial T)_V$ in this case gives, under the assumption that the electron density of states at the Fermi surface does not vary too rapidly with energy

$$\begin{aligned}\beta_e &= \kappa(\partial P/\partial T)_V \\ &= \kappa T[(\gamma/V) - \frac{\pi^2}{3}k^2 N(\partial \log n(E)/\partial E)_{E=\xi}]\end{aligned}$$

Here, N is the number of free electrons per unit volume, $n(E)$ the electron density of states, and ξ the Fermi energy. Thus, the electron contribution to thermal expansion is also a measure of the first derivative of the density of states function at the Fermi energy if the electronic specific heat γT is known. A detailed derivation of the above formula will be published elsewhere.

If the metal becomes superconducting, the electrons condense gradually into a state of zero entropy as the temperature decreases. In the picture of the two fluid model of Gorter and Casimir[18] the entropy of the electrons in a superconductor is written as

$$S_e = \gamma T^3/T_c^2$$

where γT is again the electronic specific heat per mole, and T_c is the critical temperature of the superconductor. Inserting this in Maxwell's relation, one obtains

$$\beta_{es} = \kappa(\gamma/V)(T^3/T_c^2)(g - 2s)$$

where s is written for $\partial \log T_c/\partial \log V$ and the suffix s in β_{es} refers to the superconducting state. For most of the superconductors, $g - 2s$ is negative, as Olsen and Rohrer[9, 19] have shown. The measurements on lead are in qualitative agreement with this statement.

My thanks are due to Professor P. Grassmann, the Director of this Institute, for his constant interest and encouragement in this work and to Professor J. L. Olsen and Dr. H. Rohrer for much valuable advice and many discussions. I am grateful to Dr. G. K. White for informing me of his results prior to publication. This work was supported financially by the 'Arbeitsbeschaffungsfonds des Bundes'.

REFERENCES

1. Nix, F. C., and MacNair, D. *Phys. Rev.* **60,** 597 (1941)
2. Bijl, D., and Pullan, H. *Physica* **21,** 285 (1955)
3. Gibbons, D. F. *Phys. Rev.* **112,** 136 (1958)
4. Swenson, C. A. *Phys. Rev.* **100,** 1607 (1955)
5. Fraser, D. B., and Hollis Hallett, A. C. *Proceedings of the VIIth International Conference on Low Temperature Physics, Toronto, 1961*, p. 689
6. White, G. K. *Cryogenics* **1,** 151 (1961)
7. White, G. K. *Phil. Mag.* **66,** 819 (1961)
8. Andres, K., and Rohrer, H. *Helv. phys. acta.* In press
9. Andres, K., Olsen, J. L., and Rohrer, H. *IBM Jour.* In press
10. Jones, R. V. *J. sci. Instrum.* **28,** 38 (1951)
11. Jones, R. V. *Proc. phys. Soc. Lond.* **B64,** 469 (1951)
12. Clement, J. R., and Quinnell, E. H. *Naval Research Laboratory Reprint* No. 68-52 (1952)
13. Barron, T. H. K. *Phil. Mag.* **46,** 720 (1955)
14. Blackman, M. *Proc. phys. Soc. Lond.* **B70,** 827 (1951)
15. Visvanathan, S. *Phys. Rev.* **81,** 626 (1951)
16. Varley, J. H. O. *Proc. roy. Soc.* **237,** 413 (1956)
17. Mott, N. F., and Jones, H. *The Theory of the Properties of Metals and Alloys* (Oxford University Press, London, 1936)
18. Shoenberg, D. (Ed.) *Superconductivity* (Cambridge University Press, London, 1952)
19. Rohrer, H. *Helv. phys. acta* **33,** 675 (1960)

Carbon Resistance Thermometers for Low Temperatures

N. N. Mikhailov and A. Ya. Kaganovskii

Institute for Physical Problems, Academy of Sciences, U.S.S.R.

Received 18 July 1961†

TEMPERATURE measurement below 20° K presents well known difficulties mainly connected with the fact that thermocouples and resistance thermometers of metallic conductors become very insensitive in this region. One of the convenient methods of overcoming this difficulty is the use of carbon resistance thermometers which, with semiconductor conduction characteristics, have a negative temperature coefficient of resistance and increased sensitivity with decreasing temperature. During the last twenty years different variants of such thermometers have been published on numerous occasions.

The simplest method is the application of a thin film of graphite or carbon black from the corresponding suspensions in water on a strip of insulating material, e.g. on cigarette paper.[1] Such thermometers are easy to prepare, but they are not sufficiently stable. Zavaritskii and Shal'nikov[2] have described a more reliable technique for preparing carbon film thermometers.

Several types of radio resistor have found wide application at low temperatures in recent years,[3–7] and their properties turned out by chance to be suitable for thermometers.

Sharvin, who has prepared carbon thermometers from anthracite,[8] noted that the region of their greatest sensitivity can be moved in any direction by changing the temperature of firing. It was natural to suppose that this peculiarity is not a property of anthracite alone, but of a number of other organic substances with high carbon content. In this connection we have undertaken experiments to develop the technology of preparing sturdy carbon thermometers, starting from materials which allow greater reproducibility and uniformity of the thermometers than can be obtained by using anthracite.

The technique of preparing thermometers

The initial material is petroleum pitch, part of which is used without any treatment (in the form of brickettes bonded under pressure) and part is transformed into petroleum coke. Coking of the pitch is achieved by heating it in the absence of air at 700° C for 3 hr. The coke and the pitch are separately ground in a mortar and passed through a 625 holes/cm^2 sieve. It was found that to obtain the best results the powders had to be thoroughly mixed in the proportions of 23 per cent by weight of pitch and 77 per cent coke. The charge is then weighed out into portions which are pressed at room temperature in a hydraulic press at a pressure of 12,000 kg/cm^2. For better bonding, each loading is kept under pressure for 5–10 min. The brickettes, obtained as rectangular parallelepipeds of dimensions $7 \times 3 \times 1$ mm, are fired in a quartz tube filled with finely divided charcoal. The temperature is raised over a period of $\simeq 1{\cdot}5$ hr and held at the given maximum temperature for 1 hr. After this time the oven is turned off and the brickettes cool with the oven.

Thin layers of copper are then deposited on to the ends of the brickettes by electrolysis from an acid bath and form cap-shaped contacts. Two 0·2 mm diameter copper wires are soldered at each end to the copper plated surfaces with a small quantity of tin, using a microsoldering iron. The thermometers are washed in spirits and covered with a layer of BF-2 adhesive which is polymerized in 2 hr at 180° C.

Results of the study of the thermometers

The resistance of the thermometers was measured potentiometrically using a PMS-48 potentiometer and a M-25 galvanometer. After some preliminary experiments it was established that the optimal value of the measuring current was 25 mA.

Preliminary experiments, carried out to choose the firing conditions, showed clearly (see Table 1) that raising the firing temperature leads to a reduction in the resistance of the thermometers.

This relation can be seen at any temperature of measurement, but is most strongly marked at low temperatures. As can be seen from the table, there is considerable scatter in the resistance values within each group of thermometers which have been fired at the same temperature. It is probable that this is due to the conditions of pressing (the brickettes not being exactly the same), and

---

† Received by PTÉ Editor 7 June 1960: *Pribory i Tekhnika Éksperimenta* No. 3, p. 194 (1961)

mainly to small differences of firing temperature produced by non-uniformity of temperature inside the furnace.

Table 1

Thermometer number	*Firing temperature (°C)*	*Thermometer resistance (Ω)*			
		273° K	*77° K*	*20·3° K*	*4·2° K*
5-1	750	2·4	10·2		Above 5,000
5-2	750	2·7	12·6		
5-3	750	2·35	9·5		
5-4	750	2·1	9·3		
5-5	750	2·5	12·2		
5-6	750	2·6	11·7		
7-1	770	1·5	5·75		
7-2	770	1·3	6·1		
7-3	770	1·65	6·2		
7-4	770	1·75	6·6		
7-5	770	1·87	6·8		
7-6	770	1·8	6·65		
8-1	780	1·7	6·5		
8-2	780	1·6	5·4		
8-3	780	2·0	8·1		
8-4	780	1·6	4·5		
8-5	780	1·62	4·8		
8-6	780	1·7	6·5		
9-1	790	1·24	3·57	32·8	4,348
9-2	790	1·26	3·7	32·0	3,855
9-3	790	1·17	2·7	17·1	959
9-4	790	1·23	3·6	34·1	4,768
9-5	790	0·84	2·3	13·9	836
9-6	790	0·88	2·1	12·0	544
80-1	800	0·9	1·77	6·7	145·8
80-2	800	0·7	1·37	4·1	47·7
80-3	800	0·6	1·0	2·5	17·7
80-4	800	0·64	1·2	3·7	30·2
80-5	800	0·45	0·66	1·3	6·6
80-6	800	1·1	2·0	8·0	200
81-1	810	0·55	0·95		25·7
81-2	810	0·5	0·8		13·15
81-3	810	0·54	1·0		33·5
81-4	810	0·54	0·9		12·1
81-5	810	0·5	0·8		8·75
81-6	810	0·6	0·85		12·05

Typical temperature variations of resistance for thermometers fired at three temperatures, 790°, 800°, and 810° C, are shown in Figure 1 (logarithm of the resistance as a function of the reciprocal of the absolute temperature).

It is generally assumed that the temperature dependence of resistance of semiconductors in the intrinsic region can be described approximately by the equation

$$\rho = c\exp(W_g/2kT) \qquad \ldots (1)$$

where W_g is the activation energy for the creation of carriers.

As can be seen from Figure 1, this simple formula only gives the general character of the dependence for carbon thermometers, and is insufficiently exact for practical use in temperature measurement. Calculations show that between 20° and 2° K the interpolation formula proposed by Clement and Quinnel[5] gives satisfactory results for our carbon thermometers:

$$\log R + K/\log R = A + B/T \qquad \ldots (2)$$

where K, A, and B are constants.

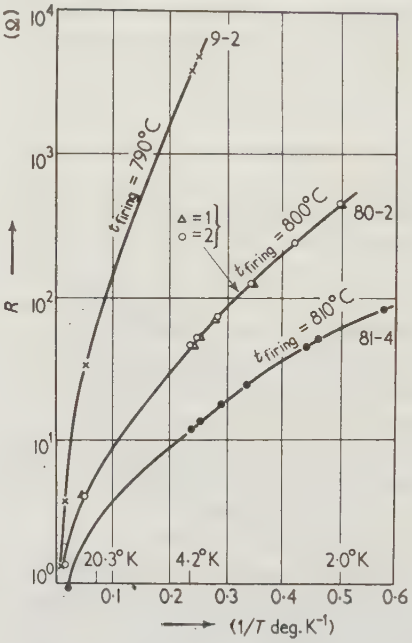

Figure 1. The temperature dependence of the resistance of thermometers which have had different thermal treatments. Thermometer 80–2 was studied before and after 100 repeated cycles of cooling and warming from room to nitrogen temperature: 1, before the 100 coolings; 2, after the 100 coolings

If these constants are determined from the resistance values at 2°, 4·2°, and 20·4° K, temperatures from 2° to 4·2° K can be calculated with an accuracy of a few hundredths of a degree. To achieve greater accuracy a detailed calibration of each thermometer is essential, and the results can be tabulated or expressed as a graph $T = f(R)$. Vroomen[9] considers it more convenient in practice to construct for each thermometer a graph of the corrections ('deviations') to function (2) which can be calculated with great accuracy and tabulated for any one thermometer of a given type.

As can be seen from Figure 1, the curve $\log R = f(T^{-1})$ becomes flatter the higher the firing temperature and corresponds to a shift of the region of a rapid increase of resistance in the direction of ever lower temperatures. The constant B in equation (2) which characterizes the slope of the curve and can be considered proportional to the activation energy rapidly decreases, as is seen from the curve in Figure 2 (constructed on the basis of studies of three thermometers Nos. 9-2, 80-2 and 81-4).

It was important to examine the reproducibility of the thermometer calibrations. One must distinguish two cases: (1) the reproducibility during one helium experiment and (2) the reproducibility after one or several cycles of cooling and heating up to room temperature. Experiments showed that during one helium experiment there is complete reproducibility, i.e. the errors in measuring the temperature are determined only by the accuracy of reading the helium vapour pressure if, as in our case, an ordinary mercury manometer is used. On the other hand, differences of resistance after repeated cycles of cooling and heating are easily observed. The temperature variation of resistance of thermometer 80-2 is shown in Figure 1 before and after a hundred coolings and heatings from room temperature to nitrogen temperature. It can be seen from Figure 1 that the change in calibration after such treatment is small. In the worst case the ambiguity in measuring temperature in the range from 2° to 4·2° K did not exceed $\simeq 0{\cdot}01°$ K.

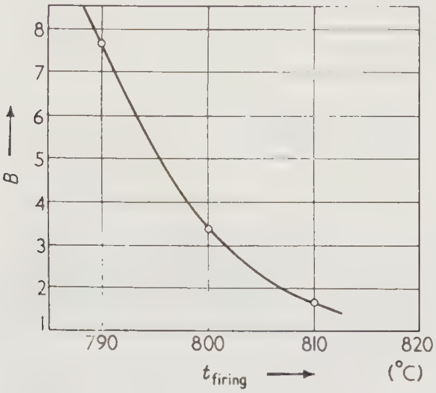

Figure 2. The variation of the constant B of the interpolation formula (2) as a function of the firing temperature of the carbon thermometers

Conclusions

A technique has been developed for preparing carbon resistance thermometers for low temperatures with sufficiently reproducible properties, using petroleum pitch as the only initial material. It is shown that the form of the temperature dependence of the resistance of the carbon thermometers is determined by the temperature of firing. Thermometers fired at 810° C are most convenient for measurements in the helium region. Thermometers fired at 790° C and 800° C are suitable for measurements in the hydrogen temperature region and in the intermediate range between hydrogen and helium temperatures.

REFERENCES

1. GIAUQUE, W. F. *Industr. Engng Chem.* **28**, 743 (1936)
2. ZAVARITSKII, N. V., and SHAL'NIKOV, A. I. *Prib. i Tekh. Eksper.* No. 1, p. 189 (1961), *Cryogenics* **1**, 235 (1961)
3. FAIRBANK, H. A., and LANE, C. T. *Rev. sci. Instrum.* **18**, 525 (1947)
4. CLEMENT, J. R., and QUINNELL, E. H. *Phys. Rev.* **79**, 1028 (1950)
5. CLEMENT, J. R., and QUINNELL, E. H. *Rev. sci. Instrum.* **23**, 213 (1952)
6. BERMAN, R. *Rev. sci. Instrum.* **25**, 94 (1954)
7. GIAUQUE, W. F., STOUT, J. W., and CLARK, C. W. *J. Amer. chem. Soc.* **60**, 1053 (1938)
8. SHARVIN, YU. V. *Prib. i Tekh. Eksper.* No. 1, p. 147 (1959)
9. VROOMEN, A. R. *Bull. Inst. Int. Froid*, Suppl. 137. Annexe 1958–1

This paper has been specially translated for CRYOGENICS and is included by permission of the Editors of *Pribory i Tekhnika Éksperimenta*. We are also indebted to the Instrument Society of America and the Plenum Press, who publish their own cover-to-cover translation of PTÉ by arrangement with the Russian publisher.

A Hydrogen Liquefier with an Output of 50 l./hr of Liquid Hydrogen

A. G. Zel'dovich and Yu. K. Pilipenko *United Institute for Nuclear Studies, U.S.S.R.*

Received 18 July 1960†

THE use of liquid hydrogen bubble chambers in physical experiments has made it necessary to provide hydrogen liquefaction plants with an output of 50–200 l./hr. The hydrogen liquefier described was designed as an independent plant or as the hydrogen section of a combined hydrogen–helium liquefier. The construction of the liquefier provides for obtaining liquid para-hydrogen and for operating as a refrigerator.

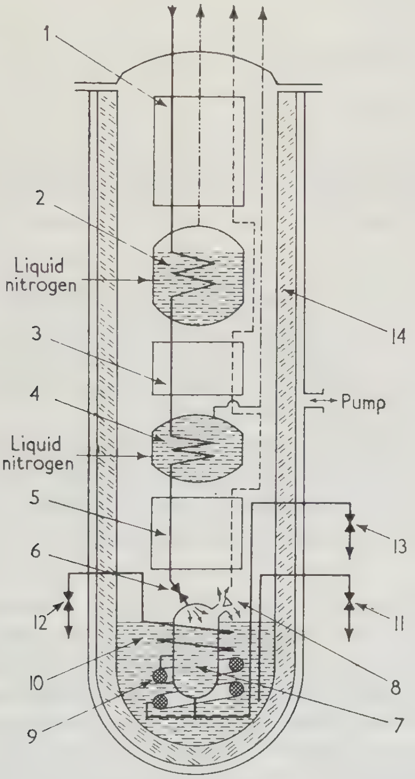

—— High pressure hydrogen - - - Low pressure hydrogen
··—·· Gaseous nitrogen —·— Pumped nitrogen

1. Warm region heat exchanger; 2, Bath of liquid nitrogen, boiling at atmospheric pressure; 3, Heat exchanger between the nitrogen baths; 4, Bath of liquid nitrogen, boiling under reduced pressure; 5, Cold region heat exchanger; 6, Throttling valve; 7, Additional collector; 8, Helium valve; 9, Reaction tube; 10, Condenser coil; 11 Draw-off valve for normal hydrogen; 12, Draw-off valve for *para*-hydrogen; 13, Draw-off valve for normal hydrogen from the additional collector; 14; Insulating Dewar

Figure 1. Arrangement of liquefier

The arrangement of the liquefier is shown in Figure 1. Liquefaction is produced by a throttling cycle with liquid nitrogen precooling. The preliminary precooling takes place in two stages: by nitrogen boiling at atmospheric pressure, and by nitrogen boiling under vacuum. The special feature of the arrangement is the presence of an additional collector, 7, with the valve 8. The through cross-section of the valve is regulated by changing the pressure of helium in a bellows volume.

For liquefying normal hydrogen the helium valve 8 is fully open and the liquid hydrogen runs over from the collector 7 into the lower part of the insulated Dewar 14, used as the collector of normal hydrogen. To obtain *para*-hydrogen, the draw-off valve 12 is opened. The liquid hydrogen passes from the additional collector into the reaction tube 9, containing a catalyst, and then into the coil condenser 10. The *ortho-para* heat of conversion given off in the reaction tube is partly taken off through its heat transfer surface. The remaining part of the heat produces evaporation of some of the converted hydrogen. Condensation and undercooling of the *para*-hydrogen obtained takes place in the coil condenser. The heat transfer is achieved by the normal hydrogen boiling in the Dewar. The quantity of *para*-hydrogen drawn off is regulated in such a way that a fraction of the liquefied normal hydrogen flows from the additional collector 7 into the Dewar 14, maintaining a fixed level there. The necessary temperature difference in the condenser coil is produced by increasing the pressure in the additional collector to 2·5–3 atm by using the helium valve. The reaction tube of the liquefier is made in the form of a coil out of 38 mm diameter copper tubing. The catalyst is ferric hydroxide, prepared in our laboratory on the basis of Buyanov's studies.[1] The volume of catalyst was reckoned according to the accepted specifications[2] and amounted to 1,300 cm^3.

The inclusion of the additional collector with the helium valve in the liquefier construction makes it possible to recover the saturated vapour pressure in the liquefier after using the necessary latent heat of evaporation of hydrogen. The refrigerating capacity is doubled by using

---

† Received by PTÉ Editor 19 April 1960: *Pribory i Tekhnika Éksperimenta* No. 2, p.185 (1961)

the cold from the evaporating hydrogen (in the refrigeration cycle). In this case the liquid hydrogen is drawn off from the additional collector through valve 13 and the evaporated hydrogen returns to the lower part of the Dewar through the draw-off valve 11 or through a special siphon. It is convenient to use such a system of operation of the liquefier in order to maintain a constant thermal regime in liquid hydrogen bubble chambers.

The liquefier is thermally insulated by a metal Dewar, filled with Mipor pumped to fore-vacuum pressure; the Mipor layer is 80 mm thick. Free space is left between the Mipor and the outer wall of the Dewar, to improve the pumping.[3] There is no liquid nitrogen shielding. The liquefier apparatus is in hydrogen vapours within the Dewar, like a number of other plants.[4] The lid is at room temperature and the base at liquid hydrogen temperature. The absence of heat exchange by convection between parts of the liquefier at different temperatures is achieved by (1) the warmer parts of the apparatus being above the colder; (2) the temperature of all parts in any horizontal section being the same; (3) insulation of any tube for which the temperature does not correspond to that of a given section.

The type of insulation used has several advantages: (1) leaks which frequently spoil the working of apparatus using the usual vacuum insulation are not dangerous in this case; (2) it is easy to achieve vacuum tightness of the Dewar because of the small number of joins; (3) it facilitates access to the heat exchange apparatus.

The heat exchangers are made of bundles of soldered tubes. Since the heat flow along the tubes is very small, all the heat exchangers (including the heat exchanger of the 'cold' region) are made of copper. The inner shell of the Dewar is made of stainless steel, the outer of ordinary carbon steel. The tubes for drawing off the liquid hydrogen and also the nitrogen siphons, have their own vacuum insulation. The usual level devices for low boiling liquids are used in the liquefier. These only give correct readings if the tube going to the lower part of the vessel is full of vapour, produced by boiling off the liquid. In our case the necessary heat supply is provided by the heat conductivity of the tubes and by the extra layers, which are insulated to prevent heat leakage.

The performance of the liquefier is given in Table 1. The experimental measurements showed that the refrigerating capacity of the liquefier (No. 2 in the table) is used in the following way:

	Q (kJ/hr)	(per cent)
On liquefying hydrogen	191	82
As a result of non-regeneration and pressure losses of the reverse flow	40·6	17·5
On heat flow from the surroundings and the spontaneous *ortho-para* conversion	1·3	0·5
Total	232·9	100

The heat flow from the surroundings is determined from the amount of hydrogen boiled off from the Dewar after the end of the operation. The loss resulting from non-regeneration is determined from the difference. If the heat flow through the insulation is referred to the parts of the Dewar inside which the hydrogen region apparatus is contained, i.e. to the region lower than the bath of pumped nitrogen, then it amounts to 1·4 kJ/m^2. The consumption of liquid nitrogen is 1·3–1·35 l. per litre of liquid hydrogen. It takes 1·5 hr to cool the apparatus to the start of liquefaction, and this requires 90 l. of liquid nitrogen. Compressors 2RG3/350 and 1 VUV are used to compress the hydrogen.

Table 1. Performance of the Liquefier

Number	1	2	3
Quantity of compressed hydrogen (m^3(n.t.p.)/hr)	150	190	150
Pressure of compressed hydrogen (atm)	140	135	140
Pressure:			
In pumped nitrogen bath (mm Hg)	140	140	140
In additional collector (atm)	0·3	0·5	2·5–3·0
In the Dewar (atm)	0·3	0·5	0·3
para-hydrogen in liquid produced (per cent)	25 (normal)	25 (normal)	99
Output of liquefier (l./hr)	40–42	50–52	28–30

We must point out that there is the possibility of boosting the liquefier by increasing the amount of compressed hydrogen to 260–280 m^3(n.t.p.)/hr and by raising the pressure in the Dewar to 1·0 atm. The expected output is then ≃ 70 l./hr of liquid hydrogen.

The efficiency of the liquefier was also tested when filling the insulating space of the Dewar with carbon dioxide at 0·2 atm (after preliminary pumping out with a fore-vacuum pump). No change in the output was observed.

The authors take this opportunity of expressing their thanks to V. A. Belushkin, L. B. Golovanov, L. P. Belonogova, and A. A. Belushkina, who took part in the construction of the liquefier; to R. A. Buyanov who made a study of the catalysis, and to K. A. Baicher, V. N. Dmitrievska, and other colleagues of the workshops and hydrogen station, by whose efforts the liquefier was built, set up, and tested.

REFERENCES

1. Buyanov, R. A. *Kinetics and Catalysis* **1,** 306, 418, 617 (1960)
2. Buyanov, R. A., Zel'dovich, A. G., and Pilipenko, Yu. K. *Prib. i Tekh. Eksper.* No. 2, 188 (1961); a translation of this paper will appear in *Cryogenics* **2,** No. 3 (1962)
3. Zel'dovich, A. G. *Automatic Indication* No. 105835, q 27/70
4. Daunt, J. G. *Low Temperature Physics* (Russian Translation, 1959)

This paper has been specially translated for CRYOGENICS and is included by permission of the Editors of *Pribory i Tekhnika Éksperimenta.* We are also indebted to the Instrument Society of America and the Plenum Press, who publish their own cover-to-cover translation of PTÉ by arrangement with the Russian publisher.

The Effect of the Martensitic Transformation on the Electrical Resistance of Lithium and Dilute Lithium–Magnesium Alloys

J. S. Dugdale *National Research Council, Ottawa*

D. Gugan *H. H. Wills Physics Laboratory, Bristol*

Received 27 September 1961

In an earlier publication[1] we described experiments from which we were able to deduce the electrical resistivity of the two phases of sodium at low temperatures. We were interested in the properties of the two phases of sodium partly because its low temperature phase provides the first known example of a hexagonal monovalent metal and partly because sodium has long been regarded from a theoretical point of view as a very good approximation to a free electron metal. Lithium also transforms at low temperatures by the martensitic mechanism, but in lithium there is an extra complication because the b.c.c. phase, which is stable at high temperatures, can transform to either of *two* faulted close-packed phases according to the conditions of the experiment.[2–5] Although lithium has only three electrons in the free atom and is thus fundamentally a simpler element than sodium, its band structure in the solid state is almost certainly more complicated than that of sodium and, at least in the body-centred phase, its Fermi surface is probably highly distorted.[6–8] Lithium therefore provides an interesting contrast to sodium and it was our intention to determine the electrical resistivity of the three phases of lithium by experiments similar to those on sodium. For reasons which we explain below, we were not in fact able to do this in full detail, but we have established certain facts about the resistivity of the different phases and these do indeed present a contrast to the corresponding data for sodium.

It turns out that in general the electrical behaviour of lithium is more complex than that of sodium; for example, in its sensitivity to small amounts of impurity. We have therefore extended our measurements to include a range of dilute alloys of lithium with magnesium and by means of these measurements we have, we believe, been able to throw some light on the behaviour of pure lithium. We have reported elsewhere the results of our experiments on the electrical resistivity of lithium-6;[9] these experiments indicate that the effects of phase transformation are essentially similar in the two isotopes.

The structure of the low temperature phases of lithium

An important fact which emerged from the experiments of Barrett[3] and of Barrett and Trautz[5] is that the low temperature phase produced spontaneously by cooling a sample of lithium is predominantly close-packed hexagonal whereas that produced by *deformation* at low temperatures is predominantly close-packed cubic; in sodium only the close-packed hexagonal phase is formed. In writing of lithium, Barrett[3] says: 'It would be appropriate to describe the structure of the spontaneously formed low-temperature phase as a nearly random placement of each successive layer of atoms in the hollows of the layer just below, or alternatively as an f.c.c. structure with very imperfect stacking of (111) planes.' Of the other close-packed phase he writes: 'In the further transition to the f.c.c. structure the sequence [of close-packed layers] becomes A′B′C′A′B′C′ . . . without change in the hexagonal atom pattern of each layer, and with relatively infrequent breaks in the sequence, a change brought about by deforming the metal at low temperatures.'

Details of the martensitic transformation in lithium

We shall give here the basic facts about the martensitic transformation in pure lithium and in lithium–magnesium alloys; for a description of the *general* features of martensitic transformation we refer the reader to reference 1.

Figure 1(a) shows schematically the proportion of the low temperature phase as a function of temperature for a substance undergoing a martensitic transformation. Figure 1(b) shows the *difference* in phase composition as a function of temperature; it is the difference between curves (1) and (2) of Figure 1(a) plotted against the temperature. This difference in phase composition shows itself as a temperature hysteresis in a number of physical properties (cf. Figure 3). The important temperatures from our point of view are M_s, the temperature at which the transformation begins; M_r, the temperature at which reversion begins; and T_B (or M_{rf} in some schemes of notation) the temperature at which reversion is complete.

Large grained specimens of pure lithium can have an M_s as high as 80° K,[10] and plastically deformed specimens can have M_s as low as 67·5° K.[11] For pure lithium, however, M_s is usually between 70° and 75° K, and the specimens used in this work nearly all had values of about 72° K.

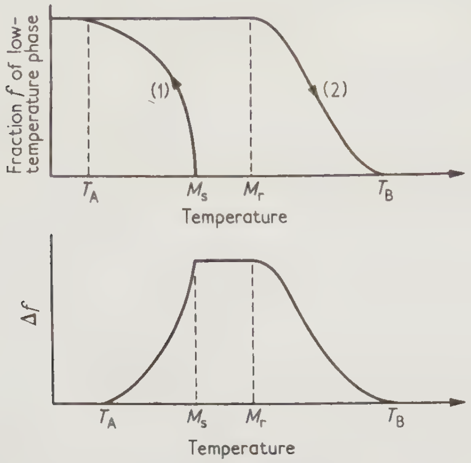

Figure 1 (a). Schematic diagram showing the fraction of the low temperature phase present at different temperatures in a substance undergoing a martensitic transformation

Figure 1 (b). The difference between the phase composition of the substance at a given temperature on first cooling to that temperature and on re-warming to that temperature after cooling to very low temperatures

The experiments on dilute alloys of magnesium in lithium show that M_s increases by about 10° K for each atomic per cent of added magnesium.[5] The reversion region in lithium (M_r to T_B in Figure 1) is from 95° to 170° K, rapid reversion beginning at about 100° K and extending to about 120° K where the rate of reversion becomes small. In the alloys the bulk of the reversion appears to occur at a temperature which is higher than in pure lithium by about 10° K per atomic per cent of added magnesium although the temperature of the end of the reversion (T_B) appears to be rather lower than in pure lithium, at about 160° K.[12]

The amount of the h.c.p. phase that can be produced by thermal cycling appears from X-ray studies on pure annealed samples of lithium to be about 50 per cent at about 60° K;[3,5] the same appears to be true in lithium magnesium alloys. According to Hull and Rosenberg[13] about 90 per cent of a pure lithium specimen transforms spontaneously by 6° K; this would seem to be consistent with Barrett's figure at 60° K if the transformation curve has the shape deduced by Martin[14] from his specific heat measurements. This large amount transformed would indicate that the transformation is not readily stopped by strain. It is therefore not surprising that the amount transformed is not very sensitive to the physical state of the specimens used. Moreover, Martin's experiments show that simple thermal cycling does not inhibit the transformation in lithium to any significant extent in contrast to the behaviour of sodium.[1,15] Because we were able to inhibit the transformation in sodium by thermal cycling, we were able to study the resistivity of the two phases of sodium in considerable detail; the absence of this effect in lithium has prevented us from obtaining such detailed information about lithium.

The effect of plastic deformation at low temperatures was studied by Barrett and Trautz[5] in pure lithium and in lithium–magnesium alloys. As already mentioned they found that plastic deformation produced an f.c.c. phase. Cold work at 78° K produced up to 50 per cent of this phase in pure lithium and higher proportions in dilute lithium–magnesium alloys. They found that the lower the temperature of deformation the greater the fraction of f.c.c. phase that was formed and although they made no deformation experiments below 78° K it seems reasonable from their work at higher temperatures to assume that at 4° K almost the whole specimen can be converted by cold work to the f.c.c. phase (cf. Figure 8 of reference 5). In the present work we have deformed wires by stretching at 4° K and by squashing at 78° K. In the experiments at 4° K we shall assume that in both pure lithium and the alloys we were able to convert the whole specimen to the f.c.c. phase; in the experiments at 78° K we shall see below that it is possible to estimate the amount of f.c.c. phase which has been produced by the deformation. All the estimates of the amounts transformed are approximate with an error of at least ± 5 per cent, and more probably ± 10 per cent.

We have considered the question of the *distribution* of the phases in our work on sodium.[1] In lithium we shall see that all the changes of resistivity on transforming are relatively small, and in this case we make no serious error in assuming that the various phases act as if they are electrically in series.

Our description of the transformation in lithium has so far been based on fairly well established facts, but there are three other phenomena which may be important in these experiments but about which little can be said with certainty.

Firstly, it is known from the experiments of Barrett and Clifton[16] that in at least some lithium–magnesium alloys there can be thermoelastic changes of phase composition (i.e. a change of composition with temperature which does not show a temperature hysteresis). However, the alloy which they studied was relatively rich in magnesium and, for the same reasons that we have already given for sodium,[1] we shall assume that none of our specimens undergoes appreciable thermoelastic transformation. Secondly, we know that in some transformations of the martensitic kind the amount of transformation can be reduced by suitable deformation or heat treatment; this is known as *stabilization*. Although these effects are small in lithium, they must modify the transformation and reversion to some extent (cf. the reversion curve for lithium observed by Martin[15]). Nevertheless, we shall ignore any effects of stabilization on our estimates of the *amount* of transformation (see, in particular, page 110).

Lastly, we have, in the outline above, taken the simple view that only the b.c.c. and h.c.p. phases are involved in the spontaneous (thermal) transformation and reversion. It appears that the thermodynamically stable phase is the f.c.c. one and it would therefore not be surprising to find that the f.c.c. phase can play some part even in the spontaneous transformation. The X-ray results seem to show quite definitely that the f.c.c. phase is *not* produced during spontaneous transformation, but there is no firm X-ray evidence on whether or not it can exist as a transient phase during the reversion. The present experiments as well as those of Martin[14] indicate that there may be some such effect in well annealed samples of pure lithium.

The specimens

In these experiments we studied samples from three batches of pure lithium which we shall refer to as A, B, and C; they were of increasing purity in that order, although B and C were rather similar. We also studied a series of dilute alloys of magnesium in lithium which were made from lithium of batch A with the appropriate amount of high purity magnesium added. A master alloy containing 10 atomic per cent of magnesium was prepared by the method described by Barrett and Trautz,[5] and alloys of the required concentration were then made by diluting the master alloy with pure lithium.

We shall distinguish between the different specimens of pure lithium by giving each one a number (which merely indicates the order in which the specimens were made) and a letter, A, B, or C, which indicates the batch from which the specimen was made. The alloys are distinguished by giving in each case the amount of magnesium in the alloy; thus the alloy containing 0·95 *atomic* per cent of magnesium we write as LiMg 0·95%.

In order to compare the alloys with each other and with pure lithium it was necessary to determine their absolute resistivities at one temperature. This was done by extruding a sample of the material into the form of a rod, about 10 cm long and 0·5 cm in diameter. The dimensions and electrical resistance of the rod were then measured at room temperature. The mean diameter was measured with a micrometer, the average random error in these measurements being about 0·5 per cent and the estimated total error in the resistivity about 1 per cent. Values of the resistivity of pure lithium and of several alloys of known composition are given in Table 1 together with the corresponding residual resistivity, ρ_0, measured at 4·2° K. Details of all the pure lithium samples are given in Table 2.

Experimental results—the h.c.p. phase

To study the electrical resistance of the spontaneously formed h.c.p. phase, we used two methods which we shall call 'the variable temperature method' and 'the reference temperature method'. In the first, we cool the specimen to a low temperature (4° or 10° K), measuring the electrical resistivity at about 10° intervals during the cooling process and then again at the same temperatures during the warming process. In this way we find out how the resistance of the specimen at various temperatures varies with the proportion of the two phases. Unfortunately this proportion is also a function of temperature and the two effects are hard to separate. In the second method, the resistance of the specimen is always measured at a fixed reference temperature above the M_s temperature and below that at which reversion begins. Between measurements the specimen is cooled to successively lower temperatures to study the effect on the resistance at the reference temperature of different proportions of the two phases. Because the reference temperature is below the reversion temperature the phase composition is not appreciably altered in warming the specimen back to the reference temperature and so the phase composition of the specimen corresponds to that of the lowest temperature to which it has been

Table 1. The Resistivity of Lithium–Magnesium Alloys

ρ_{295} (Ω*cm*)	ρ_0† (Ω*cm*)	*Magnesium in lithium*‡ (*atomic per cent*)
$9{\cdot}52 \times 10^{-6}$	$13{\cdot}8 \times 10^{-9}$	(0), pure lithium, batch B
9·58	59·5	0·05 ± 0·01
—	78	0·07 ± 0·01
9·78	250	0·21 ± 0·01
10·27	672	0·47 ± 0·015
10·68	1036	0·84 ± 0·015
11·07	1300	0·95 ± 0·015

† These results refer to two-phase mixtures (predominantly h.c.p.).

‡ We are indebted to Dr. Inman of the Department of Mines, Ottawa, for the flame-photometric analysis of these alloys.

Table 2. Summary of the Results of the Experiments on Pure Lithium

Specimen†	*Diameter* (*mm*)	*Heat treatment of specimens*	*Residual resistivity* (Ω*cm*)	*Percentage change at 80° K due to transformation*
Li (7A)	0·5	None‡	$25{\cdot}6 \times 10^{-9}$	−0·85
Li (16A)	0·5	None	30	−0·28
Li (8B)	0·5	None	13·8	+0·76
Li (12C)	0·5	None	10·6	+0·66
Li (13C)	0·5	None	10·6	+0·70
Li (15C)	0·5	None	10·9	+0·68
Li (19C)	0·5	None	10·6	+0·68
Li (18C)	3	20 hr at 150° C	8·9	−0·27
Same specimen after twice cooling to 4° K		6 hr at 50° C	9·2	0·00
Li (17C)	5	24 hr at 150° C	8·2	0 ± 0·2§

† The letter after the specimen reference number indicates the batch from which the specimen was made. Batches A and C were obtained from the Lithium Corporation of America. Batch B is of unknown origin.

‡ This means that, after extrusion, the wires were kept at room temperature for an hour or two before measurements began.

§ The specimen had such a large diameter that very accurate measurement of the resistance was not possible.

cooled. Then the specimen is warmed to successively higher temperatures between readings to study the reversion process.

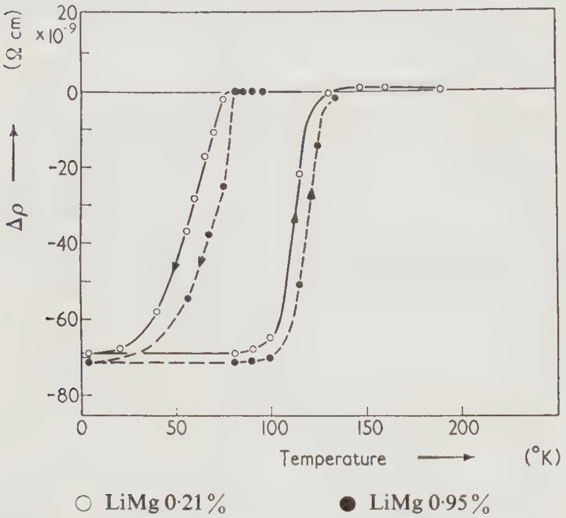

Figure 2. The change in resistivity of two lithium–magnesium alloys at 80·6° K as a function of the temperature to which the specimens were successively cooled (or heated) between readings

(1) *The alloys*

We consider first the results for the alloys since these are simpler.

The results of the reference temperature method applied to LiMg 0·21% and LiMg 0·95% are shown in Figure 2. If, as we might expect, the changes in the resistance at the reference temperature (≃ 80° K in these experiments) are proportional to the fraction of the h.c.p. phase present, then these curves should have the same shape as the transformation curves of the two specimens (cf. Figure 1(a)). The shape of these curves does indeed agree fairly well with the transformation curves deduced by other methods;[3, 14] we may therefore feel confident that we understand what is happening at this temperature. Two other features of the curves are noteworthy: first, that the resistivity of the transformed material is lower than that of the untransformed and, second, that the magnitude of the change is about the same in the two alloys. Expressed as a fraction of the *ideal* resistivity at this temperature, the three alloys (LiMg 0·21%, 0·47%, and 0·95%) all undergo a decrease of resistivity of between 5 and 8 per cent due to the transformation.

We consider now the results of the variable temperature method. Figure 3 shows the percentage difference between the resistance of the alloy specimens measured with decreasing temperature and that measured with increasing temperature, this difference being plotted as a function of the temperature. If the resistance due to impurities and that due to phonons both changed in the same way during the transformation and if Matthiessen's rule were applicable, the results of the variable temperature method would be closely related to those of the reference temperature method. The curve resulting from the former method would then roughly resemble that of Figure 1(b). A comparison of Figure 2 with the corresponding two curves in Figure 3 shows that above about 70° K the two different methods both show that the h.c.p. phase has a lower resistance than that of the b.c.c. phase. At lower temperatures, however, where the residual resistivity dominates, Figure 3 shows that the transformation now *increases* the resistance of the specimen, in complete contrast to the behaviour at 80° K shown in Figure 2. As we shall show below, this difference is attributable to departures from Matthiessen's rule.

It is possible to get a rough estimate of the magnitude of the change in residual resistance produced by the spontaneous transformation. We can use the information in Figure 2 as a guide to the amount of transformation at different temperatures. (If we use the transformation curves derived from specific heat measurements[14] we get similar results.) We see from Figure 2 that at 40° K the difference in composition on cooling and warming is rather less than 10 per cent of the total change which occurs. If the total amount spontaneously transformed at

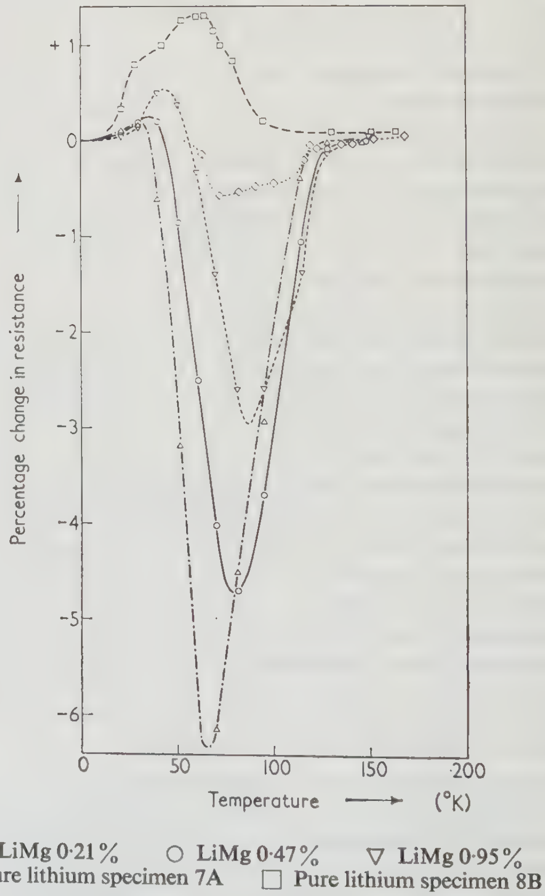

Figure 3. The percentage difference between the resistance of specimens measured with decreasing and increasing temperatures plotted as a function of temperature (the negative sign indicates a lower resistance after transformation)

4° K is about 90 per cent, the change in composition at 40° K (before and after cooling to 4·2° K) is thus about 10 per cent. According to Figure 3, this difference in composition increases the resistance of LiMg 0·95% by about 0·5 per cent, from which we deduce that a complete transformation would increase the resistance by 5 per cent. Since at 40° K most of the resistance is residual we deduce that the residual resistance of the spontaneously formed h.c.p. phase is at least 5 per cent higher than that of the b.c.c. phase. A similar result follows for the LiMg 0·21% alloy. Both these results tend to *underestimate* the change since the effect of the phonon scattering, which is in the opposite direction to that of the residual scattering, has not been taken into account. Our conclusion therefore is that the residual resistivity in the h.c.p. phase of the alloys is 5–10 per cent higher than that in the b.c.c. phase.

(2) *Pure Lithium*

Our results for several different specimens of pure lithium have been collected in Table 2. The last column gives the percentage change in resistance measured at 80°K caused by the spontaneous transformation (to transform the specimens, they were cooled to 4·2° K and brought back to 80° K). It is seen that all the changes are quite small. Certain other general features are clear: (1) the specimens from batch A, which are less pure than the others, show a *decrease* in resistance at 80° K on transforming; (2) specimens of the same size and heat treatment, but from the purer batches B and C, consistently show an *increase* of resistance on transforming; (3) the purest material (batch C) can be made to show a decrease of resistance on transforming if the specimens are big enough and are well annealed (e.g. specimen 18C; see also Table 3). Results of measurements by the variable temperature method on two pure lithium specimens have also been included in Figure 3.

Table 3. Resistance (in Arbitrary Units) of Lithium Specimen 18C after Annealing at ≃50° C for 6 hr

Temperatures to which the specimen was cooled (° *K*)	*Temperatures at which resistance was measured* (° *K*)					
	4·2	34·2	50·1	63·8	70·3	80·6
80·6	—	—	—	—	—	16035
70·3	—	—	—	—	11015	15977
63·8	—	—	—	8266	10996	15977
50·1	—	—	3824	8281	11013	15983
34·2	–	1041	3833	8297	11038	16006
4·2	143†	—	—	—	11043†	16037†

† Subsequent run after re-anneal.

Before going into further details we will give what we believe are the reasons for this behaviour. At temperatures at which the resistivity is predominantly due to phonons, the primary effect of the transformation, as in the alloys, is to *decrease* the resistivity of the specimens. However, for reasons which we shall discuss later, the magnitude of this decrease is much smaller in the pure specimens than in the alloys. In the purest specimens the decrease may be so small that if the transformation itself generates a large number of new scattering centres, thereby substantially increasing the residual resistivity of the specimen, this secondary effect can outweigh the primary effect and a net *increase* of resistivity can result. We expect that, in a large well-annealed specimen, the regions which transform (at least in the early stages of the transformation) will be comparatively big and free from defects in contrast to those in a small-grained specimen of small diameter. We thus expect the transformation to increase the residual resistivity of the small unannealed specimens much more than those which are large and well annealed. This seems to be borne out by the results in Table 2.

Another consequence of this explanation is as follows. From the nature of a martensitic transformation it is known that in general the specimens tend to become more strained as the transformation proceeds and that the regions which first transform are usually the largest and the most strain-free. This would mean that the specimen resistance as measured at a given temperature would tend to fall during the early stages of the transformation and tend to increase during the later stages. This kind of behaviour was indeed observed in an experiment on specimen 18C. In this experiment the specimen was cooled to successively lower temperatures below 80° K and after each cooling the resistance was measured at a series of reference temperatures up to and including 80° K. The temperatures and the values of resistance are given in Table 3. It is seen, for example, that as the proportion of the low temperature phase increases, the resistance at 80·6° K first falls and then rises. The resistance of the specimen at 70·3° K does likewise, but at 63·8° K, at which temperature only the later parts of the transformation take place, no decrease of resistance is seen.

Details of the reversion of specimen 18C are given in Figure 4 while in Figure 5 are shown the complete conversion–reversion cycles of specimens 7A and 8B, all obtained by the reference temperature method. (These figures should be compared with Figure 2 for the alloys.) During the reversion cycle all the pure specimens show a 'hump' just above 110° K. This is almost certainly due to an increase in the residual resistivity caused by new strains and defects generated in the specimen by the reversion processes. (This hump can also just be seen in the results of the variable temperature method although the effect is then found to be much smaller.) Ultrasonic experiments on samples of pure lithium[11] show that at this temperature during the reversion process there is a marked increase in the attentuation of the ultrasonic waves. The large peak which occurs at 160° K in the reversion curve of specimen 18C and to a lesser extent in that of specimen 7B is difficult to account for; since it occurs at a temperature at which almost all the low temperature phase is known to have disappeared it must imply that the resistivity of the body-centred phase has been substantially increased in the transformation and reversion process.

(3) *The change of shape of specimens on transformation*

The experiments of Basinski and Verdini[17] have shown that the change of specific volume on phase transformation is small. On the other hand, we know that the shear strain associated with the transformation is fairly large (cf. the discussion in the paper by Basinski and Verdini). We have therefore made some measurements to see how the change of shape of the wires we have used can affect the measured values of resistance. We measured directly the change in length of some thin wires which were prepared in the same way as the wires used in the resistance work and it appears that the change of shape in transforming can be sufficient to increase the resistance by about 0·5 per cent quite apart from any changes of resistivity which may occur. The shape factor, moreover, does not change in proportion to the phase composition of the wire, and in some cases about half of the change of shape factor persists after the specimen has completely reverted.

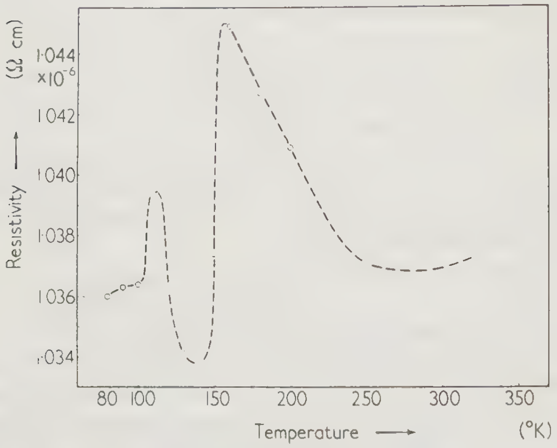

☐ Resistivity of the specimen on first cooling to 80° K
○ Resistivity after cooling to 4° K and subsequent warming to the temperature indicated

Figure 4. The change in resistivity of pure lithium specimen 18C measured at 80° K as a function of the temperature to which the specimen was successively heated between readings

In reducing the resistance results to values of resistivity we have assumed that the shape factor of our wires does not change with transformation. Thus this effect of the change of shape factor will be to give an apparent increase of resistivity. This effect shows itself to a certain extent in Figures 3, 4, and 7, for instance, where there are indications of a change of shape factor of about 0·1 per cent as a result of the transformation. This is smaller than the experiment on the change of length would lead us to expect, and it indicates that the change of shape factors are only important in our thin wires at the 0·2 per cent level. In the thicker rods, where the preferred orientation of the crystal grains is less, the effect should be less serious. This is probably a partial explanation of the change in sign of the results in the last column of Table 2 as the specimen size is changed.

This uncertainty about the shape factor means that the changes of resistivity on transformation are uncertain to about 0·2 per cent. This does not invalidate the conclusions we shall draw here, but it does mean that in a detailed interpretation of the reversion curves (cf. Figure 5) this extra effect must also be considered.

(4) *Departures from Matthiessen's rule*

From the measurements on the dilute lithium–magnesium alloys it soon became evident that Matthiessen's rule was not obeyed. In order to show this, we have subtracted from the measured resistivities of the alloys at each temperature the corresponding ideal resistivity as deduced from measurements on samples of the purest lithium. The ideal resistivity of pure lithium may itself be altered by the transformation but this uncertainty is small enough to be neglected for our present purpose.

In this way we have found out how the apparent residual resistivity, ρ_0, varies with temperature for the three alloys LiMg 0·21%, 0·47%, and 0·95%. The results are shown in Figure 6 as a function of both decreasing and increasing temperature. If Matthiessen's rule were strictly obeyed and if there were no transformation, ρ_0 would be a constant independent of temperature.

It is seen that below 100° K, ρ_0 falls markedly with falling temperature. This cannot be ascribed to the change of residual resistivity on transformation, since as we have seen from the variable temperature method, the transformation causes an increase in the resistivity at low temperatures. In other words, if the transformation did not occur the low temperature resistivity of the alloys would be even smaller thereby further decreasing the value of ρ_0 at low temperatures. It is therefore clear that

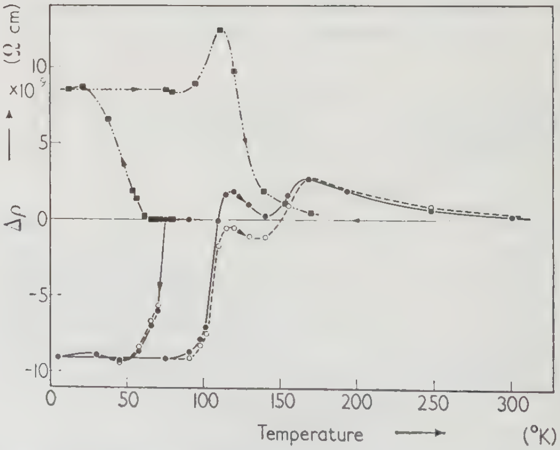

—●— Pure lithium specimen 7A measured at 74·8° K
--○-- Pure lithium specimen 7A measured at 90·4° K
-·■·- Pure lithium specimen 8B measured at 75·5° K

Figure 5. The change in resistivity of pure lithium specimens at a fixed reference temperature as a function of the temperature to which the specimens were successively cooled (or heated) between readings

in the b.c.c. phase there are large departures from Matthiessen's rule.

If at 4° K the specimens are almost completely transformed, the ρ_0 curve measured during the warming process is, up to about 90° K, essentially that of the h.c.p. phase. It is thus evident that departures from Matthiessen's rule must occur in this phase too, although they are smaller than those found in the body-centred phase.

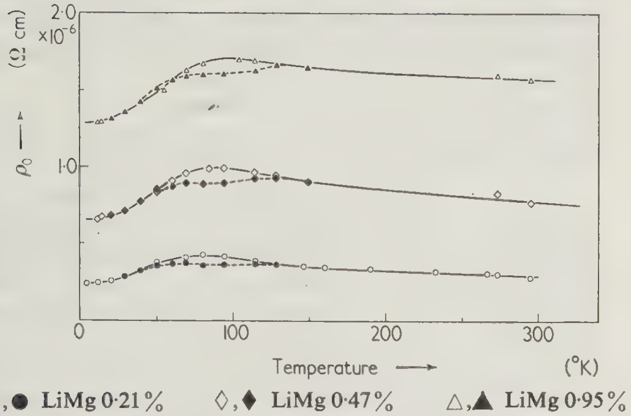

Figure 6. The apparent residual resistivity of lithium–magnesium alloys as a function of temperature, illustrating departures from Matthiessen's rule. The open symbols refer to measurements made with decreasing temperature and the full symbols to measurements made with increasing temperature

We have also compared the resistivities of specimens from two batches (A and C) of pure lithium and we find that marked departures from Matthiessen's rule occur here also as illustrated in Figure 7. In this we plot $\Delta\rho$, the difference in the resistivities of the two specimens as a function of decreasing and increasing temperature. We have indicated schematically how $\Delta\rho$ for the body-centred phase might be expected to vary with temperature if it could be measured down to the lowest temperature (dashed line in Figure 7).

Experimental results—h.c.p. phase; summary

The main features which emerge from these experiments may be summarized as follows:

(1) The spontaneous transformation from the b.c.c. to the h.c.p. phase *increases* the resistivity of the alloys at low temperatures.

(2) The spontaneous transformation always *decreases* the resistance of the alloys at 80° K.

(3) In pure samples of lithium the transformation can either increase or decrease the resistance at 80° K but all the changes are quite small. In a thick well annealed sample of the purest lithium the decrease in resistance at 80° K is about 0·25 per cent.

(4) There are large departures from Matthiessen's rule in both phases of the alloys and at least in the b.c.c. phase of quite pure lithium.

Experimental results—f.c.c. phase

(1) *The straining experiments at 4·2° K*

In order to study the residual resistivity of the f.c.c. phase, bare wires of pure lithium and of the lithium–magnesium alloys were deformed by stretching them in liquid helium. The resistance was measured as a function of strain and the results are shown in Figures 8(a) and 8(b). These show the *resistivity* of the specimens as a function of $\ln(l/l_0)$, where l is the instantaneous and l_0 the initial length of the specimen. In these curves we see that there are two regions of distinctly different character: first, the initial non-linear change of resistivity with strain and, second, the almost linear region which occurs at somewhat higher strains.

By comparison with the results of straining experiments on sodium[1] and on potassium[18] we attribute the almost linear region to the increase with strain of the number of dislocations in the specimens, whereas the curved region at low strains we attribute to the martensitic transformation, probably a transformation from the h.c.p. to the f.c.c. phase. This curved region is thus the part which interests us here and we have estimated the change in residual resistivity associated with this transformation, $\Delta\rho_0^m$, by extrapolating the linear part of the curve to zero strain as indicated in the figures. These values are listed in Table 4.

From the data shown in Figure 8 and in Table 4, we see that the transformation *increases* the residual resistivity; the values of $\Delta\rho_0^m/\rho_0$ for the alloys are all about 0·06 while the corresponding value for pure lithium is considerably greater. We discuss possible interpretations of these results below.

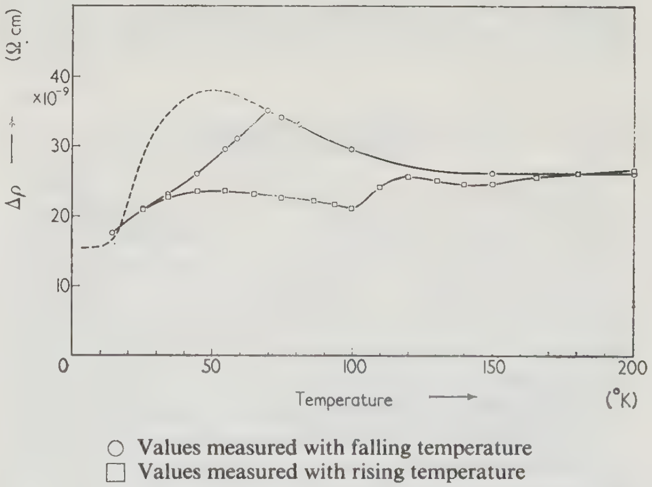

Figure 7. The difference in resistivity of two pure samples of lithium as a function of temperature. The sharp cusp at about 70° K in the falling temperature curve shows the onset of the transformation. The dashed line indicates schematically how the difference in resistivity of the pure body-centred phases might change with temperature below the transformation temperature

Table 4. Summary of the Straining Experiments

Approximate atomic percentage of magnesium in lithium	$\rho_0^\circ(\Omega cm)$	$\frac{\Delta\rho_0^m}{\rho_0}$	$\frac{\Delta\rho_0}{\Delta\epsilon}(\Omega cm)$
(0)	$15{\cdot}4\times10^{-9}$	0·11	$235\pm5\times10^{-9}$
(0)	14·6	0·17	—
0·07	82·8	0·06	335 ± 10
0·35	466	0·05	505 ± 50
0·73	969	0·065	515 ± 50
0·95	1290	0·058	550 ± 100

(2) *Deformation experiments at about 80°K*

In order to make a complete study of the temperature dependence of the resistivity of the f.c.c. phase it would be necessary to use a deformation cryostat capable of operating over a wide temperature range. It is, however, possible to obtain a certain amount of information about the f.c.c. phase from experiments using suitable fixed temperature baths and this is what we have done. The experiments consisted of first squashing a piece of wire (lithium or alloy) under liquid oxygen or nitrogen using a pair of precooled pliers; in this process the amount of deformation corresponded to an average of about 50 per cent reduction in thickness. The wire was then immersed in a series of different temperature baths (liquid helium, nitrogen, oxygen, acetone, and solid carbon dioxide) and the effect on its resistance of various thermal treatments was measured. We also made a number of experiments to test the reliability of these results and to make sure that the transient heating effects when the specimen was moved from one bath to another did not affect the results.

The sequence of the measurements and the assumed proportions of the different phases at each stage are shown in Table 5. As the table shows, the important assumptions we make are as follows: (*i*) that the deformation produces a fraction *f* of the f.c.c. phase only (we checked by measurements on the alloys at 90°K that no spontaneous transformation occurred before deformation); (*ii*) that during the subsequent cooling to 4°K, the remaining fraction (1 – *f*) of the b.c.c. phase is converted spontaneously to the h.c.p. phase while the f.c.c. phase remains unchanged; (*iii*) that in the final stage of the experiment, in which we start with the same specimens

Table 5. Sequence of Measurements in the Deformation Experiments

	Composition		
	b.c.c.	*h.c.p.*	*f.c.c.*
Squash at 77°K (or just above M_s)			
(1) Measure at 77°K, 90°K	(1–*f*)	0	*f*
(2) Cool and measure at 4·2°K	0	(1–*f*)	*f*
(3) Remeasure at 77°K, 90°K	0	(1–*f*)	*f*
Make specimen revert at 195°K (i.e. do not *anneal*)			
(4) Measure at 77°K, 90°K	1	0	0
(5) Cool and measure at 4·2°K	0	1	0
(6) Remeasure at 77°K, 90°K	0	1	0

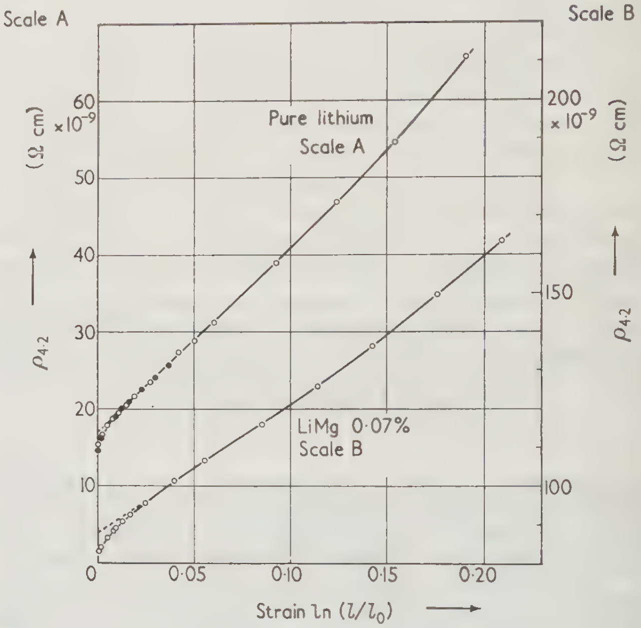

Figure 8(a). The resistivity at 4·2°K versus strain for specimens of pure lithium (B) (scale A) and for LiMg 0·07% (scale B)

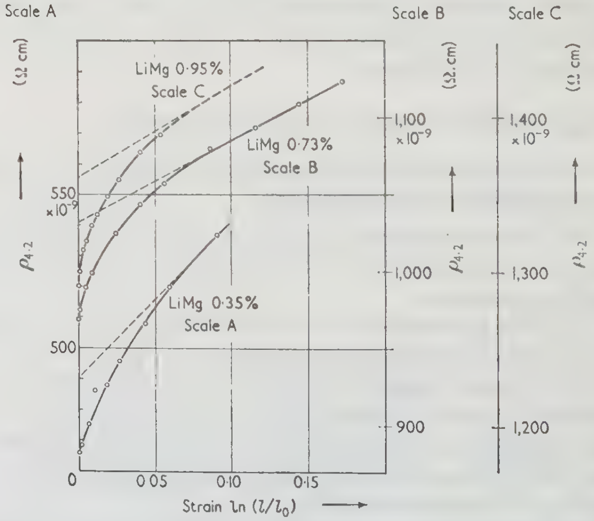

Figure 8(b). The resistivity of three lithium–magnesium alloys: LiMg 0·35% (scale A); LiMg 0·73% (scale B); LiMg 0·95% (scale C) untransformed at 77° or 90° K, cooling to 4° K converts them virtually completely to the h.c.p. phase.

Consider first the *total* resistance of the specimen at either 77° or 90° K. The effect of complete transformation from b.c.c. to h.c.p. is given by the difference between measurements (4) and (6) of Table 5. On the other hand, the effect of transforming a fraction $(1-f)$ of the specimen from b.c.c. to h.c.p. is given by the difference between (1) and (3). This therefore enables us to estimate f, the amount of f.c.c. phase formed by the deformation. If we now assume that strain contributions to the resistivity are the same at (1) and at (4), we can deduce from the difference between (1) and (4) the value of the resistance of a specimen containing only the f.c.c. phase.

This assumption about the strain contribution implies that by warming the specimens to 195° K we have caused them to revert to the b.c.c. phase without appreciably annealing them. This can be tested from the measurements at 4° K. Since we know the value of f at 4° K from the measurements at 77° or 90° K, we can use the result of section (1) above (page 109) to calculate what difference we should expect to find between the measurements (2) and (5), assuming that the same scattering centres exist in both states of the specimen. According to our findings in section (1), the intrinsic residual resistivity of the f.c.c. phase is about 6 per cent greater than that of the h.c.p. phase. Using this information we find that in our present experiments the observed difference in resistance between states (2) and (5) is close to that calculated on the assumption that the strain contribution to the resistivity is about the same for the two measurements. Our assumption is thus justified.

The results for f and for the resistance of each of the separate phases are given in Table 6 for two lithium–magnesium alloys; the values of f so found appear quite reasonable[5] and the two values for each alloy show that the measurements at the nitrogen and oxygen points are consistent. The same analysis applied to the measurements on pure lithium gave results with internal inconsistencies but in view of the results of section (1) it does not seem unreasonable to suppose that these may be due to the less predictable effects of strain in pure lithium and are not due to any fundamental error in the method.

Discussion

The following is an outline of the argument which we present in detail in the subsequent sections. In section (1) we conclude from the results of various experiments on lithium and dilute lithium–magnesium alloys (Knight shift, thermoelectric power, electrical resistivity, specific heats) that the properties of the Fermi surface at least in the b.c.c. and h.c.p. phases are not much changed by alloying with up to 1 per cent of magnesium. In section (2) we deduce from the results of the straining experiments at 4° K that there is an intrinsic difference between the electron properties of the h.c.p. and f.c.c. phases. In section (3) we argue that there is also a difference between the electron properties of the b.c.c. and h.c.p. phases and that this may explain why the b.c.c. and h.c.p. phases of pure lithium have almost the same resistivity at 80° K, in spite of their different Debye temperatures. In section (4) we observe that, because departures from Matthiessen's rule are smaller in the h.c.p. phase than in the b.c.c. phase, this difference between the phases probably accounts for the much larger changes in resistivity that are observed at 80° K when the alloys transform than are observed when pure lithium transforms. In section (5) we consider what we can deduce about the resistivity of the f.c.c. phases of the lithium–magnesium alloys at 80° K.

(1) *Change of the Fermi surface on alloying*

Hughes[19] has made measurements of the Knight shift in lithium and lithium–magnesium alloys from which it appears that the density of states in lithium is not greatly changed by alloying with magnesium. These measurements, made on the body-centred phase, show that the Knight shift decreases initially by about 1 per cent per atomic per cent of magnesium. The change in density of states, however, is thought to be considerably less than this.[19] We shall therefore assume that in the dilute alloys with which we are concerned the addition of magnesium does not significantly alter the Fermi surface in the body-centred phase.

Martin[20] has measured the electronic specific heat of both lithium and some lithium–magnesium alloys. His measurements were made on spontaneously transformed specimens at about 1° K which would thus be predominantly in the h.c.p. phase. His results show that the pure lithium specimen and the LiMg 1% alloy had the same electronic specific heat to within the experimental error of about 1 per cent. Moreover, experiments on the thermoelectric power below 1° K of lithium and its dilute alloys with magnesium[21] show no sign that the Fermi surface is changed by alloying at least up to 1 per cent of magnesium. In the discussion which follows we shall therefore assume that in none of the phases of lithium is the Fermi surface appreciably altered by the alloying with magnesium.

(2) *The change of residual resistivity in the strain-induced transformation*

The change of residual resistivity on transforming, $\Delta\rho_0^m$, as measured by the straining experiments, could arise from an intrinsic difference in the resistivity of the two phases (i.e. from a difference in electron properties in the two phases) or from changes in the number of imperfections capable of scattering the electrons or from a combination of both of these. The number of scattering centres does indeed change during the transformation; according to Barrett the large number of stacking faults in the h.c.p. phase is greatly diminished when the f.c.c. phase is formed (see page 103). On this basis we might expect the resistivity to diminish during the transformation from h.c.p. to f.c.c. However, as we have noted elsewhere, the scattering from stacking faults in pure lithium is almost certainly very small;[22] this would probably be true also of the alloys so that we shall ignore the effect of stacking faults here.

The values of $\Delta\rho_0^m/\rho_0$ (see Table 4) for the *alloys* are all fairly constant and equal to about 0·06, even though the magnitude of the residual resistivity itself changes by a factor of 15. Now we believe that the effect of tensile strain in transforming the specimens at 4° K is about the same in all the alloys, viz.: that we start with specimens predominantly in the h.c.p. phase and that strain converts them to predominantly the f.c.c. phase (cf. page 103). Thus the constancy of $\Delta\rho_0^m/\rho_0$ would seem to imply that the change is due to the different properties of the electrons in the two phases.

If we now consider the behaviour of pure *lithium*, we find that the value of $\Delta\rho_0^m/\rho_0$ is considerably higher than for the alloys. On the basis of our assumption discussed above, that the Fermi surface is not appreciably changed by alloying, we interpret this as follows. We assume that in pure lithium, as in the alloys, there is a contribution to $\Delta\rho_0^m/\rho_0$ of 0·06 from the change in electron properties, and that the remainder arises mainly from scattering by additional physical defects. (This scattering is presumably also present in the alloys but, assuming that it has approximately the same magnitude as in pure lithium, its contribution would be negligible in the more concentrated alloys. Even in the most dilute alloy it would contribute only about 25 per cent to $\Delta\rho_0^m$ and this could not be recognized with any certainty.) If this change of 0·06 corresponds to a complete change from h.c.p. to f.c.c. then the ratio of the residual resistivities in the two phases $\rho_0(\text{f.c.c.})/\rho_0(\text{h.c.p.})$ is equal to about 1·06.

(3) *The change in resistivity in the spontaneous transformation*

The residual resistivity. The spontaneous transformation increases the resistivity of the alloys at low temperatures. Since this occurs at temperatures where the scattering is almost all residual scattering, we conclude that the residual resistivity is higher in the h.c.p. phase than in the b.c.c. phase. This could arise if (1) there were an increase in the number of scattering centres in going from b.c.c. to h.c.p., and/or (2) if there were a change in the electron properties in going from one phase to the other. It is not possible to be certain which of these predominates but it does seem unlikely that additional physical defects could produce an increase in residual resistivity as large as 7×10^{-8} Ω cm (estimated from the data on the most concentrated alloy), which is five times larger than the total residual resistivity of our purest specimens. If it can be argued that the scattering from stacking faults, of which there is an abundance in the h.c.p. phase, can somehow be enhanced by the presence of impurity ions then this increase might be attributed to the formation of stacking faults. It has to be remembered, however, that the stacking faults are formed at a low temperature where appreciable diffusion is not possible (hence the martensitic nature of the transformation). We shall therefore tentatively assume that a change in electron properties is responsible for the observed increase in residual resistivity in going from the b.c.c. to the h.c.p. phase of the alloy. (Such a change in electron properties could not be a simple consequence of the volume change due to the transformation since this is known to be very small.[17])

We have, in addition, independent direct evidence for a change in the band structure of pure lithium associated with the spontaneous transformation. Recent measurements of the magnetic susceptibility of lithium in the neighbourhood of 80° K both before and after the spontaneous transformation show that the susceptibility (which is that of a paramagnetic) is greater in the h.c.p. phase than in the b.c.c. phase.[23, 24]

The change in resistivity of pure lithium on transforming at 80° K. It is clear from our experiments that in pure lithium the changes in resistivity at 80° K due to the spontaneous transformation are very small, probably less than 0·5 per cent. We know, however, from Martin's calorimetric measurements[14] that the Debye temperature θ_D is about 2·5 per cent higher in the hexagonal close-packed phase of lithium than in the body-centred phase and we should therefore expect to see a corresponding change in the ideal resistivity, as indeed we do in sodium.[1, 15]

We should expect, judging from the behaviour of sodium where our experiments show that the electron properties are *not* changed by the transformation, that at 80° K the resistivity of the hexagonal close-packed phase of lithium would be roughly 8 per cent lower than that of the body-centred phase because of the difference in θ values. The most probable reason why no such change is observed is that the change in electron properties, which in the preceding sub-section we deduced from the low temperature resistivity changes in the alloys and which would tend to increase the resistivity by 5–10 per cent, almost entirely offsets the effect at 80° K of the change in the value of θ.

(4) *The change in resistivity of the alloys on spontaneous transformation at 80° K*

The change in θ_D due to the transformation is about the same in the alloys as in pure lithium[12] and the change in electron properties is also assumed to be the same (see sub-section (2) above). We therefore expect that the change in 'ideal' resistivity (i.e. that part of the resistivity which arises from the phonon scattering) due to the transformation will be about as small in the alloys as it is in pure lithium. If, therefore, Matthiessen's rule were obeyed in both phases the change at 80° K would just reflect any change in the residual scattering. In fact the changes observed at 80° K are quite different and even in the opposite sense to those at 4° K (see page 106). We attribute this to departures from Matthiessen's rule which are greater in the b.c.c. phase than in the close-packed phase (cf. Figure 6). Departures from Matthiessen's rule not unlike those observed here have been found in dilute gold–silver and silver–gold alloys by Krautz and Schultz.[25]

Our observation that the change of absolute resistivity on transforming was about the same in all the alloys *appeared* to indicate that the changes were chiefly in the *ideal* resistivity. We now believe that this is a fortuitous appearance which arises in the alloys we have studied only because the magnitude of the departure from Matthiessen's rule is about the same for all these alloys.

In Figure 9, we show schematically what we believe to be the behaviour of the apparent residual resistivity of the two phases as a function of temperature. It is seen (Figure 9(a)) that at the lowest temperature ρ_0(b.c.c.) is less than ρ_0(h.c.p.). At high temperatures ρ_0(b.c.c.) is considerably larger than ρ_0(h.c.p.) because of the larger departures from Matthiessen's rule. In Figure 9(b) we indicate how a specimen following the transformation and reversion curves of Figure 9(c) would behave.

(5) *The change of resistivity of the alloys on strain-induced transformation at 80° K*

The results given in Table 6 show that the resistivity of the f.c.c. phase in the alloys is slightly higher than that of the h.c.p. phase. It is impossible to interpret these without knowing the resistivity of *pure* lithium in the f.c.c. phase and this we have not been able to find from our experiments. However, we have never observed a large change of resistivity on deforming pure lithium at 80° K and it would not be inconsistent to suppose that the ideal resistivity of the f.c.c. phase is quite similar to that of the b.c.c. and h.c.p. phases at 80° K. If this is the case then as with the other two phases, the f.c.c. phase of the alloys also shows large deviations from Matthiessen's rule.

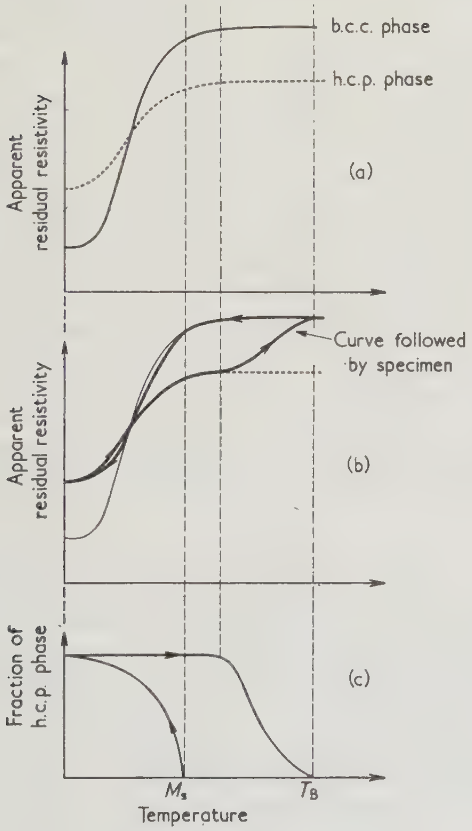

Figure 9. Schematic illustration of the variation of the apparent residual resistivity of the alloys with temperature in the two phases. (a) The apparent residual resistivity of the two pure phases. (b) The apparent residual resistivity (heavy line) which a specimen might show in following the transformation–reversion curve in (c) (cf. Figure 6). (c) The fraction of the close-packed phase present as a function of temperature on cooling and warming

Table 6. Summary of the Deformation Experiments at About 80° K

	LiMg 0·21%		*LiMg 0·95%*	
	N_2 point	*O_2 point*	*N_2 point*	*O_2 point*
Resistance (milliohms)				
b.c.c. phase	10·33	13·31	22·04	25·56
h.c.p. phase	9·93	12·97	21·66	25·11
f.c.c. phase	10·06	13·14	21·78	25·19
f, amount of f.c.c. phase produced by deformation	0·30	0·30	0·74	0·76

Summary

The changes in electrical resistivity of sodium and lithium which arise from the low temperature transformation provide an interesting contrast. At 44° K, the resistivity of the body-centred phase of sodium exceeds that of the hexagonal close-packed phase by about 15 per cent. At 80° K, which is the corresponding temperature for lithium, the difference between the ideal resistivity of the same two phases of lithium is probably less than 0·5 per cent. On the other hand the transformation has no intrinsic effect on the residual resistivity of sodium (within the experimental error of ± 1 per cent), whereas in lithium we estimate that the resistivity of the hexagonal close-packed phase exceeds that of the body-centred phase by about 10 per cent. Finally, there is in lithium the f.c.c. phase, which has no counterpart in sodium. Its residual resistivity is about 10 per cent higher again than that of the h.c.p. phase.

We are grateful to Dr. D. K. C. MacDonald for his encouragement and interest in this work. We would also like to thank our colleagues in the laboratory, in particular Doctors Z. S. Basinski, D. G. Hughes, D. L. Martin, and L. Verdini, for many helpful discussions. We are also indebted to Dr. K. Okumura for his help with the experiments, to Mr. A. A. M. Croxon for his technical assistance, and to Doctors R. G. Chambers, A. V. Gold and D. K. C.

MacDonald for reading the manuscript. One of us (D. G.) wishes to thank the University of Bristol for the award of an I.C.I. Fellowship during the tenure of which this work was completed.

REFERENCES

1. Dugdale, J. S., and Gugan, D. *Proc. roy. Soc.* **A254,** 184 (1960)
2. Barrett, C. S. *Phys. Rev.* **72,** 245 (1947)
3. Barrett, C. S. *Imperfections in Nearly Perfect Crystals*, p. 343 (Wiley, New York, 1950)
4. Barrett, C. S. *Acta Cryst. Camb.* **9,** 671 (1956)
5. Barrett, C. S., and Trautz, C. R. *Trans. Amer. Inst. min. (metall.) Engrs* **175,** 579 (1948)
6. Cohen, M. H., and Heine, V. *Advanc. Phys.* **7,** 395 (1958)
7. Ham, F. S. *The Fermi Surface*, p. 9 (Wiley, New York, 1960)
8. Cornwell, J. F. *Proc. roy. Soc.* **A261,** 551 (1961)
9. Dugdale, J. S., Gugan, D., and Okumura, K. *Proc. roy. Soc.* **A263,** 407 (1961)
10. Bowles, J. S. *J. Metals* **191** (3), 44 (1951)
11. Verdini, L. To be published.
12. Martin, D. L. *Canad. J. Phys.* **38,** 25 (1960)
13. Hull, D., and Rosenberg, H. M. *Cryogenics* **1,** 27 (1960)
14. Martin, D. L. *Proc. roy. Soc.* **A254,** 444 (1960)
15. Martin, D. L. *Proc. roy. Soc.* **A254,** 433 (1960)
16. Barrett, C. S. and Clifton, D. F. *J. Metals* **188,** 1329 (1950)
17. Basinski, Z. S., and Verdini, L. *Phil. Mag.* **4,** 1311 (1959)
18. Basinski, Z. S., Dugdale, J. S., and Gugan, D. *Phil. Mag.* **4,** 880 (1959)
19. Hughes, D. G. *Phil. Mag.* **5,** 467 (1960)
20. Martin, D. L. *Canad. J. Phys.* **39,** 1388 (1961)
21. MacDonald, D. K. C., Pearson, W. B., and Templeton, I. M. *Proc. roy. Soc.* **A256,** 334 (1960)
22. Dugdale, J. S., and Gugan, D. *Phil. Mag.* (To appear)
23. Hedgcock, F. T. *Phys. Rev. Lett.* **5,** 420 (1960)
24. Park, J. G., and Gugan, D. To be published.
25. Krautz, E., and Schultz, H. *Naturforsch.* **12a,** 710 (1957)

A Liquid Helium Level Indicator

A. E. Rovinskii *All-Union Electrotechnical Institute, U.S.S.R.*

Received 18 July 1961†

THE idea of using the phenomenon of the transition of pure tantalum into the superconducting state at 4·3° K for measuring the level of liquid helium was proposed by Feldmeier and Serin and first applied by Rasor[2] in an apparatus for continuous measurement of the quantity of liquid in a closed vessel. In a liquid level indicator with a feeler in the form of a probe it is desirable to reduce the dimensions and mass of the immersed tantalum element, so that it is advantageous to change the electrical circuit of the instrument somewhat in order to maintain a sufficiently high sensitivity.

The circuit of the level indicator is shown in Figure 1(a). The sensitive element R_E is made of 0·15 mm diameter tantalum wire (resistance $\simeq 3{\cdot}5\ \Omega$ at 293° K and $\simeq 0{\cdot}3\ \Omega$ at 10° K) and is included in an arm of a bridge formed by resistances $R_1 = 2{\cdot}6\ \Omega$, $R_2 = 14{\cdot}5\ \Omega$, and the variable resistance $R_3 = 2\ \Omega$. The supply from a 1·5 V source is fed through a button contact; a 10 mA milliameter is in the diagonal of the bridge. The bridge is balanced when the sensitive element is in vapour above the liquid; when it is immersed in liquid helium a great increase in current in the measuring diagonal takes place (up to 10 mA).

If the indicator is removed from the liquid helium vessel with the button contact made, a current of over 25 mA flows in the reverse direction in the diagonal. A shunt resistance $R_4 = 0{\cdot}55\ \Omega$ is used to protect the measuring system from such possible damage; this reduces the useful signal insignificantly but reduces the reverse current to 9 mA.

To achieve a still further decrease in the reverse current on lifting the probe out of the liquid helium vessel, an automatic reduction in bridge sensitivity was provided. A ballast resistance of nickel wire, R_N, in series with the voltage supply was placed on the probe above the sensitive element. When the probe is in the vessel of liquid the resistance of the nickel wire is small and the sensitivity of the indicator is at the maximum, but when the probe is lifted out the ballast resistance increases, producing a reduction in the voltage supply of the bridge.

The tantalum sensitive resistance and the nickel ballast resistance are made in the form of 1·5 mm spirals and are mounted at the end of the probe in channels of a Bakelite tube 4 mm in diameter and 1 mm thick (Figure 1(b)); the length of the probe is determined by the dimensions of the liquid helium vessel.

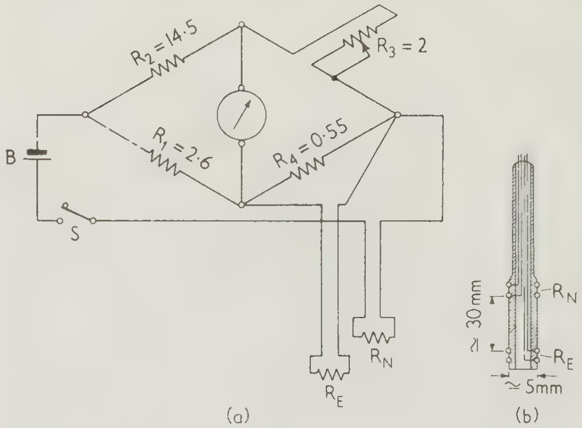

(a) (b)

Figure 1

The liquid helium level is determined by lowering the probe slowly into the vessel. The approach of the milliameter needle to the zero division shows that 40–50 mm remain before the surface of the liquid. The moment at which the sensitive element is immersed in liquid is fixed very clearly.

The tantalum wire heats up rapidly to above 4·3° K on raising the probe out of the liquid, and after 1–2 sec the instrument is ready for a repeat measurement.

REFERENCES

1. FELDMEIER, J. R., and SERIN, B. *Rev. sci. Instrum.* **19,** 916 (1948)
2. RASOR, N. S. *Rev. sci. Instrum.* **25,** 311 (1954)

This paper has been specially translated for CRYOGENICS and is included by permission of the Editors of *Pribory i Tekhnika Eksperimenta*. We are also indebted to the Instrument Society of America and the Plenum Press, who publish their own cover-to-cover translation of PTÉ by arrangement with the Russian publisher.

---

† Received by PTÉ Editor 10 April 1960; *Pribory i Tekhnika Eksperimenta* No. 2, p. 190 (1961).

Letters to the Editors

A 43 kgauss Superconducting Solenoid

THE possibility of generating high magnetic fields by means of loss-free superconducting coils is of great technological interest. For many years it was believed that because of the relatively low bulk critical fields of superconductors superconducting solenoids would be restricted to fields of a few thousand gauss. Recently, it has been realized[1] that by special treatment of materials, supercurrents can be maintained at fields between one and two orders of magnitude greater than the bulk critical field. The first superconducting coil consciously to utilize this principle appears to have been wound by Yntema[2] using cold-worked niobium. This coil generated 7 kgauss. A similar coil was constructed by Autler,[3] who also established that superconducting windings could be used effectively in an iron-cored magnet. A further advance by Kunzler et al.[4] showed that 15 kgauss could be attained in a coil of cold-worked molybdenum–rhenium wire.

A great impetus to the development of superconducting coils occurred when Kunzler and his associates[1] demonstrated high supercurrent densities in short length Nb_3Sn composite wires for externally applied fields up to 88 kgauss. Despite the fact that this material is believed to carry supercurrents up to fields in excess of 200 kgauss, metallurgical difficulties in working with such brittle material in long lengths seem to have hindered the construction of actual solenoids. Since alloys would be expected to be less brittle than intermetallic compounds, attention has turned to some of the high transition temperature alloys of niobium, in particular the niobium–zirconium system.[5–7] Again, short length heavily cold-worked specimens of niobium–zirconium wire exhibited quite high supercurrent densities up to 30 kgauss.[8]

Typical critical supercurrent densities for niobium–zirconium wire appear to be between 10^4 and 10^5 A/cm^2. Thus, it can easily be calculated that to construct a small solenoid of 10 mil wire to generate a field of 50 kgauss, one needs several thousand feet of wire. This wire must be reasonably uniform in metallurgical characteristics since the current carrying capacity of the wire is limited by the lowest value encountered along its length.

We have recently succeeded in producing niobium–zirconium wire of the desired uniformity in length up to several hundred feet. A 75 per cent niobium, 25 per cent zirconium base alloy was vacuum-arc melted and cast into $\frac{1}{2}$ in. diameter pins several inches long. These pins were canned in stainless steel and reduced by hot forging followed by cold swaging to $\frac{1}{8}$ in. diameter rods. The rods were drawn to 0·010 in. diameter wire by the Armetco Company of Wooster, Ohio.

Eighteen pieces of wire varying in length from 50 to 400 ft were insulated with several coats of epoxy enamel with a total build of $\frac{1}{2}$ mil. The wire was wound on to a $\frac{1}{2}$ in. diameter micarta phenolic resin former of length 1·4 in., resulting in a 74 layer coil of about 128 turns per layer (Figure 1). Individual lengths of wire were terminated at the end of a layer and brought out of the coil to a region of low magnetic field where a superconducting joint could readily be formed with the next piece of wire. The individual lengths were grouped into four sections consisting of 12, 24, 14, and 24 layers, respectively. Current was fed to each of the four sections from a separate individual power supply.

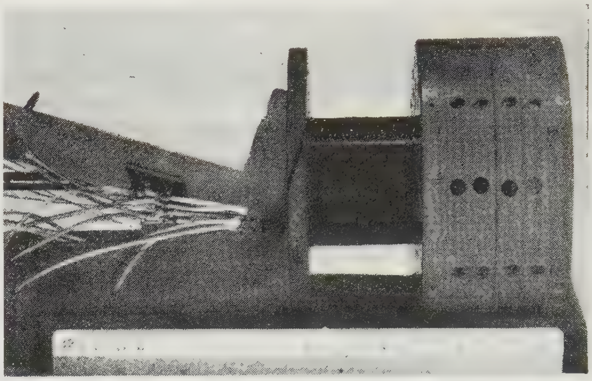

Figure 1. 43 kgauss superconducting coil

Short test samples of wire prepared in the above manner were found to carry between 20 and 40 A at 20 kgauss and 4·2° K. Individual samples frequently gave critical currents varying as much as 10 A between repeated tests. The current carrying capacity of the four sections of the solenoid ranged from 15 to 20 A depending upon whether the sections were activated together or run up separately. We conclude from this that the wire is fairly uniform in long lengths.

With the maximum permissible current in each section, a magnetic field slightly over 43,000 gauss was generated in the centre of the solenoid at 4·2° K. The field was monitored by a search coil and by a Hall probe at lower values. The field was found to be proportional to the current through the coil and in good agreement with the value calculated from the coil geometry.

When the threshold current was attained in an individual section of the coil, the impedance rose very rapidly and reduced the current in that section to a fraction of an ampere. This frequently, although not always, caused the other sections to transit to the normal state, so that the entire peak field of 43,000 gauss was switched off in a fraction of a second. This behaviour subjected the coil to a mechanical impulse which was clearly audible outside the metal cryostat in which the system was contained. Presumably, this impulse is due to the sudden release of the forces acting upon the inner windings of the coil due to the high magnetic field.

We are grateful to R. L. Ammon, W. Bagdade, J. H. Bechtold, R. T. Begley, R. D. Blaugher, G. Comenetz, R. E. Gold, G. T. Mallick, A. Patterson, S. W. Sandberg, F. A. Sattler, and C. B. Satterthwaite for active assistance in parts of this work.

REFERENCES

1. Kunzler, J. E., Buehler, E., Hsu, F. S., and Wernick, J. H. *Phys. Rev. Lett.* **6,** 89 (1961)
2. Yntema, G. B. *Phys. Rev.* **98,** 1197 (1955)
3. Autler, S. H. *Rev. Sci. Instrum.* **31,** 369 (1960)
4. Kunzler, J. E., Buehler, E., Hsu, F. S., Matthias, B. T., and Wahl, C. *J. appl. Phys.* **32,** 325 (1961)
5. Matthias, B. T. *Phys. Rev.* **92,** 874 (1953)
6. Kunzler, J. E. *Rev. mod. Phys.* (October 1961)
7. Hulm, J. K., and Blaugher, R. D. *Phys. Rev.* **123,** 1569 (1961)
8. Berlincourt, T. G., Hake, R. R., and Leslie, D. H. *Phys. Rev. Lett.* **6,** 671 (1961)

Westinghouse Research Laboratories,
Pittsburgh,
Pennsylvania.

M. J. Fraser
J. K. Hulm
H. Riemersa
A. J. Venturino
R. E. Wein

(6 October 1961)

Bibliography

The following list of papers and letters concerning low temperature physics and engineering has been compiled from a wide range of periodicals and covers the period July–September 1961.

Abrikosov, A. A., and Fal'kovskii, L. A. 'Raman Scattering of Light in Superconductors.' *J. exp. theor. Phys.* **40,** 262 (1961), *Soviet Phys. JETP* **13,** 179 (1961)

Abrikosov, A. A., and Gor'kov, L. P. 'Contribution to the Theory of Superconducting Alloys with Paramagnetic Impurities.' *J. exp. theor. Phys.* **39,** 1781 (1960), *Soviet Phys. JETP* **12,** 1243 (1961)

Adkins, C. J. 'Device for the Stabilization of Helium Cryostat Temperatures.' *J. sci. Instrum.* **38,** 305 (1961)

Alers, G. A., and Waldorf, D. L. 'Variation of the Elastic Moduli at the Superconducting Transition.' *Phys. Rev. Lett.* **6,** 677 (1961)

Alger, R. S., Anderson, T. H., and Webb, L. A. 'Trapped Radicals in Irradiated *n*-Propanol at 77°K.' *J. chem. Phys.* **35,** 49 (1961)

Allard, N. 'Spectres d'Absorption Optique, à Basse Température, de Monocristaux du Chlorure Double de Cobalt et de Cesium, $CoCs_3Cl_5$.' *C. R. Acad. Sci., Paris* **252,** 3970 (1961)

Ambler, E., and Dove, R. B. 'Continuously Operating He^3 Refrigerator for Producing Temperatures down to $\frac{1}{4}$°K.' *Rev. sci. Instrum.* **32,** 737 (1961)

Andronikashvili, E. L. 'Investigation of the Thermal Structure of Helium II by Scattering of Cold Neutrons.' *Adv. phys. Sci., Moscow* **72,** 697 (1960), *Soviet Phys. Uspekhi* **3,** 888 (1961)

Andronikashvili, E. L., et al. 'Properties of the Quantized Vortices Generated by the Rotation of Helium II.' *Adv. phys. Sci., Moscow* **73,** 3 (1961), *Soviet Phys. Uspekhi* **4,** 1 (1961)

Anon. 'Accuracy and Uniformity in Calibration of Platinum Resistance Thermometers.' *Mod. Refrig.* **64,** 698 (1961)

Anon. 'Metals for Low Temperature Service.' *World Refrig. and Air-Condit.* **12,** No. 8, 43 (1961)

Bardeen, J. 'Quantization of Flux in a Superconducting Cylinder.' *Phys. Rev. Lett.* **7,** 162 (1961)

Bekarevich, I. L., and Khalatnikov, I. M. 'Theory of the Kapitza Thermal Discontinuity of the Boundary between Liquid He^3 and a Solid Body.' *J. exp. theor. Phys.* **39,** 1699 (1960), *Soviet Phys. JETP* **12,** 1187 (1961)

Belov, K. P., Malevskaya, L. A., and Sokolov, V. I. 'Resonance and Magnetic Properties of Yttrium Iron Garnet at Low Temperatures.' *J. exp. theor. Phys.* **39,** 1542 (1960), *Soviet Phys. JETP* **12,** 1074 (1961)

Berlincourt, J. G., Hake, R. R., and Leslie, D. H. 'Superconductivity at High Magnetic Fields and Current Densities in Some Nb-Zr Alloys.' *Phys. Rev. Lett.* **6,** 671 (1961)

Bewilogua, L. 'Anwendungsmöglichkeiten sehr tiefer Temperaturen.' *Die Technik* **16,** 429 (1961)

Brandt, N. B., and Ginzburg, N. I. 'Superconductivity of Crystalline Modifications of Bismuth.' *J. exp. theor. Phys.* **39,** 1554 (1960), *Soviet Phys. JETP* **12,** 1082 (1961)

Brewer, D. F., and Edwards, D. O. 'Heat Conduction by Liquid Helium II in Capillary Tubes I: Transition to Supercritical Conduction.' *Phil. Mag.* **66,** 775 (1961)

Brewer, D. F., and Keyston, J. R. G. 'Specific Heat and Expansion Coefficient of Liquid Helium-3 under Pressure below 0·1°K.' *Nature, Lond.* **191,** 1261 (1961)

Bryant, C. A., and Keesom, P. H. 'Low-Temperature Specific Heat of Indium and Tin.' *Phys. Rev.* **123,** 491 (1961)

Byers, N., and Yang, C. N. 'Theoretical Considerations Concerning Quantized Magnetic Flux in Superconducting Cylinders.' *Phys. Rev. Lett.* **7,** 46 (1961)

Careri, G., Cunsolo, S., and Mazzoldi, P. 'Critical Drift Velocity of Ions in Liquid Helium.' *Phys. Rev. Lett.* **7,** 151 (1961)

Cataland, G., Edlow, M. H., and Plumb, H. H. 'Liquid Helium Vapor Pressure Regulator.' *Rev. sci. Instrum.* **32** (1961)

Chirlian, P. M., and Marsocci, V. A. 'On the Linear Circuit Aspects of Cryotrons.' *Proc. Inst. Radio Engrs, N.Y.* **49,** 1326 (1961)

Cini-Castagnoli, G., Giardini-Guidoni, A., and Ricci, F. P. 'Diffusion of Neon, HT, and Deuterium in Liquid Hydrogen.' *Phys. Rev.* **123,** 404 (1961)

Cooper, L. N. 'Superconductivity in the Neighborhood of Metallic Contacts.' *Phys. Rev. Lett.* **6,** 689 (1961)

Crane, L. T., and Zimmerman, J. E. 'Specific Heats of Dilute Cu-Co Alloys between 1·5° and 4·5°K.' *Phys. Rev.* **123,** 113 (1961)

Cunsolo, S., and Mazzoldi, P. 'The Influence of Pressure on the Mobility of Electric Charges in Liquid Helium II.' *Nuovo Cim.* **XX,** 949 (1961)

Danielen, A. 'Ground State of an Ising Face-centered Cubic Lattice.' *Phys. Rev. Lett.* **6,** 670 (1961)

Deaver, B. S., Jr., and Fairbank, W. M. 'Experimental Evidence for Quantized Flux in Superconducting Cylinders.' *Phys. Rev. Lett.* **7,** 43 (1961)

Doll, R., and Nabauer, M. 'Experimental Proof of Magnetic Flux Quantization in a Superconducting Ring.' *Phys. Rev. Lett.* **7**, 51 (1961)

Douglass, D. H., Jr. 'Direct Experimental Measurement of the Magnetic Field Dependence of the Superconducting Energy Gap of Aluminium.' *Phys. Rev. Lett.* **7**, 14 (1961)

Dressler, K. 'Ultraviolet Absorption Spectrum of Ammonia in Solid Argon at 4·2°K.' *J. chem. Phys.* **35**, 165 (1961)

Dugdale, J. S. 'Electrical Resistivity at Low Temperatures.' *Science* **134**, 77 (1961)

Dugdale, J. S., Gugan, D., and Okomura, K. 'The Electrical Resistivity of Lithium-6.' *Proc. roy. Soc.* **A263**, 407 (1961)

Fieschi, R., Nardelli, G. F., and Chiarotti, A. R. 'Self-Diffusion Coefficient in Solid Argon.' *Phys. Rev.* **123**, 141 (1961)

Fischer, F. 'Thermolumineszenz von KCl und NaCl nach Röntgen- und UV-Bestrahlung bei Heliumtemperatur.' *Z. Phys.* **163**, 401 (1961)

Flinn, P. A., McManus, G. M., and Rayne, J. A. 'Effective X-Ray and Calorimetric Debye Temperature for Copper.' *Phys. Rev.* **123**, 809 (1961)

Galkin, A. A., Kaner, E. A., and Korolyuk, A. P. 'Investigation of Ultrasonic Absorption by a Metal in a Magnetic Field.' *J. exp. theor. Phys.* **39**, 1517 (1960), *Soviet Phys. JETP* **12**, 1055 (1961)

Giaever, I. 'The Significance of Tunnelling into Superconductors.' *Discovery* **22**, 338 (1961)

Gindin, I. A., Lazarev, B. G., and Starodubov, Ya. D. 'Discontinuous Character of Plastic Deformation at Low Temperatures.' *Fiz. Tverd. Tela* **3**, 920 (1961), *Soviet Phys. Solid State* **3**, 669 (1961)

Ginell, R. 'Tait Coefficients and λ Transition of Helium I and II.' *J. chem. Phys.* **35**, 473 (1961)

Goodman, B. B. 'Simple Model for the Magnetic Behavior of Superconductors of Negative Surface Energy.' *Phys. Rev. Lett.* **6**, 597 (1961)

Gor'kov, L. P., and Galitskii, V. M. 'Superfluidity in a Fermi System in the Presence of Pairs with Nonzero Angular Momentum.' *J. exp. theor. Phys.* **40**, 1124 (1961), *Soviet Phys. JETP* **13**, 792 (1961)

Gossard, A. C., Jaccarino, V., and Remeika, J. P. 'Experimental Test of the Spin-Wave Theory of a Ferromagnet.' *Phys. Rev. Lett.* **7**, 122 (1961)

Gregor, L. V., and Fritz, J. J. 'Magnetic and Thermodynamic Properties of Potassium Ferricyanide at Low Temperatures.' *J. Amer. chem. Soc.* **83**, 2833 (1961)

Guénault, A. M. 'Thermal Conduction in Normal and Superconducting Tin and Indium.' *Proc. roy. Soc.* **A262**, 420 (1961)

Gygax, 'Ein supraleitender Gleichspannungsverstärker für Helium-Temperaturen.' *Z. angew. Math. Phys.* **XII**, 289 (1961)

Hein, R. A., and Falge, R. L., Jr. 'Differential Paramagnetic Effect in Superconductors.' *Phys. Rev.* **123**, 407 (1961)

Hilsch, P., and Hilsch, R. 'Zum Verhalten von Supraleitern im Kontakt mit Normalleitern.' *Naturwiss.* **48**, 549 (1961)

Hinrichs, C. H., and Swenson, C. A. 'Superconducting Critical Field of Tantalum as a Function of Temperature and Pressure.' *Phys. Rev.* **123**, 1106 (1961)

Hornung, E. W., and Lyon, D. N. 'Characteristics of Several Carbon Thermometer-heaters at Low Temperatures and in Magnetic Fields to 100 kilogauss.' *Rev. sci. Instrum.* **32**, 684 (1961)

Horwitz, N. H., and Bohm, H. V. 'Metal-to-glass Vacuum Seal for Low Temperatures.' *Rev. sci. Instrum.* **32**, 857 (1961)

Howard, R. E., Vosko, S., and Smoluchowski, R. 'Mechanism for Production of Interstitials in KCl by X-Rays at Low Temperatures.' *Phys. Rev.* **122**, 1406 (1961)

Hudson, R. P., and Hosler, W. R. 'Magnetic Susceptibility of Cerous Magnesium Nitrate.' *Phys. Rev.* **122**, 1417 (1961)

Ittner, W. B., and Kraus, C. J. 'Superconducting Computers.' *Sci. Amer.* **205**, 124 (July, 1961)

Izumi, H. 'The Silicon Cryosar.' *Proc. Inst. Radio Engrs, N.Y.* **49**, 1313 (1961)

Jennings, L. D., Hill, E., and Spedding, F. H. 'Heat Capacity of Thulium from 15° to 360°K.' *J. chem. Phys.* **34**, 2082 (1961)

Jonscher, A. K. 'p–n Junctions at Very Low Temperatures.' *Brit. J. appl. Phys.* **12**, 363 (1961)

Kamigaki, K. 'Ultrasonic Attenuation in Tin Single Crystals at Low Temperatures.' *J. phys. Soc. Japan* **16**, 1141 (1961)

Kamigaki, K. 'Ultrasonic Attenuation in Magnetite at Low Temperatures.' *J. phys. Soc. Japan* **16**, 1170 (1961)

Kan, L. S., Lazarev, B. G., and Makarov, V. I. 'On the Superconductivity of Tin and Indium under Pressure.' *J. exp. theor. Phys.* **40**, 457 (1961), *Soviet Phys. JETP* **13**, 317 (1961)

Keller, J. B., and Zumino, B. 'Quantization of the Fluxoid in Superconductivity.' *Phys. Rev. Lett.* **7**, 164 (1961)

Kenworthy, D. J., and ter Haar, D. 'Thermodynamics of Dirty Superconductors.' *Phys. Rev.* **123**, 1181 (1961)

Khesina, A. Ya. 'Spectroscopy of Some Pyrene Derivatives in Frozen Solutions.' *Bull. Acad. Sci. U.R.S.S.* **24**, 623 (1960), *English Translation* **24**, 629 (1961)

Klemens, P. G., and Maradudin, A. A. 'Lattice Distortion Due to Isotopes in Solid Helium.' *Phys. Rev.* **123**, 804 (1961)

Klipping, G. 'Ein Heliumverdampfer zur Erzeugung tiefer Temperaturen.' *Kältetech.* **13**, 250 (1961)

Knaap, H. F. P., and Beenakker, J. J. M. 'The Lennard-Jones 6-12 Potential Parameters of H_2 and D_2.' *Physica* **27**, 523 (1961)

Knorn, M. 'Absorptionsisothermen bei 78°K.' *Mber. Dt. Akad. Wiss.* **3**, 15 (1961)

Kogan, V. S., Lazarev, B. G., and Bulatova, R. F. 'Different Lattice Constants of Solid Neon Isotopes.' *J. exp. theor. Phys.* **40,** 29 (1961), *Soviet Phys. JETP* **13,** 19 (1961)

Kouvel, J. S., and Hartelius, C. C. 'Abrupt Magnetic Transition in MnSn$_2$.' *Phys. Rev.* **123,** 124 (1961)

Lange, F. 'Zur praktischen Anwendung von Supraleitern.' *Forsch. u. Fortschr.* **35,** 138 (1961)

Lazarev, B. G., Semenenko, E. E., and Sudovtsov, A. I. 'Modifications of Beryllium and Iron in Films Condensed onto Cold Substrates.' *J. exp. theor. Phys.* **40,** 105 (1961), *Soviet Phys. JETP* **13,** 75 (1961)

Lindenfeld, P. 'Thermal Conductivity of Normal and Superconducting Lead Alloys.' *Phys. Rev. Lett.* **6,** 613 (1961)

Lipsett, F. R. 'Four-specimen Liquid Helium Cryostat for Fluorescence.' *Rev. sci. Instrum.* **32,** 840 (1961)

Lipsicas, M., and Bloom, M. 'Nuclear Magnetic Resonance Measurements in Hydrogen Gas.' *Canad. J. Phys.* **39,** 881 (1961)

Little, W. A. 'Kapitza Resistance between Helium and Metals in the Normal and Superconducting States.' *Phys. Rev.* **123,** 435 (1961)

Love, W. F., and Wei, W. F. 'Longitudinal Magnetoresistance in *n*-Type Germanium: Experimental.' *Phys. Rev.* **123,** 67 (1961)

Martin, T. L. 'The Electronic Specific Heat of Lithium Isotopes.' *Proc. roy. Soc.* **A263,** 378 (1961)

Matthias, B. T., Bozorth, R. M., and van Vleck, J. H. 'Ferromagnetic Interaction in EuO.' *Phys. Rev. Lett.* **7,** 160 (1961)

Matthias, B. T., Clogston, A. M., Williams, H. J., Corenzwhit, E., and Sherwood, R. C. *Phys. Rev. Lett.* **7,** 7 (1961)

McAvoy, B. R., Feldman, D. W., Castle, J. G., Jr., and Warren, R. W. 'Optical Saturation of *F*-center Spin Resonance.' *Phys. Rev. Lett.* **6,** 618 (1961)

Meyer, L., and Reif, F. 'Ion Motion in Superfluid Liquid Helium under Pressure.' *Phys. Rev.* **123,** 727 (1961)

Miles, J. L., and McMahon, H. O. 'Use of Monomolecular Layers in Evaporated-Film Tunneling Devices.' *J. appl. Phys.* **32,** 1176 (1961)

Miller, S. C., and Omar, M. A. 'Longitudinal Magnetoresistance in *n*-Type Germanium: Theoretical.' *Phys. Rev.* **123,** 74 (1961)

Milligan, D. E. 'Infrared Spectroscopic Study of the Photolysis of Chlorine Azide in Solid Argon at 4·2°K.' *J. chem. Phys.* **35,** 372 (1961)

Milne, D. K. 'Simple Approach to Cryogenic Waveguide.' *J. sci. Instrum.* **38,** 335 (1961)

Mittendorf, H. 'Zur Struktur dünner, bei tiefer Temperatur kondensierter Salzschichten.' *Z. Phys.* **163,** 321 (1961)

Mönch, W. 'Messung der Fehlordnungsenergie an abschreckend kondensierten Metallschichten bei tiefer Temperatur.' *Z. Phys.* **164,** 229 (1961)

Morgand, P. 'Étude Spectroscopique de la Photolyse du Toluene en Solution Rigide à 77°K.' *C. R. Acad. Sci., Paris* **252,** 3577 (1961)

Morris, D. E., and Tinkham, M. 'Effect of Magnetic Field on Thermal Conductivity and Energy Gap of Superconducting Films.' *Phys. Rev. Lett.* **6,** 600 (1961)

Mycielski, J. 'Mechanism of Impurity Conduction in Semiconductors.' *Phys. Rev.* **123,** 99 (1961)

Näbauer, M. 'Experimentelle und theoretische Untersuchung des Beginns der Umwandlung Supraleitung—Normalleitung unter der Wirkung eines überkritischen Magnetfelds bei verschiedenen Einschaltgeschwindigkeiten des Feldes.' *Z. Phys.* **163,** 119 (1961)

Nash, F. R. 'Size-dependent Relaxation Times at Liquid Helium Temperatures.' *Phys. Rev. Lett.* **7,** 59 (1961)

Navarro, Q. O., and Shirley, D. A. 'Nuclear Orientation of Dy^{155} and Dy^{157},' *Phys. Rev.* **123,** 186 (1961)

Nelson, D. T., and Legvold, S. 'Adiabatic Demagnetization with Yttrium-Rare Earth Alloys.' *Phys. Rev.* **123,** 80 (1961)

Netzel, R. G., and Dillinger, J. R. 'Epoxy Resin as a Material for Constructing Cryogenic Apparatus.' *Rev. sci. Instrum.* **32,** 855 (1961)

Newhouse, V. L., and Edwards, H. H. 'Thin-Film Cryotrons.' *Proc. Inst. Radio Engrs, N.Y.* **49,** 1318 (1961)

Ohlmann, R. C., and Tindham, M. 'Antiferromagnetic Resonance in FeF$_2$ at Far-Infrared Frequencies.' *Phys. Rev.* **123,** 425 (1961)

Onsager, L. 'Magnetic Flux through a Superconducting Ring.' *Phys. Rev. Lett.* **7,** 50 (1961)

Pace, E. L., and Bobka, R. J. 'Thermodynamic Properties of Trifluoroacetonitrile from 12°K to its Boiling Point.' *J. chem. Phys.* **35,** 454 (1961)

Parkinson, D. H. 'Summarized Proceedings of a Symposium on Electronic Devices at Helium Temperatures —London, November 1960.' *Brit. J. appl. Phys.* **12,** 353 (1961)

Pearson, R. F., and Cooper, R. 'Magnetic Anisotropy and Rotational Hysteresis in Single Crystals of Magnetite below the Transition Temperature.' *Proc. phys. Soc. Lond.* **78,** 17 (1961)

Pearson, W. B., and Templeton, I. M. 'The Effect of Dissolved Iron on the Thermoelectricity of Silver at Very Low Temperatures.' *Canad. J. Phys.* **39,** 1084 (1961)

Pershaw, P. S., and Bloembergen, N. 'Electrically Induced Shift of the F^{19} Resonance Frequency in MnF$_2$.' *Phys. Rev. Lett.* **7,** 165 (1961)

Personov, R. I. 'Absorption and Fluorescence Spectra of Perylene at Low Temperatures.' *Bull. Acad. Sci. U.R.S.S.* **24,** 620 (1960), *English Translation* **24,** 624 (1961)

Peshkov, V. P. 'Critical Velocities in Superfluid Helium.' *J. exp. theor. Phys.* **40,** 379 (1961), *Soviet Phys. JETP* **13,** 259 (1961)

Pfeffer, W. 'Spezifische Wärmen von $DyCl_3.6H_2O$ und $NdCl_3.6H_2O$ im Temperaturbereich zwischen 1,2°K und 220°K.' *Z. Phys.* **164,** 295 (1961)

Podgurski, H. H., and Davis, F. N. 'Thermal Transpiration at Low Pressure. The Vapor Pressure of Xenon below 90°K.' *J. phys. Chem.* **65,** 1343 (1961)

Pokrovskii, V. L. 'Threshold Phenomena in Superconductors.' *J. exp. theor. Phys.* **40,** 143 (1961), *Soviet Phys. JETP* **13,** 100 (1961)

Pokrovskii, V. L. 'Thermodynamics of Anisotropic Superconductors.' *J. exp. theor. Phys.* **40,** 641 (1961), *Soviet Phys. JETP* **13,** 447 (1961)

Pokrovskii, V. L. 'Absorption of Ultrasound in an Anisotropic Superconductor.' *J. exp. theor. Phys.* **40,** 898 (1961), *Soviet Phys. JETP* **13,** 628 (1961)

Pokrovskii, V. L., and Toponogov, V. A. 'Reconstruction of the Energy Gap in a Superconductor by Measurement of Sound Attenuation.' *J. exp. theor. Phys.* **40,** 1112 (1961), *Soviet Phys. JETP* **13,** 785 (1961)

Pollak, M., and Geballe, T. H. 'Low-Frequency Conductivity Due to Hopping Processes in Silicon.' *Phys. Rev.* **122,** 1742 (1961)

Quinn, D. J., and Budnick, J. I. 'Study of the Superconducting Transition Temperature in Dilute Thallium Solid Solutions.' *Phys. Rev.* **123,** 466 (1961)

Rauch, C. J. 'Millimeter Cyclotron Resonance Experiments in Diamond.' *Phys. Rev. Lett.* **7,** 83 (1961)

Rayne, J. A., and Chandrasekhar, B. S. 'Elastic Constants of Iron from 4·2 to 300°K.' *Phys. Rev.* **122,** 1714 (1961)

Reinberg, A. R., and Grossweiner, L. I. 'Low-Temperature Optical Bleaching of *F* Centers in KCl.' *Phys. Rev.* **122,** 1734 (1961)

Rodbell, D. S. 'Possibility of Exchange Magnetostriction Yielding Negative Thermal Expansion in Solid He^3.' *Phys. Rev. Lett.* **7,** 1 (1961)

Rolfe, J., Lipsett, F. R., and King, W. J. 'Optical Absorption and Fluorescence of Oxygen in Alkali Halide Crystals.' *Phys. Rev.* **123,** 447 (1961)

Roncin, J., and Damany-Astoin, N. 'Spectre d'Absorption, entre 1650 et 2600 Å, du Mercure Piégé dans des Matrices d'Isopentane et d'Argon à 20°K.' *C. R. Acad. Sci., Paris* **252** (1961)

Salinger, G. L., and Wheatley, J. C. 'Magnetic Susceptibility of Materials Commonly Used in the Construction of Cryogenic Apparatus.' *Rev. sci. Instrum.* **32,** 872 (1961)

Schirber, J. E., and Swenson, C. A. 'Superconductivity of α- and β-Mercury.' *Phys. Rev.* **123,** 1115 (1961)

Schuch, A. F. 'Bond-lengths in Solid Helium.' *Nature, Lond.* **191,** 591 (1961)

Seraphim, D. P., and Marcus, P. M. 'First and Second Order Stress Effects on Superconducting Transitions in Ta and Sn.' *Phys. Rev. Lett.* **6,** 680 (1961)

Sevast'yanov, B. K. 'Magnetic Properties of Thin Superconducting Tin and Indium Films.' *J. exp. theor. Phys.* **40,** 52 (1961), *Soviet Phys. JETP* **13,** 35 (1961)

Shirley, D. A., Kaplan, M., and Axel, P. 'Recoil-Free Resonant Absorption in Au^{197}.' *Phys. Rev.* **123,** 816 (1961)

Slack, G. A. 'Thermal Conductivity of CaF_2, MnF_2, CoF_2 and ZnF_2 Crystals.' *Phys. Rev.* **122,** 1451 (1961)

Smith, P. H., Shapiro, S., Miles, J. L., and Nicol, J. 'Superconducting Characteristics of Superimposed Metal Films.' *Phys. Rev. Lett.* **6,** 686 (1961)

Sosin, A., and Neely, H. H. 'Cryostat for Irradiating at 4·2°K.' *Rev. sci. Instrum.* **32,** 922 (1961)

Springer, T., and Wiedemann, W. 'Untersuchung des Streuquerschnittes von Eis für sehr langsame Neutronen bei 4°K.' *Z. Phys.* **164,** 111 (1961)

Stelzried, C. T. 'A Liquid-helium-cooled Coaxial Termination.' *Proc. Inst. Radio Engrs, N.Y.* **49,** 1224 (1961)

Stiles, P. J., Burstein, E., and Langenberg, D. N. 'Observations of de Haas-van Alphen Oscillations in *p*-type PbTe.' *Phys. Rev. Lett.* **6,** 667 (1961)

Sujak, B. 'Thermal Conductivity Changes of $ZnSO_4.7H_2O$ below 10°K.' *Acta phys. Polon.* **XX,** 167 (1961)

Suzuki, R., and Akano, M. 'The Knight Shift in the Superconducting State.' *Nuovo Cim.* **XXI,** 559 (1961)

Thorsen, A. C., and Berlincourt, T. G. 'De Haas-van Alphen Effect in Potassium.' *Phys. Rev. Lett.* **6,** 617 (1961)

Townsend, P., and Sutton, J. 'A Study of Superconducting Niobium by Electron Tunnelling.' *Proc. phys. Soc. Lond.* **78,** 309 (1961)

Toxen, A. M. 'Size Effects in Thin Superconducting Indium Films.' *Phys. Rev.* **123,** 442 (1961)

Van den Beukel, A. 'Stored Energy Measurements on Copper and Nickel Cold Worked at Liquid Nitrogen Temperature.' *Physica* **27,** 603 (1961)

Van den Broek, J., Van der Marel, L. C., and Gorter, C. J. 'Paramagnetic Relaxation in Crystals of Copper Potassium Chloride and Chromium Potassium Alum at Liquid Helium Temperatures.' *Physica* **27,** 661 (1961)

Verkin, B. I., Dmitrenko, I. M., and Svechkarev, I. V. 'The Magnetic Properties of Beryllium in the Temperature Range 300 to 4·2°K.' *J. exp. theor. Phys.* **40,** 670 (1961), *Soviet Phys. JETP* **13,** 468 (1961)

Voorhoeve, W. H. M., and Dokoupil, Z. 'The Specific Heat of $MnCl_2.4H_2O$ between 0·9°K and 4·2°K at Three Different Magnetic Fields: 2·84, 7·61 and 10·48 kOe. ' *Physica* **27,** 777 (1961)

Ward, J. B., and Kauffman, J. W. 'Low-Temperature Recovery of Resistivity in Electron-Irradiated Gold.' *Phys. Rev.* **123,** 90 (1961)

Watanabe, T. 'The Magnetic Investigation of Mn^{++}, Co^{++}, Ni^{++} and Cu^{++} Ammine and Anhydrate Salts at Low Temperatures.' *J. phys. Soc. Japan* **16,** 1131 (1961)

WHITE, G. K. 'Thermal Expansion at Low Temperatures II: Electronic Component in Metals.' *Phil. Mag.* **66,** 815 (1961)

WILKINSON, M. K., CHILD, H. R., MCHARGUE, C. J., KOEHLER, W. C., and WOLLAN, E. O. 'Neutron Diffraction Investigations of Metallic Cerium at Low Temperatures.' *Phys. Rev.* **122,** 1409 (1961)

WOODS, A. D. B. 'Inelastic Scattering of Neutrons from Rotating Liquid Helium II.' *Canad. J. Phys.* **39,** 1082 (1961)

YOUNG, D. R. 'Recent Developments in High Speed Superconducting Devices.' *Brit. J. appl. Phys.* **12,** 359 (1961)

ZAVARITSKII, N. V. 'The Thermal Conductivity of High Purity Thallium and Tin.' *J. exp. theor. Phys.* **39,** 1571 (1960), *Soviet Phys. JETP* **12,** 1093 (1961)

ZIMMERMAN, J. E., and ROOT, R. C. 'Level Indicator for Permanent Installation in Liquid Helium Storage Dewar.' *Rev. sci. Instrum.* **32,** 853 (1961)

EDITORIAL NOTE

IN our first issue of September 1960 we mentioned that bibliographical material covering the low temperature field was being made available to our Journal through the kindness of Arthur D. Little Inc. of Cambridge, Massachusetts. In 1952 A. D. Little published a list of publications, each with a short abstract, comprising just under 1,000 entries, covering the years 1944–51. This material was broken down into a number of subsections and the publication was sent out to workers in the field of cryogenics and others. This first publication was augmented by nine supplements, giving titles of papers only, covering the years 1952–57. These supplements were in alphabetical order of authors. Although no further publication was made, A. D. Little kept their records up to date and kindly offered us the whole of the material.

The publishers of CRYOGENICS accepted this offer and the whole bibliography has been re-classified and brought up to date by Dr. D. F. Brewer of the Clarendon Laboratory. There are about 5,000 entries altogether, covering publications in the low temperature field from 1944 up to 1960 when the quarterly bibliographies published in CRYOGENICS began to appear.

This bibliography has now been published as a supplement to CRYOGENICS. The entries, each giving the authors and title of paper, are arranged alphabetically under 22 headings in five main groups. Copies are obtainable from: CRYOGENICS, Carlton House, Great Queen Street, London, W.C.2, price 25*s*.